UNIVERSITA' DEGLI STUDI DI PADOVA

Sede Amministrativa: Università degli Studi di Padova

Dipartimento di Scienze Chimiche

SCUOLA DI DOTTORATO DI RICERCA IN SCIENZE MOLECOLARI

INDIRIZZO SCIENZE CHIMICHE

CICLO XXI

Functionalisation of aromatic C-H bonds with dicarbene transition metal catalysts

Direttore della Scuola: Ch.mo Prof. Maurizio Casarin

Supervisore: Ch.mo Prof. Marino Basato

Dottoranda: Gabriella Buscemi

INDEX

ABSTRACT

The present research project concerns the catalytic application of transition metal dicarbene complexes, with the general structure reported in **Figure 1**, in aromatic C-H bond functionalisation/activation reactions.

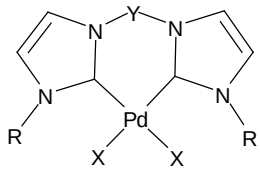

R = Me, Ph
X = Cl, Br, I, TFA
Y = methylene, *o*-phenylene, *o*-xylylene, *m*-xylylene

Figure 1 General structure of complexes with chelating N-heterocyclic dicarbene ligands.

The efficiency of this kind of complexes has been mainly examined in the hydroarylation of alkynes (*Fujiwara reaction*, **Figure 2**), which involves the addition of arenes to a wide range of internal and terminal alkynes [1]. It was already known that this reaction is catalysed by simple palladium(II) compounds, such as $Pd(OAc)_2$, in a trifluoroacetic acid environment. It occurs at room temperature and is characterised by a high and quite unusual regio- and stereoselectivity: remarkably the thermodynamically less favoured *cis*-arylalkenes are often obtained as major products.

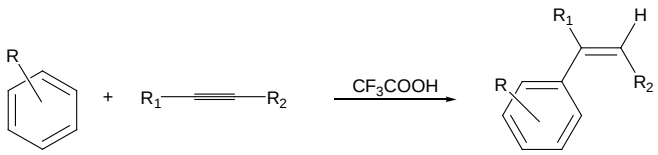

Figure 2 The Fujiwara reaction.

The Fujiwara reaction appears very promising from the synthetic point of view also because both the inter- and intra-molecular versions of the reaction are known, thus expanding its applicability to the functionalisation of aromatic heterocycles [2] and to the synthesis of coumarins [3]. However, the possible industrial application requires the optimisation of the reaction conditions since the reaction is often quite slow, needs an excess of arene substrate, and it usually requires 1-5 mol% palladium

which heavily affects the cost of the process. In the literature other metal centres, such as platinum(II) [4], gold(I) and gold(III) [5] have been successfully employed as alternative catalysts, but their efficiency appears to be lower than that of palladium(II). Also the use of non-noble, electrophilic metal centres has been reported, but their reactivity is lower and/or their applicability limited to aryl-acetylenes [6].

The initial aim of the present research project was to improve the yields of the reaction and decrease the catalyst loading. N-heterocyclic carbene ligands [7] can improve the stability of the catalyst under the reaction conditions as well as its reactivity. Monocarbene Pd(II) complexes $(IPr)Pd(OAc)_2$ and $(IPr)Pd(OOCCF_3)_2$ (IPr = *N*,*N*'-bis(2,6-diisopropylphenyl)-imidazol-2-ylidene) are indeed the only complexes which have been reported to be active in the Fujiwara reaction in the absence of other promoters, though their activity is comparable to that of simple $Pd(OAc)_2$ [8].

In the initial part of this research work it has been shown that the dicarbene palladium(II) complexes reported in **Figure 3** are able to catalyse the hydroarylation of alkynes at 80 °C, with excellent conversions and selectivities at low catalyst loading (0.1 mol%) and with equimolar amounts of reagents.

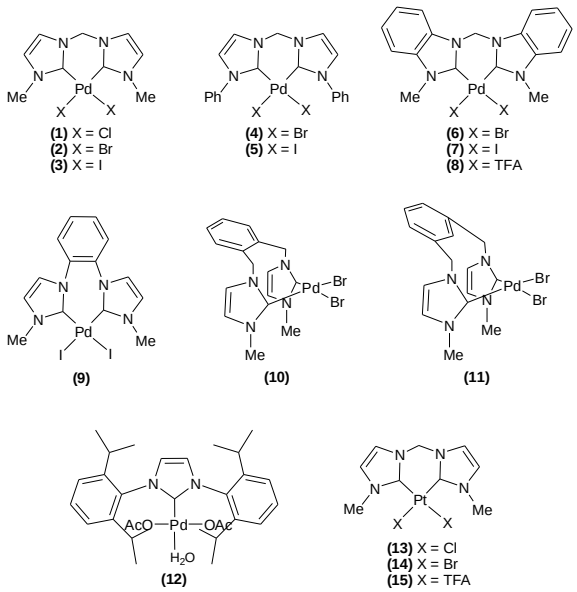

Figure 3 N-Heterocyclic dicarbene complexes employed in the work.

These dicarbene complexes have displayed a reactivity higher than simple palladium acetate and monocarbene palladium complex **(12)** tested in the same reaction conditions (**Figure 4**). Dicarbene platinum(II) complexes have also been employed and have performed an efficiency superior than Pt salts based systems reported in the literature [4].

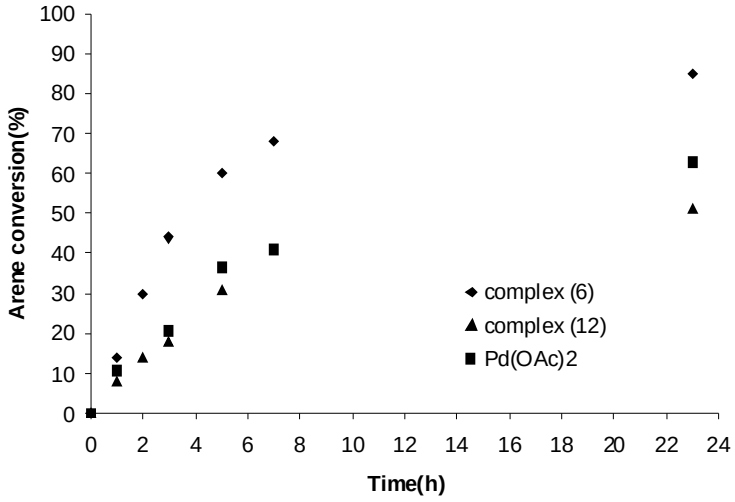

Figure 4 Conversion(%) *vs* time diagram for the reaction between pentamethylbenzene and ethyl propiolate catalysed by complex **(6)**, complex **(12)** and $Pd(OAc)_2$.

The optimised protocol has resulted quite general with respect to the alkyne, while its applicability to arene substrates is at present limited to electron-rich molecules. However this is a limitation occurring with all Pd- and Pt-catalytic systems reported in the literature for the hydroarylation reaction [1-6, 8].

Another part of the work has concerned the identification of the catalytic active species. Mechanistic studies, performed at 80 °C and made varying both the dicarbene ligand and the halide ligands at the metal, have revealed that the catalytic active species retains the dicarbene ligand in its coordination sphere. Halide anionic ligands are instead removed from the complex by exchange with the trifluoroacetate anion deriving from the acidic solvent media. In fact, looking at **Figure 5** and **6**, it is evident that the catalytic efficiency of the complex does not depend on the kind of

halide ligands (the catalytic species indeed does not possess halide ligands), but it is influenced by the nature of the dicarbene ligand [9].

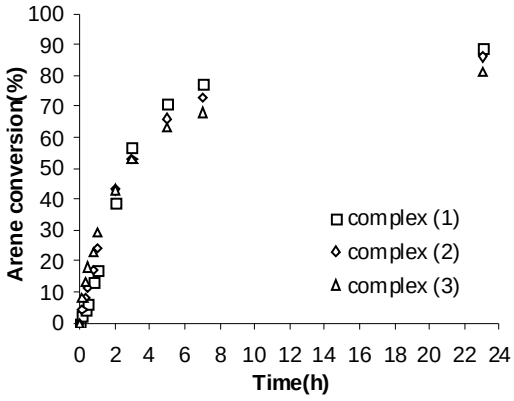

Figure 5 Conversion(%) *vs* time diagram for the reaction between pentamethylbenzene and ethyl propiolate: effect of the anionic ligand.

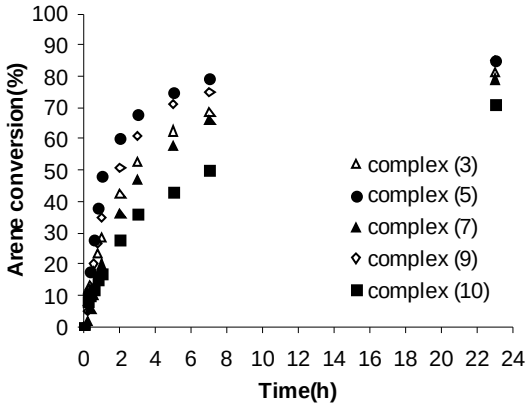

Figure 6 Conversion(%) *vs* time diagram for the reaction between pentamethylbenzene and ethyl propiolate: effect of the dicarbene ligand.

Parallel electrochemical studies have been therefore made to evaluate the electronic density at the metal centre in different dicarbene complexes [10]. The aim is to clarify if the catalytic efficiency of the complex is predominantly influenced by its electronic or steric properties, in order to design the best catalyst for the reaction.

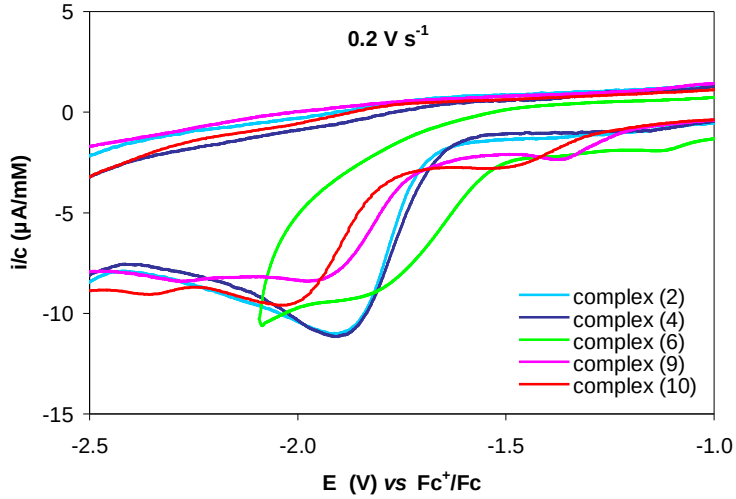

Figure 7 Cyclic voltammetry of Pd(II) complexes in DMSO + Bu_4NClO_4 0.1 M recorded at v = 0.2 V s^{-1}.

Cyclic voltammetries have shown that the electronic density at the metal changes depending on the dicarbene ligand (**Figure 7**), but the scale of reduction potentials Pd(II)-Pd(0) is not correlated to the scale of catalytic activity. This suggests that the catalytic efficiency of such complexes in the Fujiwara reaction is predominantly influenced by the steric hindrance at the metal centre.

A successive optimisation of the reaction parameters (nature of the solvent system, concentration of the reagents, reaction temperature [11] and use of co-catalysts [12]) has allowed to further increase the selectivity of the reaction under mild reaction conditions. It has indeed found that, in the presence of silver salts (like AgTFA) as co-catalysts, the reaction can be run at room temperature, with conversion higher than the one displayed by palladium acetate in the same reaction conditions (**Figure 8**). Differently from at 80 °C, isomerisation to the more thermodinamically stable *trans*-arylalkene and hydrolysis reactions of the ester functions do not occur at room temperature, so that selectivity towards the *cis*-arylalkene product has been significantly improved.

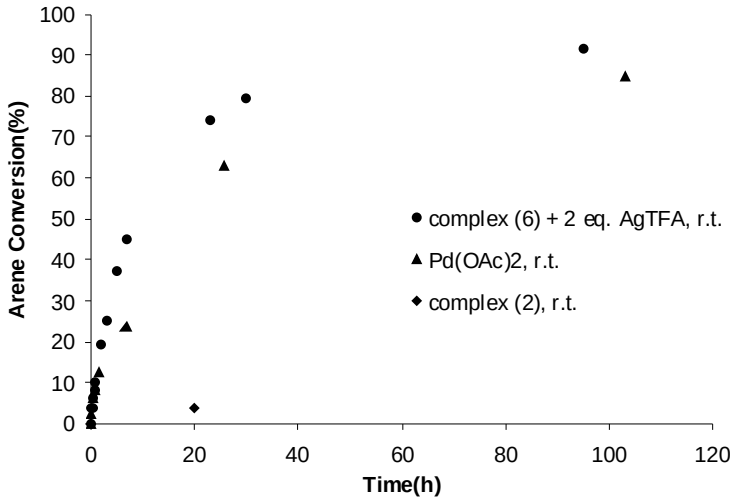

Figure 8 Conversion(%) *vs* time diagram for the reaction between pentamethylbenzene and ethyl propiolate: effect of the silver salt.

Finally, the optimised catalytic system has been used with other substrates, such as aromatic heterocycles, obtaining also in this case high yields in products. However,

the selectivity towards the desired product decreases by the formation of adducts heterocycle/alkyne 2/1 [13].

A preliminary investigation of the reaction mechanism through kinetic studies has been also started. There is indeed at present some controversy about the reaction mechanism, that could be an electrophilic arene metalation [1b] or a Friedel-Crafts-type alkenylation [14].

The kinetic law has resulted of the first order in palladium and, in the adopted reaction conditions, of the first order also in arene or in alkyne. It remains to evaluate the dependence of the kinetic law from the concentration of the acid, which seems to have an important role in the reaction mechanism. However, it needs to be used in large excess with respect to the substrates and probably its principal role is to hydrolyse the vinyl-palladium species, invoked as catalytic intermediate in both the proposed mechanisms.

Dicarbene complexes of palladium(II) and platinum(II) have been also tested in other aromatic C-H bond functionalisation reactions, such as the *ortho*-functionalisation of acetanilides [15].

SOMMARIO

Il presente progetto di ricerca riguarda l'applicazione di complessi dicarbenici di metalli di transizione, con la struttura generale riportata in **Figura 1**, in reazioni di funzionalizzazione/attivazione di legami C-H aromatici.

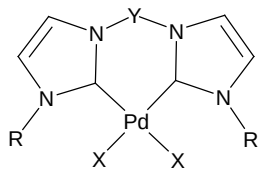

R = Me, Ph
X = Cl, Br, I, TFA
Y = metilene, *o*-fenilene, *o*-xililene, *m*-xililene

Figura 1 Struttura generale di complessi con leganti dicarbenici N-eterociclici.

L'efficienza catalitica di questi complessi è stata principalmente valutata nella reazione di idroarilazione di alchini (*reazione di Fujiwara*, **Figura 2**), che consiste nell'addizione di areni ad alchini interni o terminali catalizzata da semplici composti di palladio(II), come $Pd(OAc)_2$ [1]. Questa reazione decorre in ambiente acido, generalmente acido trifluoroacetico, a temperatura ambiente e presenta una elevata ed inusuale regio- e stereoselettività: si ottengono infatti come prodotti principali i *cis*-arilalcheni, che sono le olefine termodinamicamente meno favorite.

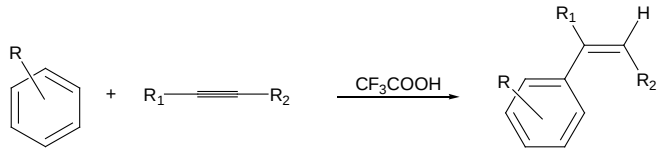

Figura 2 Reazione di Fujiwara.

La reazione appare molto promettente dal punto di vista tecnologico, anche perché sono conosciute sia la versione inter- che quella intramolecolare, permettendo quindi la funzionalizzazione di eterocicli aromatici [2] e la sintesi di cumarine [3]. La potenziale applicazione industriale richiede però l'ottimizzazione delle condizioni di reazione, poichè la reazione è spesso lenta, necessita di un eccesso di arene rispetto

all'alchino e viene condotta con un elevato tenore di catalizzatore (1-5%), fattore che incide pesantemente sul costo del processo.

Altri centri metallici, come Pt(II) [4], Au(I) e Au(III) [5], sono stati impiegati come catalizzatori alternativi, ma la loro reattività sembra essere inferiore a quella mostrata dai composti di palladio(II). Sono stati utilizzati anche centri metallici elettrofilici non nobili, ma la loro reattività è inferiore e/o la loro applicabilità limitata ai soli aril-acetileni [6].

L'obiettivo iniziale di questo progetto di tesi è stato quindi quello di migliorare le rese della reazione e diminuire il tenore di catalizzatore. Leganti carbenici N-eterociclici [7] possono aumentare la stabilità del catalizzatore nelle condizioni di reazione e quindi la sua reattività. I complessi monocarbenici di palladio(II), $(IPr)Pd(OAc)_2$ e $(IPr)Pd(OOCCF_3)_2$ (IPr = *N*,*N*'-bis(2,6-diisopropylphenyl)-imidazol-2-ylidene) sono infatti gli unici complessi ad essere risultati attivi nella reazione di Fujiwara senza bisogno di promotori, sebbene la loro reattività sia comparabile a quella mostrata da $Pd(OAc)_2$ [8].

Nella prima parte di questo lavoro di ricerca è stato dimostrato che i complessi dicarbenici di palladio(II) riportati in **Figura 3** catalizzano la reazione ad 80 °C, con eccellenti conversioni e selettività a basso tenore di catalizzatore (0.1%) e con i reagenti in rapporto equimolare.

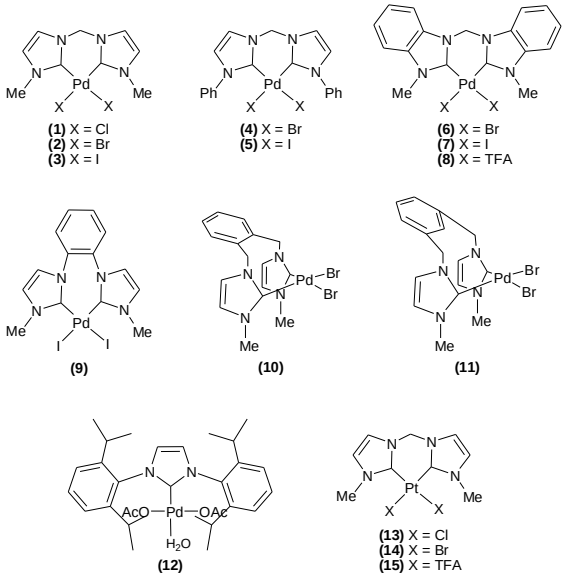

Figura 3 Complessi dicarbenici N-eterociclici impiegati in questo lavoro.

Questi complessi hanno mostrato una reattività maggiore rispetto al semplice palladio acetato ed al complesso monocarbenico **(12)** testati nelle stesse condizioni di reazione (**Figura 4**). Sono stati impiegati in questo studio anche complessi dicarbenici di Pt(II), che si sono dimostrati più attivi dei sistemi catalitici di platino riportati in letteratura [4].

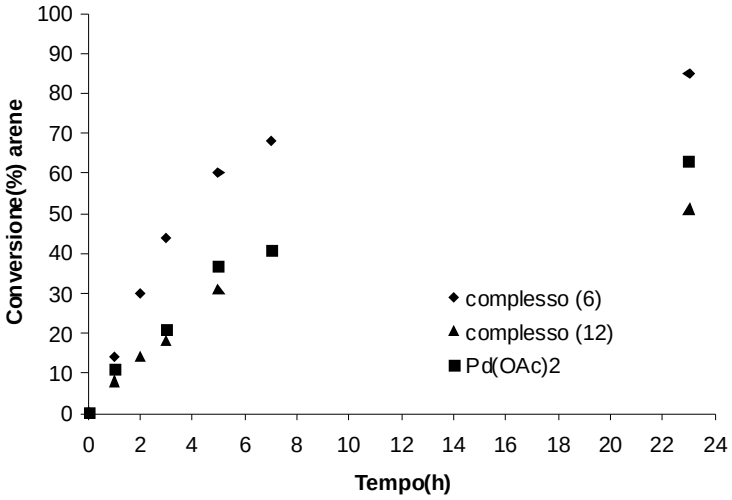

Figura 4 Diagramma di conversione(%) *vs* tempo per la reazione tra pentametilbenzene ed etil propiolato catalizzata da complesso **(6)**, complesso **(12)** e $Pd(OAc)_2$.

Il protocollo ottimizzato è risultato abbastanza generale per quanto riguarda gli alchini, mentre la sua applicabilità agli areni è al momento limitata a molecole elettron-ricche. Questa è comunque una limitazione di tutti i sistemi catalitici di Pd e Pt riportati in letteratura per l'idroarilazione di alchini [1-6, 8].

Una seconda parte del lavoro ha riguardato l'identificazione della specie cataliticamente attiva. Studi meccanicistici condotti ad 80 °C, variando sia il legante dicarbenico che i leganti anionici al metallo, hanno mostrato che la specie cataliticamente attiva mantiene il legante dicarbenico nella sua sfera di coordinazione, mentre i leganti anionici vengono rimossi dal complesso attraverso uno scambio con l'anione trifluoroacetato derivante dal solvente acido. Infatti, dalle **Figure 5** e **6** è possibile osservare come l'efficienza catalitica del complesso non

dipenda dal tipo di leganti anionici (in quanto la specie catalitica non li possiede), ma dipenda invece dalla natura del legante dicarbenico [9].

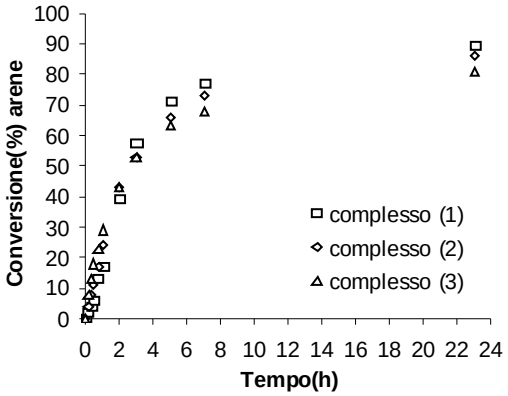

Figura 5 Diagramma di conversione(%) *vs* tempo per la reazione tra pentametilbenzene ed etil propiolato: effetto del legante anionico.

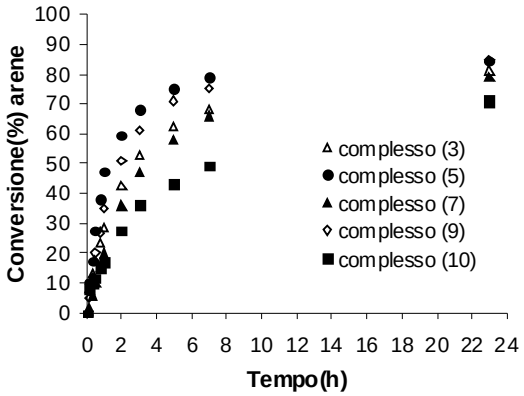

Figura 6 Diagramma di conversione(%) *vs* tempo per la reazione tra pentametilbenzene ed etil propiolato: effetto del legante dicarbenico.

Sono stati inoltre effettuati studi elettrochimici per determinare la densità elettronica presente al centro metallico in complessi con diverso legante dicarbenico [10], con lo scopo di chiarire se l'efficienza del complesso sia principalmente influenzata dalle proprietà elettroniche o da quelle steriche di questo legante e di progettare così il migliore catalizzatore per la reazione.

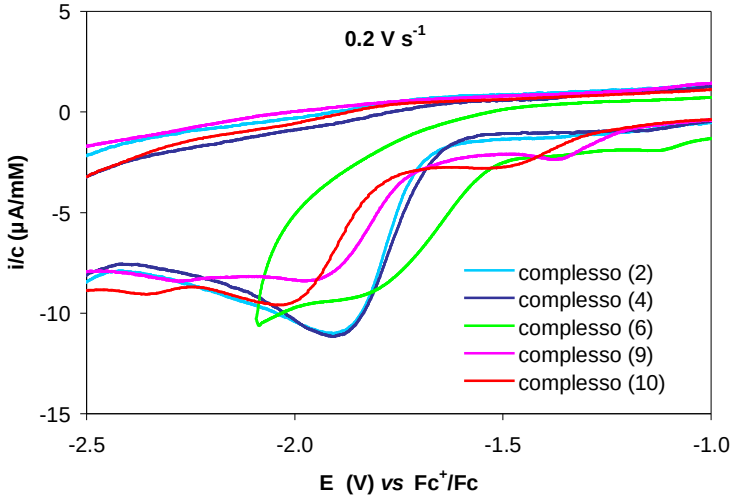

Figura 7 Voltammetria ciclica dei complessi di Pd(II) in DMSO + Bu_4NClO_4 0.1 M registrata a v = 0.2 V s^{-1}.

Le voltammetrie cicliche hanno mostrato che la densità elettronica al centro metallico varia a seconda del legante dicarbenico (**Figura 7**), ma che la scala di potenziali di riduzione Pd(II)-Pd(0) non è correlabile alla scala di attività catalitica. L'efficienza di questo tipo di complessi nella reazione di Fujiwara sembra quindi essere principalmente influenzata dall'ingombro sterico al centro metallico.

La successiva ottimizzazione dei parametri di reazione (natura del solvente, concentrazione dei reagenti, temperatura di reazione [11] ed utilizzo di co-catalizzatori [12]) ha permesso di incrementare ulteriormente la selettività della reazione in condizioni di reazione blande. E' stato infatti dimostrato che in presenza di sali di argento come co-catalizzatori (per esempio AgTFA) la reazione avviene anche a temperatura ambiente, con conversioni maggiori di quelle ottenute con palladio acetato nelle stesse condizioni di reazione (**Figura 8**). Diversamente che a 80 °C, le reazioni di isomerizzazione a *trans*-arilalchene (prodotto più stabile termodinamicamente) e le reazioni di idrolisi delle funzioni esteree non avvengono a temperatura ambiente, cosicché la selettività verso il *cis*-arilalchene viene notevolmente migliorata.

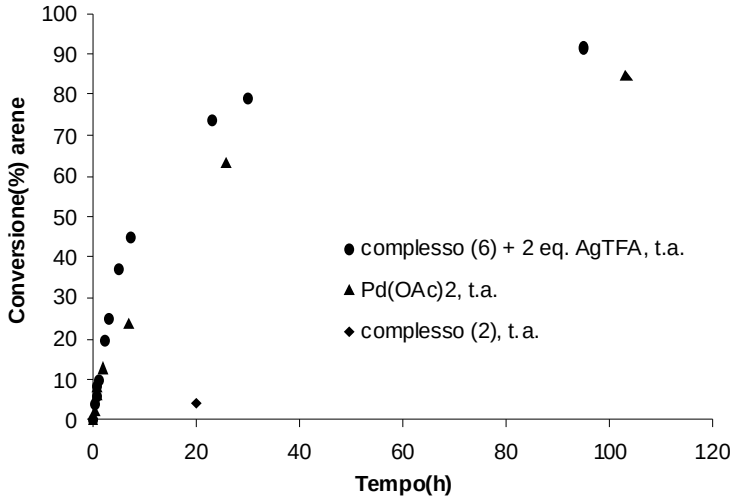

Figura 8 Diagramma di conversione(%) *vs* tempo per la reazione tra pentametilbenzene ed etil propiolato: effetto del sale di argento.

Infine, sono state determinate le condizioni sperimentali adatte per estendere questo protocollo sintetico ad eterocicli aromatici, ottenendo anche in questo caso elevate rese nei prodotti. La selettività della reazione verso il prodotto desiderato è però diminuita dalla formazione di addotti eterociclo/alchino 2/1 [13].

Analisi preliminari di tipo cinetico hanno inoltre dato una prima indicazione sul tipo di meccanismo coinvolto nella reazione, che non è ancora del tutto chiarito e che potrebbe coinvolgere la metallazione elettrofilica dell'arene [1b] oppure una alchenilazione di tipo Friedel-Crafts [14].

La legge cinetica è risultata essere del primo ordine in palladio e, nelle particolari condizioni dei reazione adottate, anche del primo ordine in arene o in alchino. Rimane da valutare la dipendenza della legge cinetica dalla concentrazione di acido, che sembra avere un ruolo importante nel meccanismo di reazione. Deve essere infatti utilizzato in largo eccesso rispetto ai substrati e probabilmente il suo ruolo principale è quello di idrolizzare la specie vinilica di palladio, proposta come intermedio catalitico in entrambi i cicli riportati in letteratura.

I complessi dicarbenici di palladio(II) e platino(II) sono stati testati anche in altre reazioni di funzionalizzazione di legami C-H aromatici, come l'*orto*-funzionalizzazione di acetanilidi [15].

References

[1] a) C. Jia, D. Piao, J. Oyamada, W. Lu, T. Kitamura, Y. Fujiwara, *Science* **2000**, *387*, 1992; b) Y. Fujiwara, C. Jia, W. Lu, J. Oyamada, T. Kitamura, K. Matsuda, M. Irie, *J. Am. Chem. Soc.* **2000**, *122*, 7252; c) C. Jia, T. Kitamura, Y. Fujiwara, *Acc. Chem. Res.* **2001**, *34*, 633; d) T. Kitamura, *Eur. J. Org. Chem.*, DOI: 10.1002/ejoc.200801054.

[2] a) W. Lu, C. Jia, T. Kitamura, Y. Fujiwara, *Org. Lett.* **2000**, *2*, 2927; b) J. Oyamada, W. Lu, C. Jia, T. Kitamura, Y. Fujiwara, *Chem. Lett.* **2002**, *1*, 20; c) M. L. Keita, T. Mizuhara, J. Oyamada, T. Kitamura, *Chem. Lett.* **2007**, *36*, 1150.

[3] a) J. Oyamada, C. Jia, Y. Fujiwara, T. Kitamura, *Chem. Lett.* **2002**, 380; b) T. Kitamura, K. Yamamoto, M. Kotani, J. Oyamada, C. Jia, Y. Fujiwara, *Bull. Chem. Soc. Jpn.* **2003**, *76*, 1889; c) M. Kotani, K. Yamamoto, J. Oyamada, Y. Fujiwara, T. Kitamura, *Synthesis* **2004**, *9*, 1466; d) J. Oyamada, T. Kitamura, *Tetrahedron* **2006**, *62*, 6918; e) K. Li, L. N. Foresee, J. A. Tunge, *J. Org. Chem.* **2005**, *70*, 2881; f) B. M. Trost, F. D. Toste, K. Greenman, *J. Am. Chem. Soc.* **2003**, *125*, 4518.

[4] a) J. Oyamada, T. Kitamura, *Chem. Lett.* **2005**, *34*, 1430; b) J. Oyamada, T. Kitamura, *Tetrahedron Lett.* **2005**, *46*, 3823; c) J. Oyamada, T. Kitamura, *Tetrahedron* **2006**, *62*, 6918; d) J. Oyamada, T. Kitamura, *Tetrahedron* **2007**, *63*, 12754.

[5] a) M. T. Reetz, K. Sommer, *Eur. J. Org. Chem.* **2003**, 3485; b) Z. Shi, C. He, *J. Org. Chem.* **2004**, *69*, 3669; c) Z. Li, Z. Shi, C. He, *J. Organomet. Chem.* **2005**, *690*, 5049; d) C. Ferrer, C. H. M. Amijs, A. M. Echavarren, *Chem. Eur. J.* **2007**, *13*, 1358.

[6] a) T. Tsuchimoto, T. Maeda, E. Shirakawa, Y. Kawakami, *Chem. Commun.* **2000**, 1573; b) C. E. Song, D.-u. Jung, S. Y. Choung, E. J. Roh, S.-g. Lee, *Angew. Chem. Int. Ed.* **2004**, *43*, 6183; c) M. Y. Yoon, J. H. Kim, D. S. Choi, U. S. Shin, J. Y. Lee, C. E. Song, *Adv. Synth. Catal.* **2007**, *349*, 1725; d) R. Li, S. R. Wang, W. Lu, *Org. Lett.* **2007**, *9*, 2219;

[7] a) D. Bourissou, O. Guerret, F. P. Gabbai, G. Bertrand, *Chem. Rev.* **2000**, *100*, 39; b) W. A. Herrmann, *Angew. Chem. Int. Ed.* **2002**, *41*, 1290; c) N. M. Scott, S. P. Nolan, *Eur. J. Inorg. Chem.* **2005**, 1815; d) S. P. Nolan, (Ed.), *N-Heterocyclic Carbenes in Synthesis* Wiley-VCH, Weinheim, **2006**; e) F. Glorius, (Ed.), N-Heterocyclic Carbenes in Transition Metal Catalysis, *Topics in Organometallic Chemistry*, Vol. 21, Springer, Heidelberg, **2007**.

[8] M. S. Viciu, E. D. Stevens, J. L. Petersen, S. P. Nolan, *Organometallics* **2004**, *23*, 3752.

[9] A. Biffis, C. Tubaro, G. Buscemi, M. Basato , *.Adv. Synth. Catal.* **2008**, *350*, 189.

[10] Article in preparation.

[11] G. Buscemi, A. Biffis, C. Tubaro, M. Basato, *Catal. Today* **2009**, *140*, 84.

[12] Article in preparation.

[13] Article in preparation.

[14] a) J. A. Tunge, L. N. Foresee, *Organometallics* **2005**, *24*, 6440; b) E. Soriano, J. Marco-Contelles, *Organometallics* **2006**, *25*, 4542.

[15] M. D. K. Boele, G. P. F. van Strijdonck, A. H. M. de Vries, P. C. J. Kamer, J. G. de Vries, P. W. N. M. van Leeuwen, *J. Am. Chem. Soc.* **2002**, *124*, 1586.

ABBREVIATIONS

A = area of the electrode (cm^2)

Ar = generic aryl ring

α = group next to an atom or electron transfer coefficient

c (or C^*) = concentration (or bulk concentration of the electroactive species) (M)

CV = cyclic voltammetry

D = diffusion coefficient ($cm^2\ s^{-1}$)

Dba = (E,E)-dibenzylideneacetone

DCE = 1,2-dichloroethane $ClCH_2CH_2Cl$

DCM = dichloromethane CH_2Cl_2

DFT = density functional theory

DMF = dimethylformamide $(CH_3)_2NCOH$

DMSO = dimethylsulfoxide $(CH_3)_2SO$

Δ = heat

E (V) = potential (Volt)

$E^{\ominus}$ (V) = standard potential (Volt)

$E^{0'}$ (V) = formal potential (Volt)

E_p (V) = peak potential (Volt)

E_{pa} (V) = anodic peak potential (Volt)

E_{pc} (V) = cathodic peak potential (Volt)

E_λ (V) = switching potential (Volt)

eq. = equivalents

Et = ethyl group (CH_3CH_2-)

ET = electron transfer

F ($C\ mol^{-1}$) = Faraday constant (Coulomb/mole)

Fc^+/Fc = redox couple ferricinium/ferrocene

HTFA = trifluoroacetic acid CF_3COOH

I (A) or i (A) = current (Ampère)

i_p (A) = peak current (Ampère)

i_{pa} (A) = anodic peak current (Ampère)

i_{pc} (A) = cathodic peak current (Ampère)

IPr = *N*,*N*'-bis(2,6-diisopropylphenyl)-imidazol-2-ylidene

k^0 = standard electron transfer rate constant

k_{ET} = electron transfer rate constant

Li^{n}Bu = *n*-butyl lithium

L =generic neutral ligand

M = metal

Me = methyl group (CH_3-)

n = number of electrons involved in an electrochemical process

NaH = sodium hydride

NEt_3 = triethylamine

NHC = N-heterocyclic carbene

NOE = Nuclear Overhauser Effect

v (V s^{-1})= scan rate (Volt/sec)

O = generic oxised species of a redox couple

OAc = acetate anion ($CH_3CO_2^-$)

OEt = ethoxy group (CH_3CH_2O)

OEt_2 = diethyl ether $(CH_3CH_2)_2O$

OTf = triflate anion ($CF_3SO_3^-$)

P = generic product

Ph = phenyl group (C_6H_5-)

PEt_3 = triethylphosphane

PPh_3 = triphenylphosphane

PR_3 = generic phosphane

p-Tol = 4-methylphenyl

R = generic alkyl group or generic reduced species of a redox couple

r.t. = room temperature

S-DOSP = *S*-(*N*-dodecylbenzenesulfonyl)prolinate

t_λ (sec) = switching time (seconds)

^{t}Bu = *tert*-butyl group $(CH_3)_3C$-

TFA= trifluoroacetate anion ($CF_3CO_2^-$)

X = generic anionic ligand

Y = generic electron-withdrawing group

CHAPTER 1
INTRODUCTION

1.1 Imidazolin-2-ylidene complexes

Imidazolin-2-ylidenes were introduced by Arduengo *et al.* in 1991 with the isolation and crystallisation of the first stable *N*-heterocyclic carbene (**Figure 1.1a)** [1]. This important breakthrough has stimulated considerable interest in this area of chemistry and new improved methodologies for the synthesis of stable nucleophilic carbenes have been subsequently reported [2].

Several families of stable carbenes are known to date, but only five-member cyclic diamino carbenes (NHCs) have found numerous applications, since they possess an unexpected stability mainly arising from the presence of α-amino groups. Theoretical and experimental reports have indeed proved that a charge-transfer from the carbenic carbon to the more electronegative neighbouring nitrogen atoms is present together with a simultaneous donation from the nitrogen lone pairs into the formally empty p(π) orbital of the carbenic carbon atom (**Figure 1.1b)** [3]. These effects, namely inductive and mesomeric effect, largely contribute to stabilise the carbenic atom.

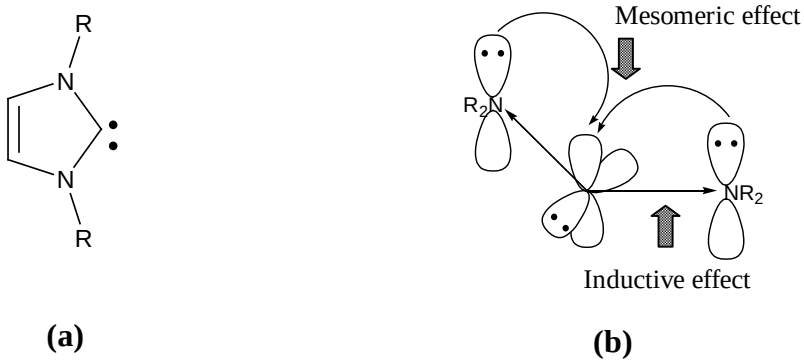

Figure 1.1 (a) General structure of NHC ligands;
(b) inductive and mesomeric effects in N-heterocyclic carbenes.

Additionally, it has been suggested that imidazolin-2-ylidenes present a certain aromatic character due to a cyclic electron stabilisation, which is however significantly smaller than the one of benzene or imidazolium salts [4].

Upon binding to transition metals these ligands exhibit strong σ-donor properties with negligible π-acceptor ability. This is also confirmed by their ability to coordinate both high- and low-valent transition metals (such as Ti^{IV}, Nb^{V}, Re^{VII} or Pd^{0}, Rh^{I}) or electron-poor cations such as Be^{2+} [5].

These characteristics render nucleophilic carbenes similar to electron-rich trialkylphosphanes, although the reactivity of the corresponding complexes is quite different. NHCs-complexes are indeed less sensitive than phosphane-complexes to air and moisture and have proved high resistance to thermal and oxidative conditions [6], thereby resulting in several reactions more active and robust catalysts with respect to their phosphane-based analogues. Moreover, they do not easily dissociate from the metal centre during a catalytic cycle; this avoids the necessity of excess ligand.

In catalysis, not only the stability of the catalyst but also the possibility to control the regio- and stereochemistry of the reaction is important; this is generally achieved modifying the catalyst structure through the appropriate choice of ligands. For this reason, phosphanes have been for many years the most widely used ligands in homogeneous transition metal catalysis, since it is possible to finely control both the steric and electronic properties at the metal centre by small changes in the phosphane structure. In this connection also NHC-complexes can be easily modulated in their characteristics, incorporating different groups on the nitrogen atoms or in the carbon backbone of the carbene.

Because of these peculiar properties, N-heterocyclic carbenes can be therefore successfully utilised in catalysis and they are usually not used as reactive fragments but as ancillary ligands, able to control and determine the activity and the selectivity of the catalyst.

For the preparation of metal carbene complexes two general procedures, involving the selective abstraction of the imidazolium H(2)-proton followed by metalation, are widely applied. One occurs through the preliminary isolation of free N-heterocyclic carbene that can be generated with various synthetic methods, among which the deprotonation of the imidazolium salt with a strong base (for example NEt_3, KO^tBu, Li^nBu, NaH...) [2] (**Figure 1.2**).

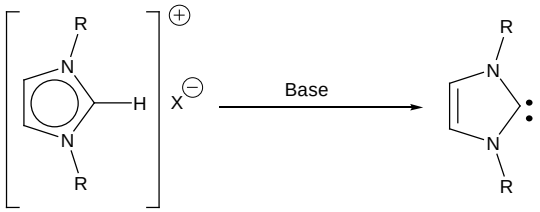

Figure 1.2 Deprotonation of imidazolium salt.

The second method avoids the pre-isolation of the free carbene by heating the corresponding imidazolium ligand with the anhydrous metal salt, in the presence of a deprotonating agent (which could even be the anion of the metal salt).

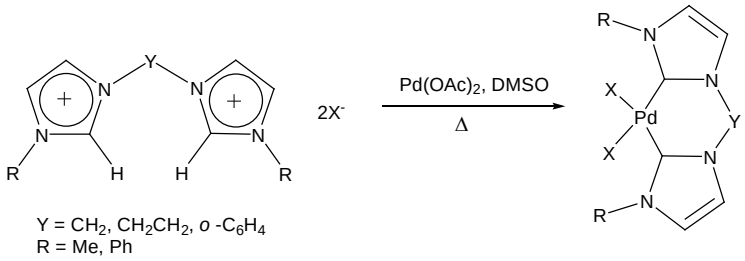

Figure 1.3 Synthesis of dicarbene complexes.

The procedure is particularly efficient for the preparation of dicarbene complexes, which have been synthesised in our laboratories by reacting the imidazolium salts with palladium(II) acetate (**Figure 1.3**) [7]; the acetate anion is indeed a basic ligand which is able to deprotonate the CH group and *in situ* generate free carbenes that can subsequently react to give the corresponding complexes. An analogue procedure is applicable to obtain Pt(II) dicarbene complexes; in this case Pt halide as metallic precursor and two equivalents of sodium acetate as deprotonating agent are used.

1.2 Catalytic applications of chelating dicarbene complexes: aromatic C-H bond functionalisation reactions

Thanks to the ability of N-heterocyclic carbenes to stabilise highly reactive organometallic species [4, 8] many research groups have been recently interested in the catalytic properties of NHC-complexes, founding that a large number of them are efficient catalysts in several metal-catalysed transformations, such as for example olefin metathesis [9], hydrosilylations [10], hydrogenations and hydrogen transfer reactions [11].

However, the applicability of these complexes has been predominantly evaluated in transition-metal catalysed C-C coupling reactions [11e, 12], that are at present one of the most important reaction classes for the synthesis of pharmaceutical agents, organic materials and natural products. In particular the Heck [13] and the Suzuki–Miyaura [14] reactions have been developed up to a very high degree of synthetic utility (**Figure 1.4**).

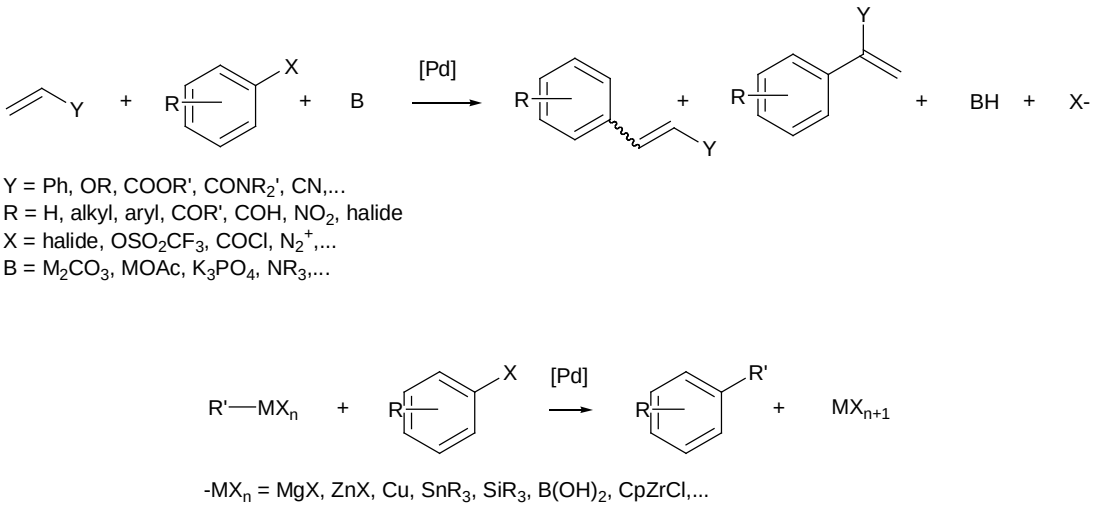

Figure 1.4 Heck (above) and cross-coupling (below) reactions; the Suzuki reaction is a cross-coupling reaction with arylboronic acids as the organoelement reagent.

The major drawbacks of such methodologies are the need to use aryl bromides or iodides as reagents, more reactive but also more costly and less widely available than the corresponding chlorides, and the co-production of salt wastes. Because of these disadvantages, synthetic chemists are looking for alternative cheaper and cleaner

routes for the synthesis of organic molecules. In this context, the direct functionalisation of an aromatic C-H bond would be the preferable way, since it involves an environment-friendly chemical transformation requiring no-halogen-containing substrates.

The initial limitation of these procedures is due to the high strength of the C-H bond, which is therefore difficult to cleave directly (105 kcal/mol in methane and 110 kcal/mol in benzene). An important breakthrough was carried out after the discovery that organotransition-metal complexes are capable to catalyse the direct functionalisation of C-H bonds [15]. The interest towards the metal-mediated routes has been so increased and numerous reviews have subsequently appeared [16]. These reactions usually occur under relatively mild conditions and aromatic hydrocarbons usually react faster than alkanes, even if they possess a greater C-H bond strength.

Three main types of C-H activation/functionalisation mechanisms have been reported in the literature [17]:

1) Metal-through-Ligand Activation (MeLA):

In this mechanism the metal centre coordinates an organic species **(1.1)**, which therefore becomes active enough to react with a substrate breaking the C-H bond **(1.2)**. Some authors define this kind of mechanism as *C-H Functionalisation*, since it does not involve the formation of a σ C-M bond.

$$A\text{-}B + L_nM \rightarrow L_nM(A\text{-}B) \qquad \textbf{(1.1)}$$

$$L_nM(A\text{-}B) + R\text{-}H \rightarrow L_nM + R\text{-}(A\text{-}B)\text{-}H \quad (\text{or } R\text{-}A(H)\text{-}B) \qquad \textbf{(1.2)}$$

An example is represented by the coordination of a diazo derivative N_2=C(R)R' to the metal and successive insertion of the metal-carbene fragment M=C(R)R' into the C-H bond of an organic moiety [18] (**Figure 1.5**). In this specific case the driving force of the reaction comes from the production of N_2, which accompanies the formation of the reactive carbenic intermediate.

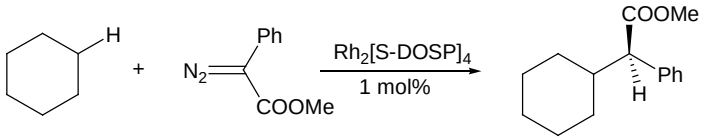

Figure 1.5 Example of a reaction between an organic species and a diazo derivative N_2=C(R)R'.

2) Metal-Initiated Activation (MIA):

The role of the metal complex is simply to generate a reactive species able to attack the C-H bond **(1.3)**. The best example of this kind of mechanism is represented by Fenton's reagent: a Fe complex catalyses the oxidation of hydrocarbons through the use of H_2O_2 or O_2. Involvement of radical species implies, as expected, poorly selective reactions.

$$H_2O_2 + Fe^{2+} \rightarrow HO\cdot + HO^- + Fe^{3+} \qquad \textbf{(1.3)}$$

$$HO\cdot + RH \rightarrow HOH + R\cdot$$

$$R\cdot + O_2 \rightarrow ROO\cdot$$

$$ROO\cdot + Fe^{2+} \rightarrow ROO^- + Fe^{3+}$$

$$ROO^- + H^+ \rightarrow ROOH$$

3) True Organometallic Activation (TOA):

In general this mechanism involves the substitution of H in the C-H bond with the metal centre, forming a direct σ C-M bond. This is achieved through three different routes: *Oxidative Addition*, *Electrophilic Substitution*, *σ-Bond Metathesis*.

Oxidative Addition	$R\text{-}H + M^{n+} \rightarrow R\text{-}M^{(n+2)+}\text{-}H$
Electrophilic Substitution	$R\text{-}H + M^{n+} \rightarrow R\text{-}M^{(n-1)+} + H^+$
σ-Bond Metathesis	$R\text{-}H + X\text{-}M^{n+} \rightarrow R\text{-}M^{n+} + X\text{-}H$

The *oxidative addition* pathway occurs with electron rich metal centres, which are capable to coordinate a hydrocarbon and transfer two electrons on the antibonding C-H molecular orbital. This causes C-H bond breaking and coordination of the formed

R and H fragments to the metal. The crucial step of this mechanism is the coordination of the hydrocarbon, thus a vacant coordination site on the metal is necessary. Unsaturated hydrocarbons are better nucleophiles than saturated ones and are therefore more coordinating and easily activated for the reaction.

The *intramolecular oxidative addition* way allows to overcome the difficult step involving the C-H metal interaction, through the use of an electron-withdrawing group Y able to anchor the metal centre (**Figure 1.6**); this functionality increases the hydrogen acidity thus favouring the C-H activation. However, this process results obviously limited in scope.

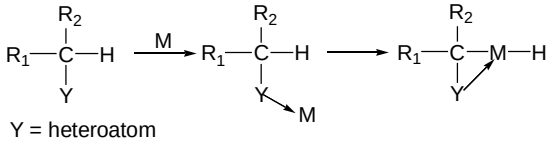

Figure 1.6 Intramolecular oxidative addition through the use of a directing group.

The *electrophilic substitution* mechanism requires, instead, electron poor metal centres capable of replacing the proton on the C-H group. The metal reacts with an arene affording the cationic Wheland intermediate, whereas with alkanes it generates a high energy activated complex (**Figure 1.7**).

Figure 1.7 Electrophilic substitution mechanism with arenes and alkanes.

The Shilov reaction represents the first historical example of this kind of C-H activation and it involves the oxidation of CH_4 to CH_3OH catalysed by a Pt(II)

complex; unfortunately the reaction suffers of low selectivity and the oxidant is an expensive Pt(IV) complex. More recently a new synthetic method (the "Catalytica system") for the same reaction has been developed, which utilises oleum as oxidant and as reaction medium, affording sulphuric acid methyl ester which can be easily hydrolysed to methanol [16i].

In this specific case the electrophilic activation step is favoured by the double positive charge on the complex. Also the results obtained by Strassner's group has confirmed the validity of this procedure; in this case potassium peroxodisulfate is used as oxidant and Pd(II) or Pt(II) dicarbene complexes are employed as catalysts [19] (**Figure 1.8**).

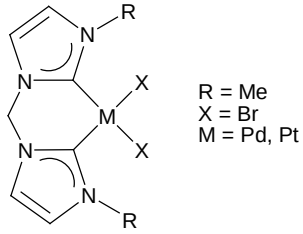

Figure 1.8 Pd(II) and Pt(II) dicarbene complexes utilised in the oxidation of methane to methanol.

The σ-*Bond Metathesis* mechanism, instead, concerns the transfer of an hydrogen atom from an organic moiety to one metal ligand, in a concerted fashion involving a four centre and four electron transition state (**Figure 1.9**).

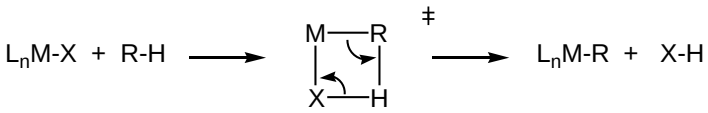

Figure 1.9 General example of a σ-*Bond Metathesis* mechanism.

This route does not imply a change in the formal oxidation state of the metal centre and for this reason it is similar to the electrophilic substitution way.

CHAPTER 2
C-H BOND FUNCTIONALISATION REACTIONS

2.1 Background of C-H bond functionalisation reactions

The catalytic formation of C-C bonds by C-H functionalisation is a topic of much current interest and significant progresses have been made in the last years, especially regarding the addition of arenes to unsaturated molecules. This synthetic process is very attractive and useful for both agricultural and pharmaceutical businesses and has the advantage to be a more environmentally benign methodology with respect to the conventional methods, such as for example the Heck-type reactions. A large number of stoichiometric reactions are known in the literature [20], while the catalytic systems available to date are still few [21]. From one side, the chelate-assisted oxidative addition of aromatic C-H bonds to metal centres in low oxidation state (e.g. Ru(0)) has been exploited [21, 22]. The mechanism involves the previous coordination of an arene chelating group to the metal and the subsequent oxidative addition of an *ortho* C-H bond, affording a σ-arylruthenium(II) intermediate (**Figure 2.1**).

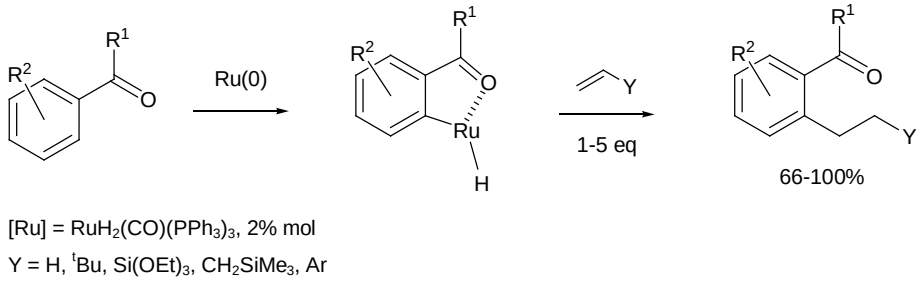

Figure 2.1 Chelate-assisted oxidative addition of an olefin to an aromatic ring.

This intermediate can subsequently transfer the aryl to an unsaturated organic molecule, such as an olefin, through a mechanism involving olefin insertion followed by reductive elimination of a formal olefin hydroarylation anti-Markovnikov product.

The reaction is obviously limited to functionalised arenes, as aromatic ketones, and it only occurs at high temperatures (135 °C) with a low stereoselectivity when alkynes are used as substrates.

The second strategy is based on an electrophilic arene metalation reaction with the formation of σ-arylmetal complexes, effected by metal centres such as for example Pd(II) [21, 23]. The reaction takes place without chelating directing groups on the arene reagent, although the presence of such groups may contribute to increase the selectivity of the reaction. The mechanism involves olefin insertion and β-elimination, yielding a formal olefin *trans*-arylation product and a metal hydride species which subsequently decomposes to Pd(0) (**Figure 2.2**).

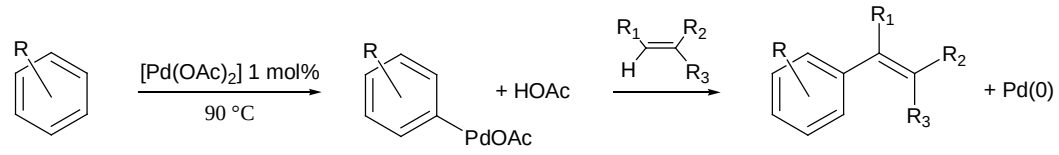

Figure 2.2 Oxidative coupling of olefins to arenes.

Therefore, the presence in the reaction environment of stoichiometric species capable of reoxidising Pd(0) to Pd(II) is necessary and further complicates the reaction. In spite of the numerous proposed oxidising systems, among others benzoquinone/^{t}BuOOH [21, 23], benzoquinone/O_2 [24], benzoic acid/O_2 [25], the efficiency of the process is actually still too low for viable industrial applications.

Simple Pd(II) compounds, such as $Pd(OAc)_2$, in an acidic environment can also promote the reaction of arenes with alkynes at room temperature [23, 26]. In this case, however, products of formal hydroarylation of the triple bond are formed and the proposed catalytic cycle does not involve changing in the oxidation state of the metal, so the use of oxidants is not required.

2.2 Intermolecular hydroarylation of alkynes

There are several examples of alkynes addition to aromatic rings catalysed by transition metals [27]. Some of these reactions involve a true *C-H activation* mechanism, in which an interaction of the arene with the metal is present. However, in most cases there is no formation of a σ C-M bond, so in this context the term "*C-H functionalisation*" is preferred.

The first example of a C-H bond activation reaction was reported by Yamazaki *et al.* [28]. They described the addition of benzene to diphenylacetylene catalysed by $Rh_4(CO)_{12}$ (1 mol%) under CO pressure to give triphenylethylene and 2,3-diphenylindenone (**Figure 2.3**). The proposed mechanism implies the initial oxidative addition of the benzene C-H bond to the Rh(0) catalyst, giving the Rh(II) H-Rh-Ph species. Subsequently, insertion of the alkyne into Rh-Ph bond occurs, followed by reductive elimination to give the product. The major drawbacks of such reaction are the severe conditions (220 °C) and the low selectivity in the case of mono-substituted arenes.

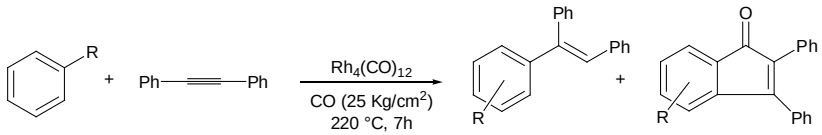

Figure 2.3 Addition of alkynes to arenes catalysed by $Rh_4(CO)_{12}$.

Regarding the processes not involving a change in the oxidation state of the metal, different mechanistic proposals have been formulated for the hydroarylation of alkynes depending on the catalyst system but, in general, two main reaction pathways are reported in the literature (**Figure 2.4**) [29].

In one pathway the hydroarylation reaction proceeds *via* σ-arylmetal species **2**, generated through electrophilic metalation of the arene with metal cationic species **1** (**path A**). The second pathway involves, instead, the previous coordination of the alkyne to the metal, which is therefore activated enough to react with the arene substrate (Friedel-Crafts mechanism, **path B**). Both these mechanism involve a metal-vinyl intermediate **4**, which is protonolysed by an H^+, derived from the arene or in some cases by an added acid, to give the final product.

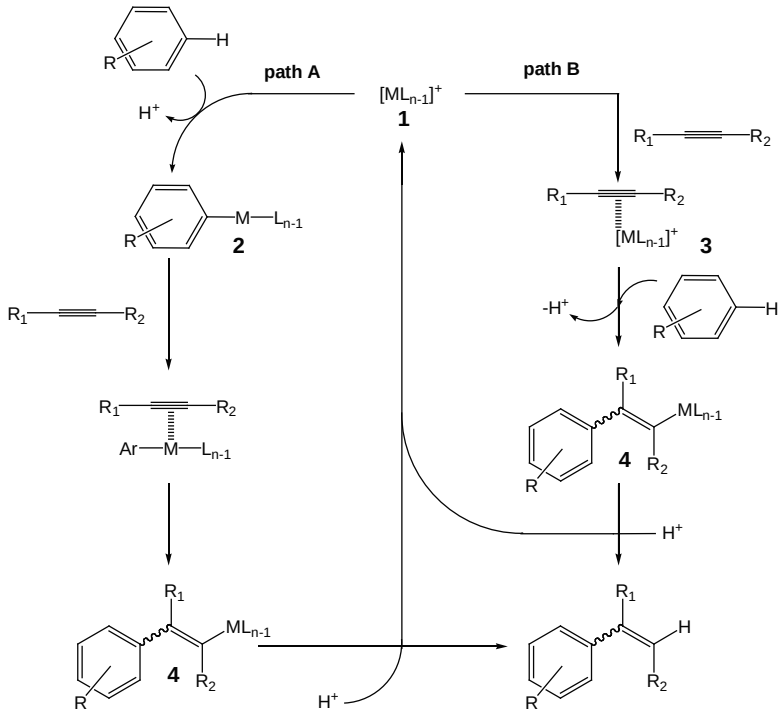

Figure 2.4 Proposed pathways for the hydroarylation of alkynes.

In the hydroarylation of alkynes catalysed by 10 mol% metal triflates (M = Sc, Zr, In) at 85 °C a Friedel-Crafts mechanism is suggested (**Figure 2.5**) [29-30]. The presence of both stereoisomer *E* and *Z* at the initial stage of the reaction indicates, moreover, that the reaction does not proceed *via* a concerted mechanism (**path a**), but through a vinyl cationic intermediate (**path b**). Oligomerisation of the alkyne is an important collateral reaction because of the instability of the vinyl cationic intermediate **3** reported in **Figure 2.4**.

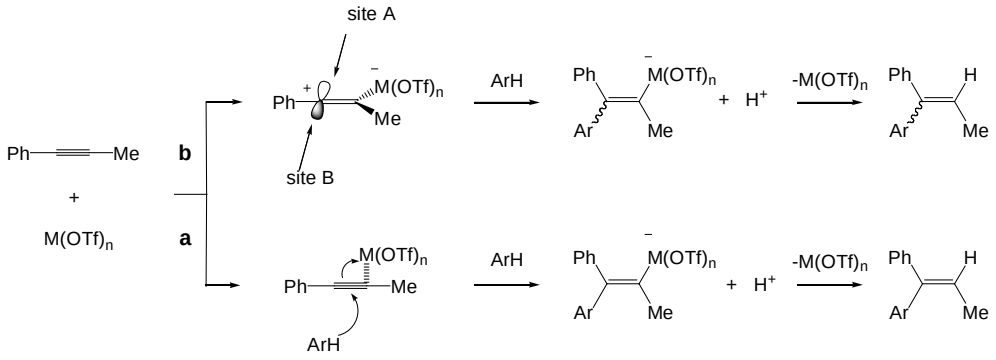

Figure 2.5 Possible pathways for the hydroarylation of alkynes catalysed by metal triflates. M = Sc, Zr, In.

Also $FeCl_3$ in CH_3NO_2 catalyses the alkenylation of electron-rich arenes with aryl-substituted alkynes, under mild conditions and 10 mol% catalyst load [31]. Like in the case of early-groups metal triflates, the use of an acid is not necessary and the reaction goes through a Friedel-Crafts pathway; this procedure is however quite limited in scope, being applied at the moment only to aryl-acetylenes.

Recently, Reetz and Sommer have reported that the present reaction is also catalysed by Au(III) or Au(I) salts in the presence of silver additives [32]. The catalytic system $AuCl_3$(1.5mol%)/2$AgSbF_6$ is the most efficient catalyst in the case of terminal aryl-substituted alkynes, whereas [Au(PEt_3)Cl] or [Au(PPh_3)Cl] (1 mol%) activated with $AgSbF_6$ or $BF_3{\cdot}OEt_2$ (5 mol%) are superior when electron-poor terminal alkynes are used. In the case of internal electron-poor alkynes no reaction is observed. Also with these systems, the use of strong acids is not necessary and the reaction occurs in CH_3NO_2 with good yields at 50-60 °C. Although the reaction mechanism is still not clear, the authors have proposed the coordination of the alkyne to the metal forming a π-complex which undergoes a kind of electrophilic aromatic substitution with the arene (**Figure 2.4 path B**). Therefore, the metal exclusively acts as a Lewis acid to increase the electrophilicity of the alkyne. Similar results have been reported with an $AuCl_3$(2.5mol%)/3AgOTf system at room temperature and under solvent-free conditions; in this case the authors have suggested a different reaction mechanism involving the direct metalation of the arene forming an arylgold intermediate (**Figure 2.4 path A**) [33].

In all these examples, the regio- and stereochemistry is similar and governed by the set of substituents on the alkyne. In fact, alkyl- and aryl-alkynes usually react to form 1,1-disubstituted alkenes, whereas terminal alkynes conjugated to electron-withdrawing groups give 1,2-disubstituted alkenes. Moreover, electron-rich arenes are the most reactive giving elevated yields in the products.

Dinuclear palladium complexes at 2 mol% loading (**Figure 2.6**) in the presence of trialkylboranes are also efficient catalysts for this reaction at 100 °C [34], *via* a mechanism involving an electrophilic C-H activation of the arene. Trialkylborane seems to serve as a hydride source to convert hydroxo-bridged complexes into hydrido-bridged complexes.

In this case the major product is the *trans*-arylalkene, indicating that *cis*-addition is more kinetically favoured, and the reaction does not occur with mononuclear palladium complexes, $Pd(OAc)_2$ and $Pd_2dba_3 \cdot CHCl_3$.

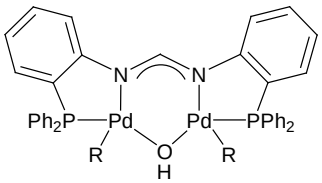

R = *p*-Tol or Me

Figure 2.6 Dinuclear palladium complexes $Pd_2R_2(\mu\text{-OH})(\mu$-dpfam). dpfam = *N*,*N*'-bis[2-(diphenylphosphino)phenyl]-formamidinate.

Differently from the catalytic systems described above, electron-deficient arenes are the most active and terminal alkynes are not reactive in the reaction.

2.3 The Fujiwara reaction [26]

The Fujiwara reaction involves the hydroarylation of a wide range of internal and terminal alkynes, catalysed by simple Pd(II) and Pt(II) compounds [26, 35]. In contrast with the previously described catalytic systems it exclusively occurs in a strong acidic environment. It is a very advantageous reaction since it requires the minimal number of reactants and "low-energy" starting materials as substrates, fulfilling the basic principles of atom economy. Moreover, it is also very interesting from the economic point of view being achievable under acceptable thermodynamic conditions such as mild temperatures and low pressures.

Unlike the "Heck reactions", it does not afford waste products and in most cases it presents a high and quite unusual regio- and stereoselectivity towards the thermodynamically unfavourable product *cis*-arylalkene (**a**, **Figure 2.7**).

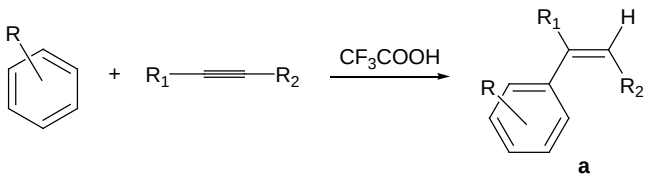

Figure 2.7 The Fujiwara reaction.

All these factors render the reaction very advantageous over the other methods available to synthesise such molecules and it has been defined as *"the most general and efficient method for the one-step hydroarylation of internal and terminal alkynes by simple arenes"* by Pfeffer [21a] and *"among the most expansive in terms of scope of aromatic and alkyne substrates that can be successfully transformed into functionalised aromatic products"* by Gunnoe [21d].

The reaction mechanism originally proposed by Fujiwara (**Figure 2.8**, **left cycle**) involves highly electrophilic Pd(II) and Pt(II) cationic species (**A**), generated *in situ via* reaction with trifluoroacetic acid [26].

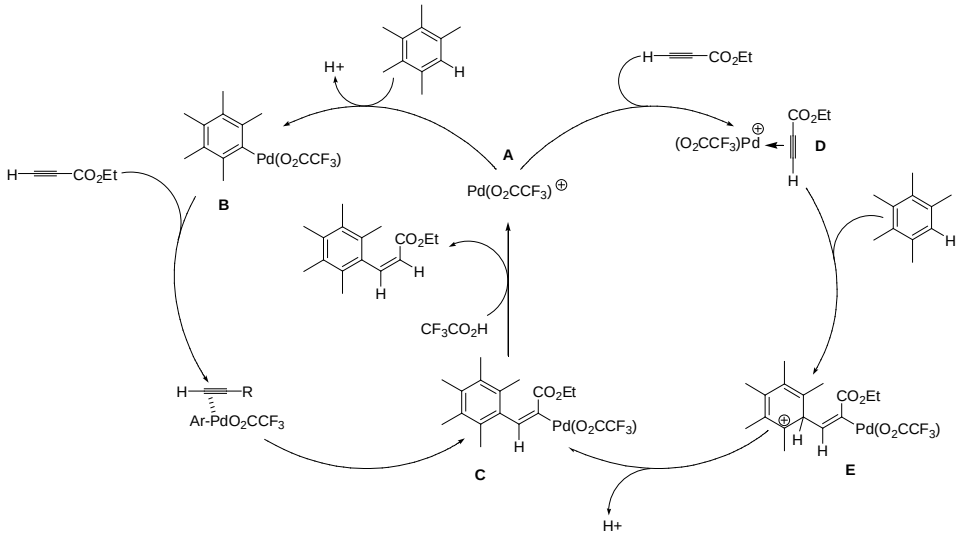

Figure 2.8 Proposed mechanisms for the Fujiwara reaction.

It is believed that such cationic species are sufficiently activated to form σ-arylpalladium(II) complexes after metalation of the aromatic C-H bond. The formation of these complexes has been supported by ^{1}H-NMR studies showing the fast disappearance at room temperature of the aryl hydrogen of pentamethylbenzene in the presence of 1 eq. of $Pd(OAc)_2$ in HTFA, and by isotopic experiments which tend to exclude the involvement of a Pd(II) insertion into the C-H bond of terminal alkynes, as well as the involvement of vinylidene complexes [26b].

Such complexes are supposed to be intermediates also in the coupling of arenes with olefins [23] and arenes with aryl halides, as proposed by Fagnou and co-workers [36]. Both intra- and intermolecular versions of this last reaction involve oxidative addition of the aryl halide to the metal, forming a σ-arylintermediate which subsequently attacks the arene through an electrophilic metalation reaction. It has been demonstrated that this process occurs through a σ-bond metathesis mechanism when electron-withdrawing groups are present on the arene, whereas electron-donating groups favour a concerted electrophilic aromatic substitution involving an external base B (**Figure 2.9**).

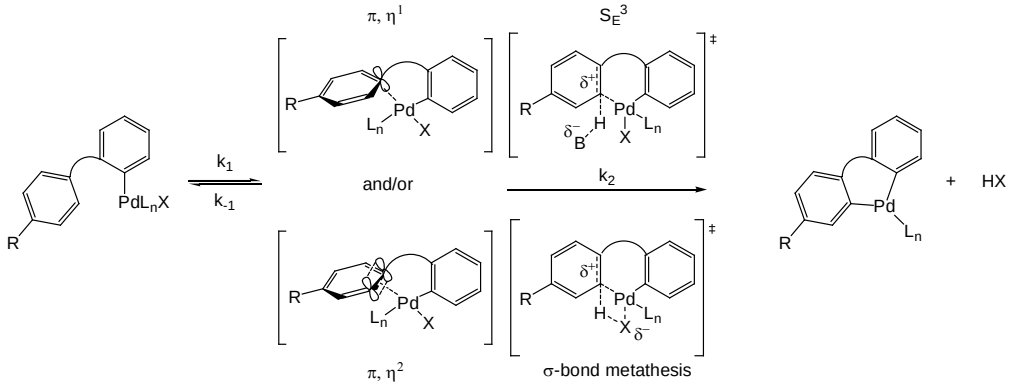

Figure 2.9 Electrophilic aromatic substitution and σ-bond metathesis pathways in the coupling of arenes with aryl halides.

However, coming back to the Fujiwara reaction, the subsequent alkyne insertion in the σ-arylcomplex (**B**, **Figure 2.8**) occurs in an unusual *trans* fashion leading to a Pd-vinyl complex (**C**), which is then hydrolysed by HTFA giving the catalytic species $Pd(O_2CCF_3)^+$ **A** and the hydroarylation product. The reaction does not occur in less acidic solvents, such as acetic acid, and it is necessary a large amount of HTFA to improve the yields.

This mechanistic proposal is in contrast with subsequent studies of Tunge [37a] and Marco-Contelles [37b] based on kinetic isotope effects, which suggest a preliminary coordination/electrophilic activation of the alkyne (**Figure 2.8**, **right cycle**), so that the attribution to a TOA (*True Organometallic Activation*) or MeLA (*Metal-through-Ligand Activation*) mechanism is not sure. In this second hypothesis the electrophile

is an alkyne-metal complex (**D**) that attacks the arene leading to the Pd-vinyl complex (**C**); therefore, in this case, there is not a direct interaction of the arene with the metal. Finally, protonolysis of the Pd-vinyl bond liberates the product and regenerates the catalyst.

As previously mentioned, the reaction is highly selective towards the *cis*-arylalkene **a**, but small percentages of other products, like the alkyne double-insertion product (**c**, **Figure 2.10**), are also observed.

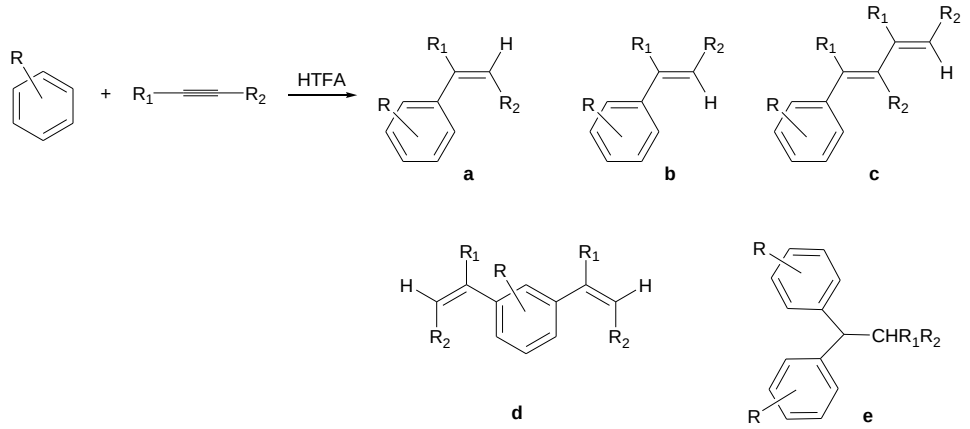

Figure 2.10 Possible products in the Fujiwara hydroarylation of alkynes.

This product comes from a second insertion of the alkyne on the palladium-vinyl complex (**Figure 2.11**) [26b], which is an intermediate proposed in both the mechanisms shown in **Figure 2.8**.

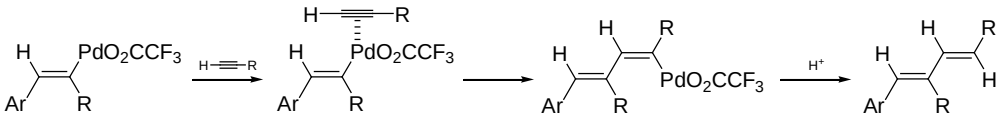

Figure 2.11 Proposed mechanism for the formation of product **c** in **Figure 2.10**.

In other cases, isomerisation of the major product to give more thermodynamically stable products (*trans*-arylalkenes **b**, **Figure 2.10**) occurs. When alkoxyarenes are used as substrates, the formation of adducts 2/1 arene/alkyne (**e**, **Figure 2.10**) is

obtained, further lowering the selectivity of the reaction. These adducts come from the addition of an arene molecule to the 1/1 product and their formation is mainly influenced by the coordination ability of the arene substituents. However, the yields in 1/1 or 2/1 adducts can be controlled by varying the reaction time and the concentration of catalyst. Indeed, using 1 mol% palladium acetate adduct 2/1 is the secondary product of the reaction, whereas using 5 mol% $Pd(OAc)_2$ the 2/1 adduct becomes the main product. Use of the catalytic system $PtCl_2$/2AgOAc, (or 2AgOTf) instead, totally suppresses formation of 2/1 adducts increasing the selectivity of the reaction towards the desired product; however, this latter catalytic system performs a lower activity than the Pd(II)-based one [35]. Furthermore, arenes with more than one C-H bond available for the functionalisation can afford double-hydroarylation products as **d** (**Figure 2.10**).

In general, the efficiency of the reaction is enhanced by increasing the number of electron-donating substituents on the arene and by the presence of electron-withdrawing groups, such as CHO, COMe, CO_2H, CO_2Me, CO_2Et on the alkyne, thus displaying characteristics of an electrophilic substitution. The nature of the substituents on the alkyne has a considerable effect on the regioselectivity of the reaction as well; indeed, internal alkynes with phenyl groups react to give α-arylalkenes, whereas alkynes conjugated with electron-withdrawing groups provide β-aryl substituted alkenes.

Moreover, steric hindrance at the arene is not limiting for the reaction, since pentamethylbenzene is the substrate which reacts more rapidly with several alkynes. The reaction is therefore driven by the electronic properties of the arene rather than by steric effects; this is in contrast with other Pd-catalysed reactions such as the Heck reaction.

The Fujiwara reaction appears a very promising synthetic process, being a simple and economic method to form *cis*-arylalkenes in one step. Moreover, the inter- and intramolecular [29, 30b, 31, 38] version of the reaction, upon reacting propiolic acids or esters with phenols, gives the possibility to synthesise in high yields coumarins, which are natural products of great interest in pharmaceutical industry. The process is also applicable to other substrates such as aromatic heterocycles, providing addition products with high conversions and selectivities [39].

However, a potential industrial application requires the optimisation of the reaction conditions; indeed the reaction is often quite slow and it usually needs 1-5 mol% palladium, which heavily affects the cost of the process; moreover, an excess of arene is often needed to enhance conversions and selectivities. Although other metal centres have been used as catalyst in the hydroarylation of alkynes, the turnover numbers of these processes are not exceedingly high.

A solution to improve this methodology could be the use of complexes with ligands capable to increase the stability of the catalyst under the reaction conditions as well as its reactivity. N-heterocyclic carbene ligands [40] appear particularly suited to this purpose, in fact it is known that their Pd(II) complexes possess a high thermal and hydrolytic stability, even under the strongly acidic conditions necessary for this reaction [19a, 19b]. Not surprisingly, monocarbene Pd(II) complexes $(IPr)Pd(OAc)_2$ and $(IPr)Pd(OOCCF_3)_2$ (IPr = *N*,*N*'-bis(2,6-diisopropylphenyl)-imidazol-2-ylidene) have been reported to be active in the Fujiwara reaction in the absence of other promoters, although their activity is comparable to that of simple $Pd(OAc)_2$ [42]. Their selectivity is even superior to the one given by palladium acetate, because the formation of dienes is not observed with these complexes.

AIM OF THE PROJECT

The present research project involves the individuation of novel catalysts for carbon-carbon coupling reactions, with the primary aim to significantly improve the synthetic method for the technological application of the process in fine chemistry.

The attention has been focused on complexes possessing chelating N-heterocyclic carbene ligands in view of their promising characteristics of stability under harsh reaction conditions [19a, 19b, 41].

Our research group has already been interested in the catalytic application of transition metal carbene complexes, which have been tested in other catalytic reactions such as Heck reactions and C-N and C-O coupling [7b, 7d]. The goal of this thesis is to expand their applications to novel reactions as the C-H functionalisation reactions [21], which have recently achieved a promising development.

The steric and electronic properties of the complexes have been systematically modulated through choice of metal (Pd, Pt) and by ligand design (**Figure 1**).

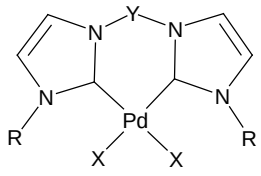

R = Me, Ph
X = Cl, Br, I, TFA
Y = methylene, *o*-phenylene, *o*-xylylene, *m*-xylylene

Figure 1 General structure of complexes with chelating N-heterocyclic ligands.

In particular, these properties have been properly tuned by changing:

a) the nature of the heterocyclic ring (imidazole, benzimidazole);
b) the nature of the bridge between the two carbene groups (Y);
c) the nature of the nitrogen substituents in the carbene groups (R);
d) the nature of the anionic ligands (X).

With regard to the Fujiwara reaction [26], the objectives of the project are:

- Optimisation of the reaction conditions (catalyst load, temperature, solvent, co-catalysts) using palladium(II) dicarbene catalysts.
- Application of such an optimised catalyst to explore the generality and regio- and stereoselectivity of the synthesis as a function of the nature of the reagents and of the catalyst.
- Extension of the synthetic protocol to other compounds such as aromatic heterocycles [39].
- Systematic evaluation of the steric and electronic properties of the complexes on their catalytic efficiency and identification of an optimal catalyst both in terms of nature of the dicarbene ligand and of the anionic ligands.
- Electrochemical characterisation of the complexes and of the corresponding imidazolinium precursors, for which literature reports are rather lacking [51, 52, 76, 78] to evaluate their electronic properties and support the catalytic results obtained in the Fujiwara reaction.
- Identification of the catalytically active species through mechanistic and electrochemical studies.
- Investigation on the reaction mechanism through kinetic studies to gain information useful for modelling better catalytic systems.

Another part of the study concerns the extension of this investigation to other aromatic C-H bond activation reactions correlated to the Fujiwara reaction, as the *ortho*-functionalisation of anilides with olefins, reported by van Leeuwen *et al.* [66a].

CHAPTER 3
THE FUJIWARA REACTION

3.1 Preliminary optimisation of the reaction conditions [43]

The complexes utilised in this study are shown in **Figure 3.1**. Some of them are known in the literature whereas others have been prepared in our laboratories according to standard procedures [44, 19c].

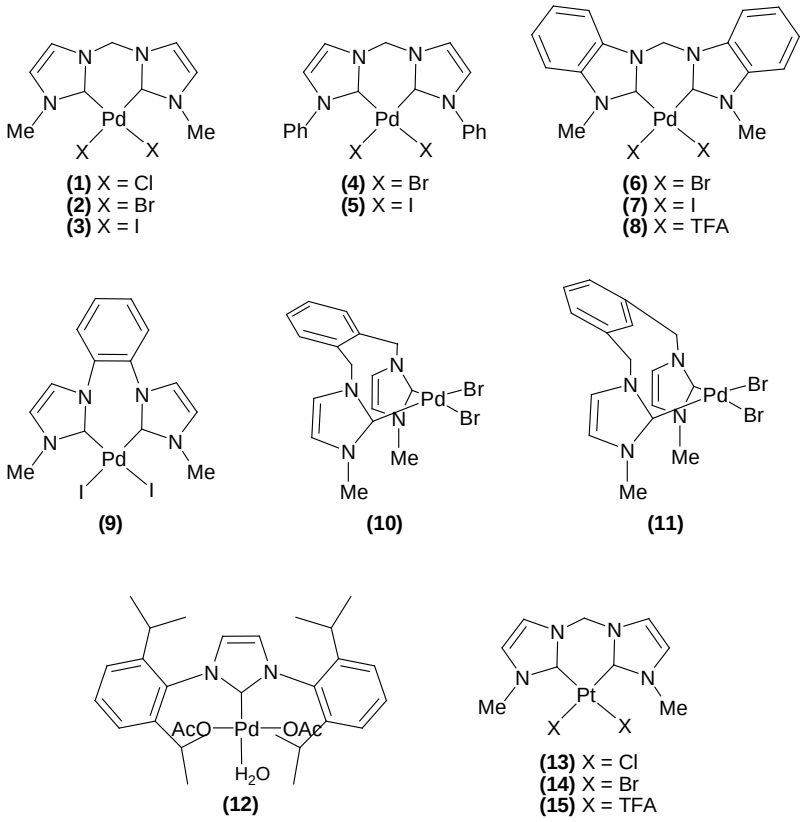

Figure 3.1. Library of palladium(II) and platinum (II) complexes employed in the work.

The standard reaction between pentamethylbenzene and ethyl propiolate (**Figure 3.2**) has been initially considered, since it gives elevated yields with palladium acetate [26b] and the arene has only one C-H bond available for activation, thus simplifying the interpretation of the data.

The reaction conditions usually employed by Fujiwara *et al.* have been initially adopted (1 eq. alkyne, 2 eq. arene, 0.01 eq. catalyst, solvent: CF_3COOH/CH_2Cl_2 4mL/1mL, room temperature, 20h).

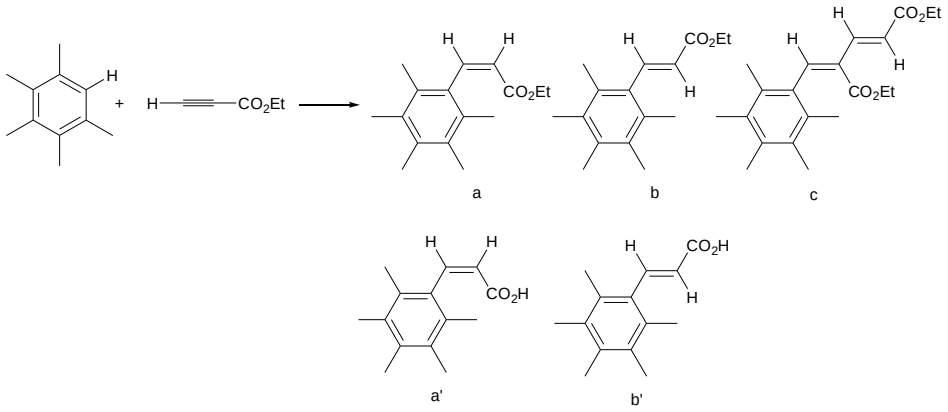

Figure 3.2 Possible reaction products in the reaction between pentamethylbenzene and ethyl propiolate.

Table 3.1 Conversion(%) for the reaction between pentamethylbenzene and ethyl propiolate under Fujiwara's conditions

Complex	Time(h)	Arene/Alkyne conversion(%)[a]	Yield(%)[a]		
			a	b	c
(2)	20	4/4	4	-	-
$[Pd(OAc)_2]$[26b]	2	91/97	85	-	6

Reaction conditions: 0.03 mmol catalyst, 3 mmol alkyne, 6 mmol arene, solvent: CF_3COOH/CH_2Cl_2 = 4mL/1mL, room temperature. [a] Conversions(%) and yields(%) determined by ^{1}H-NMR. For more details see the Experimental Section.

Under these conditions the conversion has amounted to only 4% with complex **(2)** (**Table 3.1**), albeit with complete selectivity towards the *cis*-product **a**, whereas palladium acetate gives 91% arene conversion and 93% selectivity [26b] (the minor product is the diene **c**, **Figure 3.2**).

This is a clear evidence that the reaction is not catalysed by trifluoroacetic acid alone. Instead, employing stronger acids as triflic acid, the reaction goes also in the absence of a metal centre [45]. Other strong acids (HBF_4, HSO_3F-SbF_5, CF_3SO_3H-SbF_5,

$HAlBr_4$) do not catalyse the reaction with ethyl propiolate, but promote the hydroarylation of phenyl-acetylenes [46].

By increasing the reaction temperature to 80 °C and by replacing dichloromethane with 1,2-dichloroethane all dicarbene complexes have given very high conversions and selectivities towards the *Z* product (**a** + **a'**), other products being the *E* isomer (**b** + **b')** and the product of double alkyne insertion (**c**) (see **Figure 3.2**).

Table 3.2 Conversion(%) for the reaction between pentamethylbenzene and ethyl propiolate catalysed by 1 mol% different dicarbene palladium(II) complexes at 80 °C. Arene/alkyne ratio = 2/1.

Complex	Arene/Alkyne conversion(%)[a]	Yield(%)[a]			Selectivity(%) in a
		a/a'	b/b'	c	
(1)	98/98	49/33	10/6	-	50
(2)	96/98	54/28	9/3	2	58
(3)	84/96	45/17	7/3	12	53
(5)	100/100	84/9	6/1	-	84
(7)	97/100	73/15	5/1	3	75
(9)	92/92	84	8	-	91

Reaction conditions: 0.0265 mmol catalyst, 2.65 mmol alkyne, 5.3 mmol arene, solvent: CF_3COOH/DCE = 4mL/1mL, 80 °C, 20h. [a] Conversions(%) and yields(%) determined by GC-MS and/or ^{1}H-NMR. For more details see the Experimental Section.

At 80 °C some side-products, identified as hydrolysed *cis*- and *trans*-products (**a'** and **b'**) have been observed, thus decreasing the selectivity of the reaction towards the desired product **a**. The hydrolysed products can be removed from the product mixture after the basic workup reported in the literature [26b], giving the corresponding salts which remain in the aqueous layers. To calculate the yield of every product, the workup has been avoided in the subsequent experiments and the yields have been calculated by simply analysing by ^{1}H-NMR small portions of solution, drawn off from the reaction mixture.

The subsequent optimisation of the catalyst amount and of the reaction time has been carried out mainly with complexes possessing bromides as anionic ligands, since

bromide is expected to be more easily displaced than iodide [47]. This expectation is also supported by the results of Strassner *et al.* with related palladium(II) and platinum(II) complexes, whose reactivity in the methane C-H activation reaction is markedly enhanced on going from iodide to bromide complexes [19a, 19b, 41].

To optimise the catalyst load, an experiment has been made using only 0.1 mol% complex **(6)** and again very high conversion (96%) and selectivity (86%) towards the *Z* product (**a** + **a'**) have been obtained after 20h.

Optimisation of the reaction time has been carried out under these new reaction conditions determining the conversion curve (**Figure 3.3**).

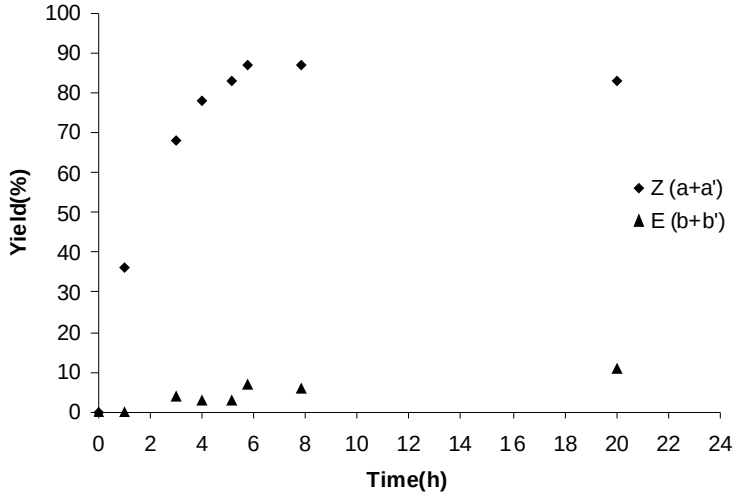

Figure 3.3 Yields(%) in the main products *vs* time diagram for the reaction between pentamethylbenzene and ethyl propiolate catalysed by complex **(6)**. Reaction conditions: 0.00265 mmol catalyst, 2.65 mmol alkyne, 5.3 mmol arene, solvent: CF_3COOH/DCE = 4mL/1mL, 80 °C.

It is evident from the figure that the reaction is very fast during the first five hours, reaching 88% arene conversion with 93% selectivity; after this time there is a slow but continuous increase in the concentration of the *E* product, due to a background isomerisation process which decreases the selectivity of the reaction towards the *Z* product.

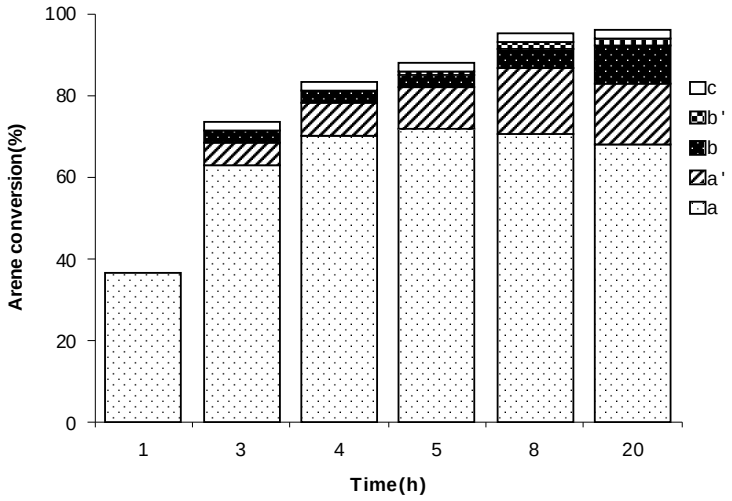

Figure 3.4 Products conversion(%) *vs* time diagram for the reaction between pentamethylbenzene and ethyl propiolate catalysed by complex **(6)**. Reaction conditions: see **Figure 3.3**.

Table 3.3 Time course of the reaction between pentamethylbenzene and ethyl propiolate catalysed by 0.1 mol% complex **(6)**. Arene/alkyne ratio = 2/1.

Time(min)	Arene/Alkyne conversion(%)[a]	Yield(%)[a] a/a'	b/b'	c	Selectivity(%) in a
60	36/36	36/-	-	-	100
180	74/76	63/6	3/-	2	85
240	83/85	70/8	3/-	2	84
310	88/90	72/10	3/1	2	82
345	95/97	70/16	5/2	2	74
470	96/98	71/16	5/2	2	74
1200	96/98	68/15	9/2	2	71

Reaction conditions: 0.00265 mmol catalyst, 2.65 mmol alkyne, 5.3 mmol arene, solvent: CF_3COOH/DCE = 4mL/1mL, 80 °C. [a] Conversions(%) and yields(%) determined by ^{1}H-NMR. For more details see the Experimental Section.

In conclusion, longer reaction times cause an increase in the amounts of by-products because of hydrolysis of the ester function and thermally induced *cis/trans*

isomerisation of the main reaction product *Z*. The concentration of the double insertion product **c**, instead, remains almost constant during the reaction (**Figure 3.4** and **Table 3.3**).

After these preliminary results, in which reaction times and catalyst loading have been optimised, it is apparent that the reaction could be run in just 5 hours with only 0.1 mol% catalyst. In **Table 3.4** results obtained under these new reaction conditions are reported.

Table 3.4 Conversion(%) for the reaction between pentamethylbenzene and ethyl propiolate catalysed by 0.1 mol% different dicarbene palladium(II) complexes. Arene/alkyne ratio = 2/1.

Complex	Arene/Alkyne conversion(%)[a]	Yield(%)[a]			Selectivity(%) in a
		a/a'	b/b'	c	
(1)	78/78	68/6	2/2	-	87
(2)	88/88	79/7	2	-	90
(3)	89/91	76/8	3	2	85
(4)	96/96	86/8	2	-	90
(6)	85/87	75/6	2	2	88
[$Pd(OAc)_2$]	42/45	36/1	1/1	3	86

Reaction conditions: 0.00265 mmol catalyst, 2.65 mmol alkyne, 5.3 mmol arene, solvent: CF_3COOH/DCE = 4mL/1mL, 80 °C, 5h. [a] Conversions(%) and yields(%) determined by GC-MS and/or ^{1}H-NMR. For more details see the Experimental Section.

All the dicarbene complexes tested have exhibited high reactivities and selectivities, both higher than the ones observed with palladium acetate tested in the same reaction conditions. In this preliminary screening, complex **(4)** has resulted to be the most active and the most selective dicarbene catalyst.

It has been also noticed that use of excess arene is not necessary in order to achieve good results (**Table 3.5**), although the reaction rate is slower: 60% conversion with 92% selectivity for the *Z* product has been obtained after 5 hours using catalyst **(6)** with only 1 eq. of pentamethylbenzene, compared to 85% conversion but 88% selectivity obtained using 2 eq. of pentamethylbenzene (**Table 3.4**).

Table 3.5 Conversion(%) for the reaction between pentamethylbenzene and ethyl propiolate catalysed by 0.1 mol% different dicarbene palladium(II) complexes. Arene/alkyne ratio = 1/1.

Complex	Arene/Alkyne conversion(%)[a]	Yield(%)[a]			Selectivity(%)
		a/a'	b/b'	c	in a
(1)	70/71	61/7	1/-	1	87
(2)	66/67	56/7	2	1	85
(3)	62/63	53/6	2	1	85
(4)	75/76	65/7	2	1	87
(5)	75/77	64/6	2/1	2	85
(6)	60/62	55/1	2	2	92
(10)	43/47	32/6	1	4	74
(11)	51/53	43/4	2	2	84

Reaction conditions: 0.00265 mmol catalyst, 2.65 mmol alkyne, 2.65 mmol arene, solvent: CF_3COOH/DCE = 4mL/1mL, 80 °C, 5h. [a] Conversions(%) and yields(%) determined by GC-MS and/or ^{1}H-NMR. For more details see the Experimental Section.

A close examination of the data reported in **Table 3.5** reveals, moreover, that all the analysed complexes exhibit more or less the same catalytic activity, except complexes **(10)** and **(11)** which display a significantly lower reactivity.

Complex **(6)** has been therefore chosen as standard catalyst to continue the optimisation of the reaction conditions.

3.2 Optimisation of the solvent

Further experiments have been carried out to optimise the nature of the solvent system made out of trifluoroacetic acid and an organic solvent, usually 1,2-dichloroethane, added in order to help the dissolution of the reagents. The choice of alternative organic solvents is however restricted to dimethylsulfoxide or acetonitrile because of the scarce solubility of the catalyst in the other ones. The use of coordinating solvents such as DMSO has given worse results, lowering the conversion from 73% to 23% under our standard reaction conditions (4.28 mmol arene, 4.28 mmol alkyne, 0.00428 mmol complex **(6)**, 80 °C, 5h). This is probably due to the strong coordination of DMSO molecules to the metal, which deactivates

the complex. Moreover, it has been confirmed that excess trifluoroacetic acid is fundamental, as in Fujiwara's case. Using CF_3COOH/DCE = 1mL/4mL the conversion is indeed halved, whereas selectivity remains high (94%).

3.3 Optimisation of the reagent concentration

Other investigations have been set out in order to evaluate how a variation of the concentration of substrates affects the performance of the catalytic system.

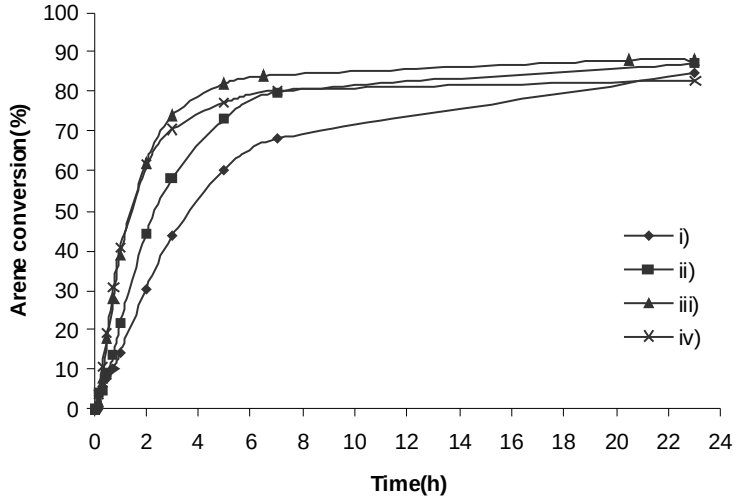

Figure 3.5 Conversion(%) *vs* time diagram for the reaction between pentamethylbenzene and ethyl propiolate catalysed by complex **(6)** at different concentrations of organic reagents.
i): arene = alkyne (0.5 M, 2.65 mmol), catalyst (0.1%). Molar ratio HTFA/substrates = 20/1.
ii): arene = alkyne (0.8 M, 4.28 mmol), catalyst (0.1%). Molar ratio HTFA/substrates = 12/1.
iii): arene = alkyne (1.4 M, 7.94 mmol), catalyst (0.1%). Molar ratio HTFA/substrates = 7/1.
iv): arene = alkyne (2.1 M, 13.25 mmol), catalyst (0.1%). Molar ratio HTFA/substrates = 4/1.
Conversions(%) determined by ^{1}H-NMR. Reaction conditions: see the Experimental Section.

The ratio between the concentrations of arene, alkyne and catalyst **(6)** has been kept constant at 1:1:1000 and the absolute concentration of the organic reagents has been varied between 0.5 M and 2.1 M.

It is apparent from the curves reported in **Figure 3.5** that the conversion at prolonged reaction times (23h) is the same irrespective of the concentrations employed. On the other hand, at shorter reaction times the conversion at a given time increases with increasing concentration. It is important to notice that the initial reaction rate remains constant for concentrations greater than 1.4 M because presumably, above such

concentration of substrates, the amount of trifluoroacetic acid becomes limiting for the reaction rate; this fact further confirms the need of using a large excess acid to improve the yields and additional studies have been started during a parallel master thesis in our research group [48] in order to understand the role of trifluoroacetic acid in greater detail.

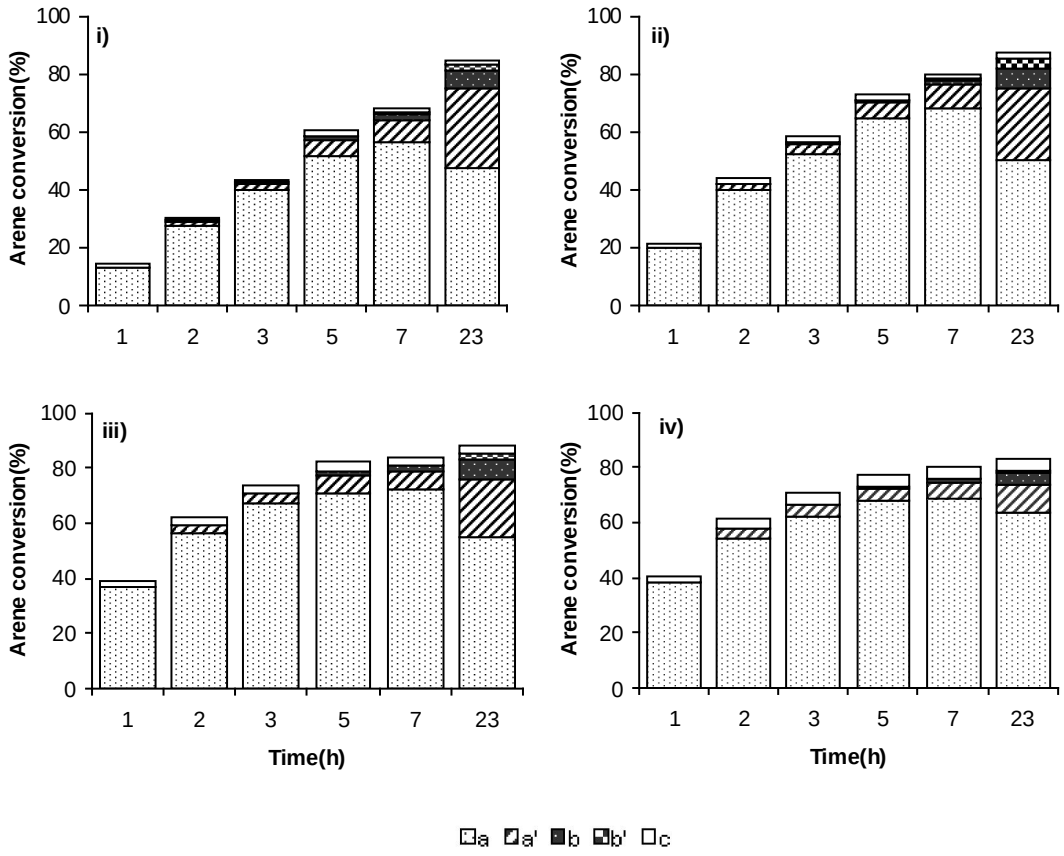

Figure 3.6 Products distribution for the reaction between pentamethylbenzene and ethyl propiolate catalysed by complex **(6)** at different concentrations of organic reagents.

Most importantly, looking at the composition of the product mixture at different concentrations and reaction times, it is apparent that the overall selectivity of the reaction increases at higher reagent concentration, the incidence of hydrolysis/isomerisation products becoming lower (**Figure 3.6**).

3.4 Optimisation of the reaction temperature

Subsequently, the reaction temperature has been optimised. Given that at room temperature the catalytic cycle does not proceed at a significant rate (see results listed in **Table 3.1**), a comparison has been made between reactions carried out at 50 and at 80 °C. In **Figure 3.7** the conversion profiles, obtained at the two temperatures with catalyst **(6)**, are reported. As expected, the reaction rate at 50 °C is much lower than at 80 °C, but it still allows to reach high conversions in reasonable reaction times.

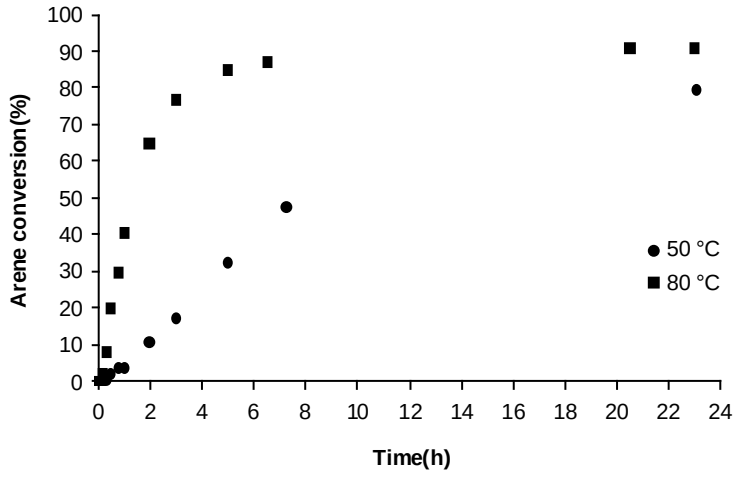

Figure 3.7 Conversion(%) *vs.* time diagram for the reaction between pentamethylbenzene and ethyl propiolate catalysed by complex **(6)** at different temperatures. Reaction conditions: arene (7.94 mmol, 1.4 M), alkyne (7.94 mmol, 1.4 M), catalyst (0.0079 mmol, 1.4 mM), CF_3COOH/DCE = 4mL/1mL.

Most notably, the overall selectivity of the catalytic system is much better at 50 °C than at 80 °C (**Figure 3.8**). In fact, hydrolysis and isomerisation reactions of the main product are significantly reduced.

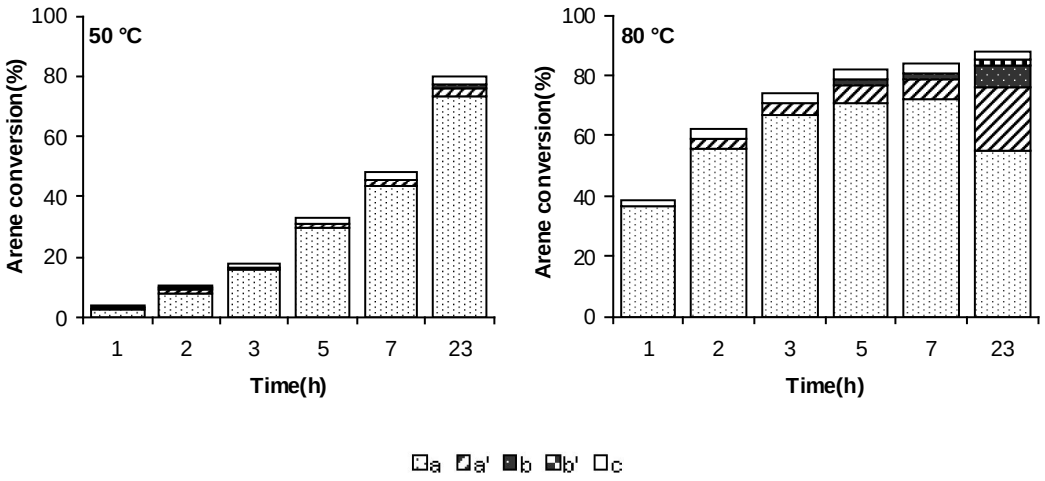

Figure 3.8 Products distribution for the reaction between pentamethylbenzene and ethyl propiolate catalysed by complex **(6)** at different temperatures.

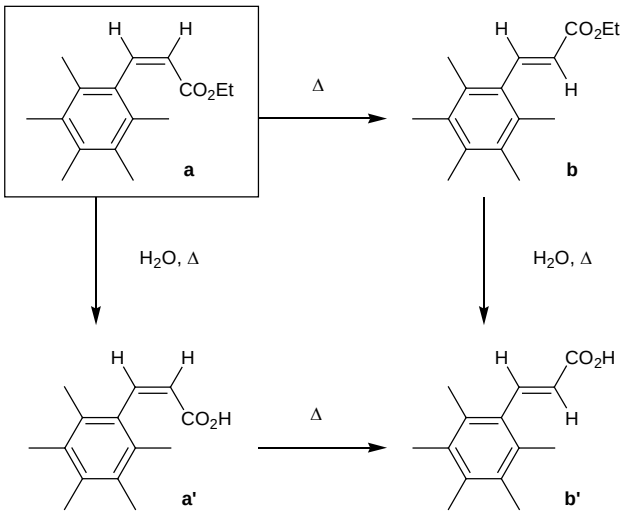

Figure 3.9 Evolution reactions (isomerisation and hydrolysis) of the main hydroarylation product **a** under catalytic conditions.

In **Figure 3.9** evolution reactions (isomerisation and hydrolysis) of the main hydroarylation product **a** are shown. Higher temperatures favour the *cis*/*trans* isomerisation process, thereby decreasing the selectivity of the reaction. Traces of water present in the reaction mixture can, moreover, react with ester functions of the main products giving the corresponding cinammic acids **a'** and **b'**.

In conclusion, at the end of this preliminary study, the reaction can be performed in high yields and selectivities at 80 °C for 5 hours with stoichiometric reagents and using only 0.1 mol% catalyst.

3.5 Study on the structure of the catalyst [49]

On the basis of the previous investigations, the catalytic efficiency of the studied complexes has appeared in all cases superior to $Pd(OAc)_2$ (see **Table 3.4**). However, more detailed experiments have been performed, determining the conversion curves of complex **(6)**, complex **(12)** and $Pd(OAc)_2$ under the optimised reaction conditions in order to compare more directly their efficiency (**Figure 3.10**). The hydroarylation reaction between pentamethylbenzene and ethyl propiolate has been employed also in this case as standard test reaction.

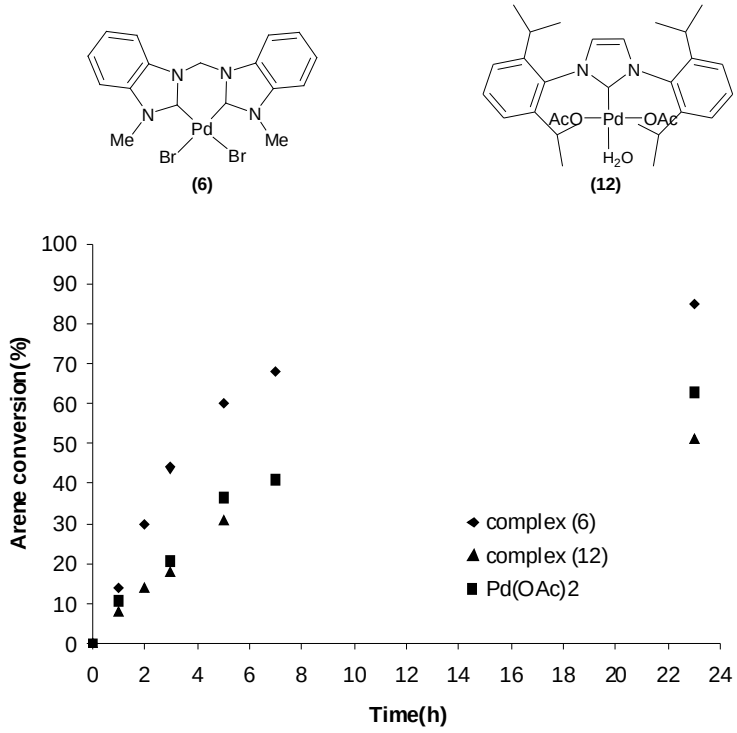

Figure 3.10 Conversion(%) *vs.* time diagram for the reaction between pentamethylbenzene and ethyl propiolate catalysed by complex **(6)**, complex **(12)** and $Pd(OAc)_2$. Reaction conditions: 0.00265 mmol catalyst, 2.65 mmol alkyne, 2.65 mmol arene, solvent: CF_3COOH/DCE = 4mL/1mL, 80 °C.

Dicarbene complex **(6)** has been found to be the most efficient catalyst for the reaction, with an initial activity almost two times higher than that of both $Pd(OAc)_2$ and monocarbene palladium complex **(12)** [44g], which expectedly forms Nolan's bis(trifluoroacetate) complex *in situ* [42] (**Figure 3.10**). The high reactivity of N-heterocyclic dicarbene complexes in this reaction is probably due to their elevated stability in the reaction conditions (high temperatures and acidic environment).

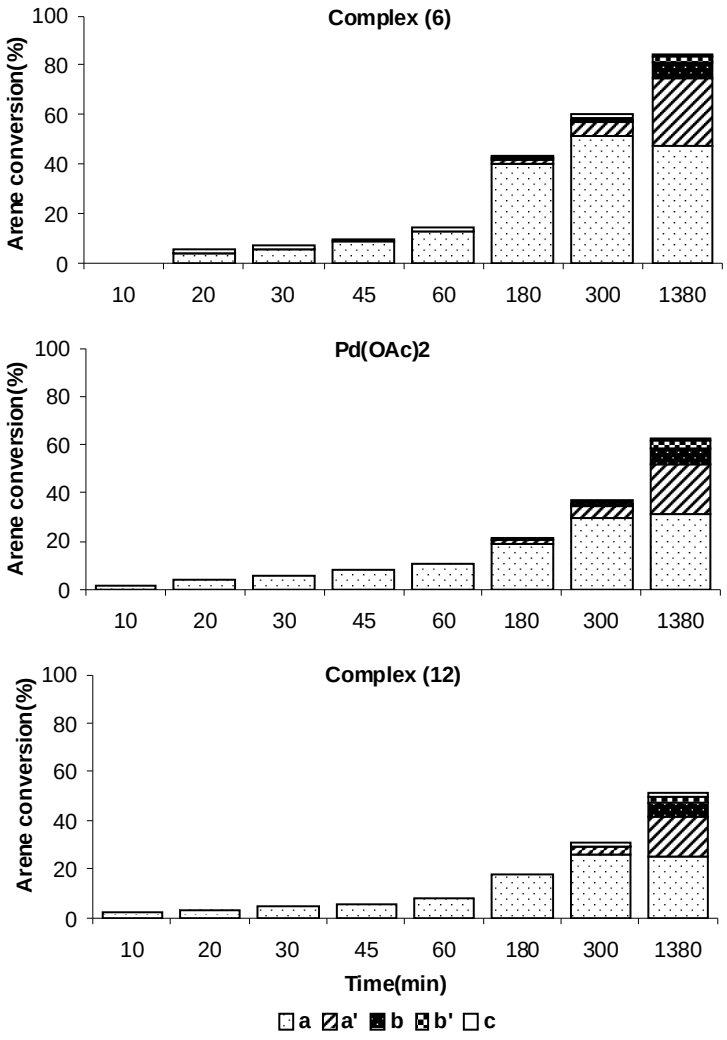

Figure 3.11 Products distribution for the reaction between pentamethylbenzene and ethyl propiolate catalysed by complex **(6)**, complex **(12)** and $Pd(OAc)_2$. Reaction conditions: see **Figure 3.10**.

Looking at **Figure 3.11**, it is evident that the highest yields in the *cis*-product **a** are obtained after 5 hours of reaction. After this time, complex **(6)** has given namely 60% arene conversion, while $Pd(OAc)_2$ has given only 37% conversion and complex **(12)** 31% conversion. The selectivity of the reaction is very similar in these three cases, but it appears to be however slightly influenced by the steric hindrance at the metal (87% selectivity for complex **(6)**, 84% for complex **(12)** and 78% for $Pd(OAc)_2$ after 5h).

Having established the high catalytic efficiency of complex **(6)**, a series of chelating dicarbene palladium(II) complexes, characterised by different sets of dicarbene and anionic ligands (**Figure 3.12**), have been tested as catalysts. The comparison of their efficiency has been made determining also in this case the conversion curves.

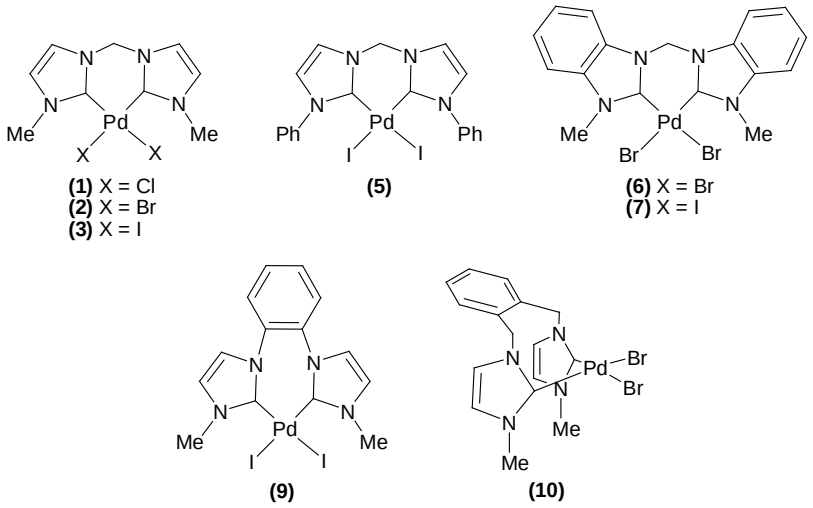

Figure 3.12 Palladium(II) dicarbene complexes employed as catalysts in this study.

3.6 Effect of the anionic ligand

Conversion curves for complexes possessing the same dicarbene ligand and different halide ligands have been firstly determined (**Figure 3.13** and **3.14**), in order to evaluate how the nature of the anionic ligand influences the activity of the complex.

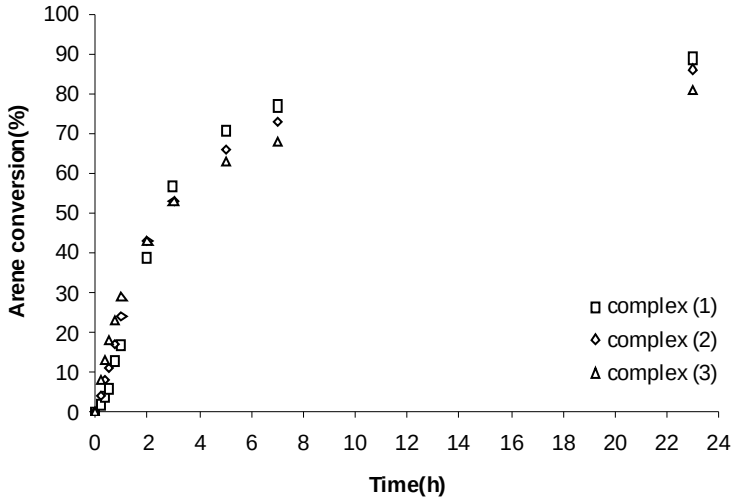

Figure 3.13 Conversion(%) *vs.* time diagram for the reaction between pentamethylbenzene and ethyl propiolate catalysed by complexes **(1)-(3)**. Reaction conditions: 0.00265 mmol catalyst, 2.65 mmol alkyne, 2.65 mmol arene, solvent: CF_3COOH/DCE = 4mL/1mL, 80 °C.

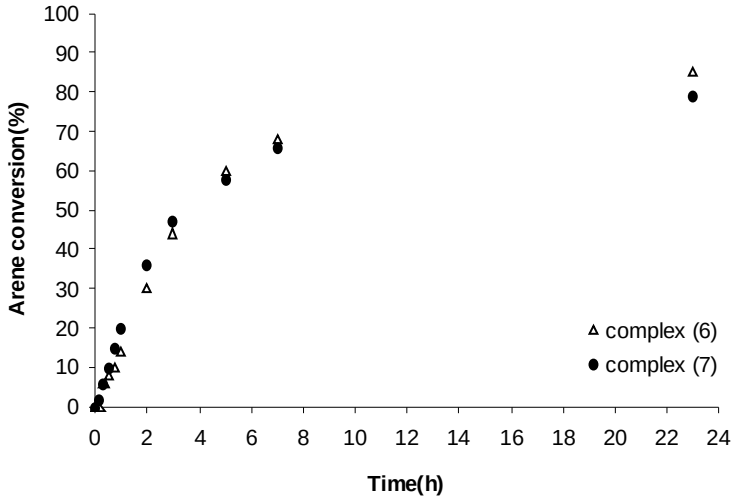

Figure 3.14 Conversion(%) vs. time diagram for the reaction between pentamethylbenzene and ethyl propiolate catalysed by complexes **(6)** and **(7)**. Reaction conditions: 0.00265 mmol catalyst, 2.65 mmol alkyne, 2.65 mmol arene, solvent: CF_3COOH/DCE = 4mL/1mL, 80 °C.

The catalytic activity displayed by complexes **(1)-(3)** (**Figure 3.13**) and by complexes **(6)** and **(7)** (**Figure 3.14**) has resulted comparable within the margin of experimental error, irrespective of the nature of the halide counterion, thereby demonstrating that this influence is very small. These results strongly support the

hypothesis that the actual catalytically active species do not contain halide ligands, which at 80 °C are removed through exchange with trifluoroacetate anions of the solvent. This experimental evidence is in agreement with DFT calculations, performed by Strassner *et al.*, which have predicted that replacement of the two halides by trifluoroacetate anions takes place at high temperatures. Moreover they have demonstrated that the binding energy difference between the various halides and the metal is not large enough to produce effects on the kinetic outcome of the reaction (**Figure 3.15**) [19b].

B3LYP/6-311+G(d,p) calculated free energies (kcal/mol) for the replacement of the halogen ligands by trifluoroacetic acid.

	First replacement	**Second replacement**	**Overall reaction**
F	-2.8	+1.2	-1.6
Cl	+11.1	+3.5	+14.7
Br	+14.1	+6.3	+20.4
I	+16.8	+9.2	+26.0

Figure 3.15 Free energies values calculated by Strassner *et al.*

Considering for example complexes **(1)**, **(2)**, **(3)** (**Figure 3.16**) the catalytically active species is therefore the same, so that selectivity of the reaction is very similar.

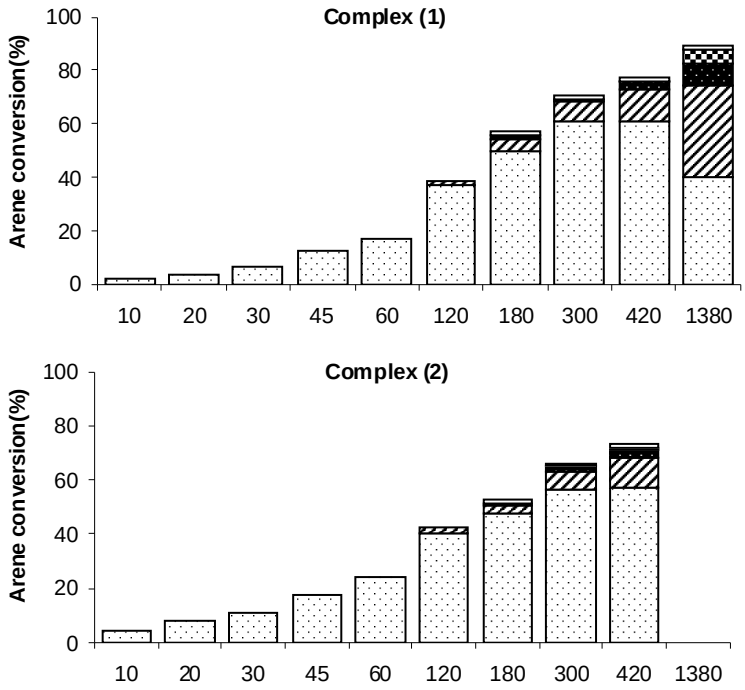

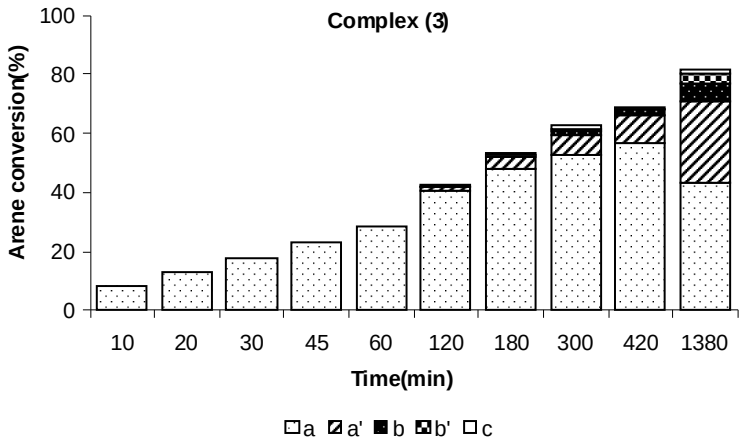

Figure 3.16 Products distribution for the reaction between pentamethylbenzene and ethyl propiolate catalysed by complexes **(1)-(3)**. Reaction conditions: see **Figure 3.13**.

3.7 Effect of the dicarbene ligand

Subsequently, a comparison among the activity of a series of complexes with the same anionic ligand but different dicarbene ligand has been made in order to elucidate the influence of the dicarbene ligand on the catalytic activity of the complex.

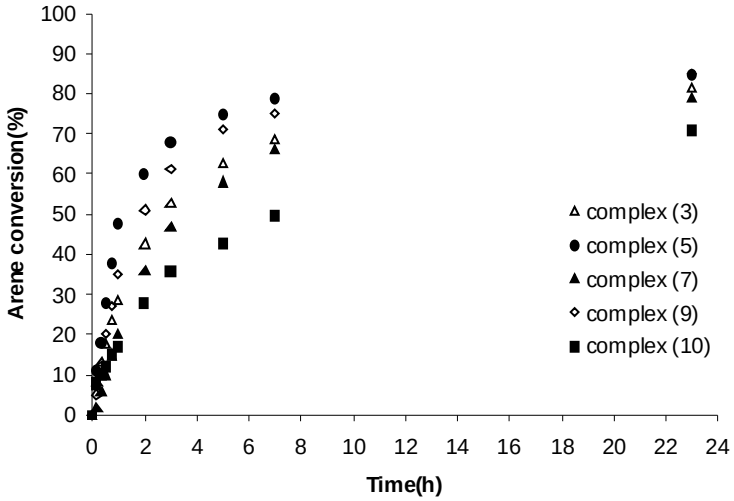

Figure 3.17 Conversion(%) *vs.* time diagram for the reaction between pentamethylbenzene and ethyl propiolate catalysed by complexes **(3)**, **(5)**, **(7)**, **(9)**, and **(10)**. Reaction conditions: 0.00265 mmol catalyst, 2.65 mmol alkyne, 2.65 mmol arene, solvent: CF_3COOH/DCE = 4mL/1mL, 80 °C.

Analysis of conversion curves (**Figure 3.17**) reveals that all complexes perform in similar manner over long reaction times (23h), reaching comparable conversions. However, during the first 5 hours of reaction, the catalytic performances are quite different and, in particular, it turns out that complexes with the more hindering NHC ligands **(5)** and **(9)** present higher activities.

These results suggest that the actual catalytically active species still contains the dicarbene ligand, which influences the reactivity of the catalyst.

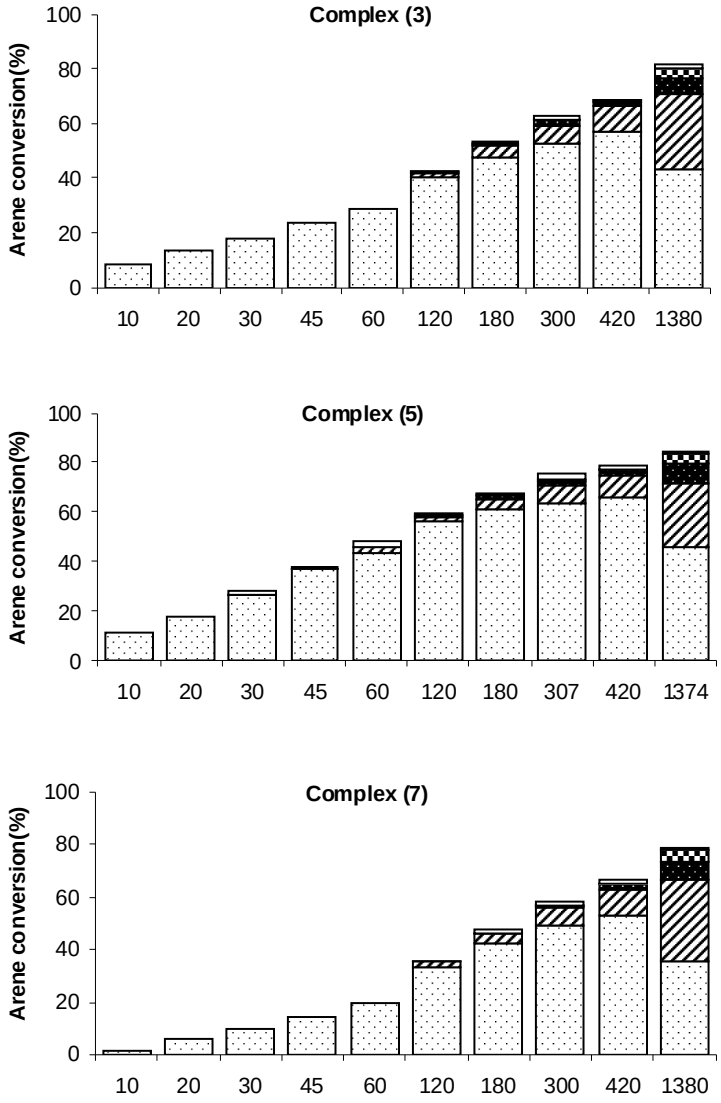

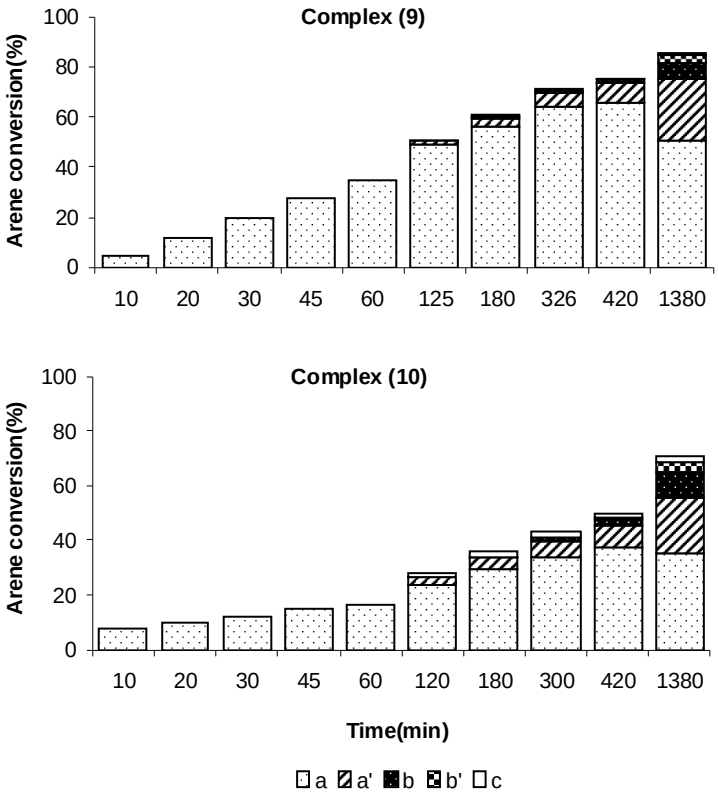

Figure 3.18 Products distribution for the reaction between pentamethylbenzene and ethyl propiolate catalysed by complexes **(3)**, **(5)**, **(7)**, **(9)**, and **(10)**. Reaction conditions: see **Figure 3.17**.

3.8 Effect of the silver salts [45]

The data reported above show that the catalytic species is simply formed after substitution of the halides with more labile ligands, which are in this case the trifluoroacetate anions coming from the acid employed in the reaction; the dicarbene ligand, instead, remains bonded to the metal, as already predicted in view of the strength of the metal-carbene bond. The presence of labile ligands at the metal favours the coordination of the substrates, increasing the rate of the reaction. Silver salts have been therefore added to the reaction mixture in order to facilitate the formation of the catalytically active species and to further improve the activity of the catalytic system. In particular AgTFA has been chosen, with the purpose to retain the same counter-anion of the acid. The conversion curves obtained at 80 °C using complex **(6)** with and without the silver salt are reported in **Figure 3.19**.

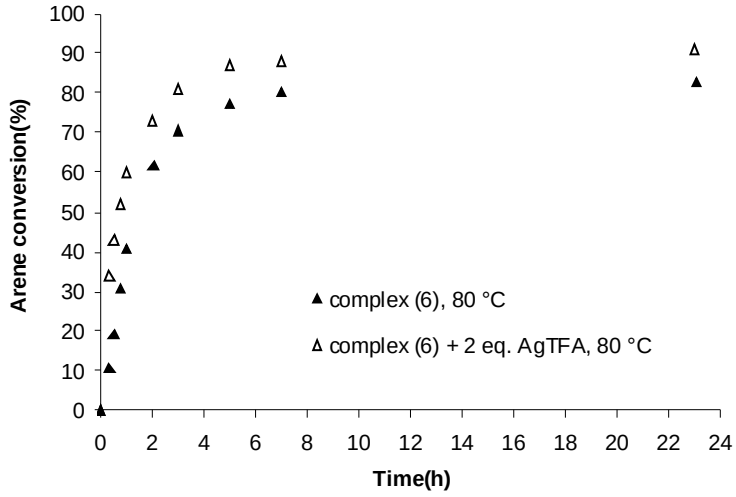

Figure 3.19 Conversion(%) *vs.* time diagram for the reaction between pentamethylbenzene and ethyl propiolate catalysed by complex **(6)**. Effect of the silver salt at 80 °C. Reaction conditions: 0.01325 mmol catalyst, 13.25 mmol alkyne, 13.25 mmol arene, solvent: CF_3COOH/DCE = 4mL/1mL.

The catalytic system is, at 80 °C, more efficient in the presence of two equivalents of the silver salt. Moreover, utilising this co-catalyst, the reaction takes place even at room temperature achieving acceptable conversions, differently to the system without AgTFA in which conversions are instead very low (**Figure 3.20**).

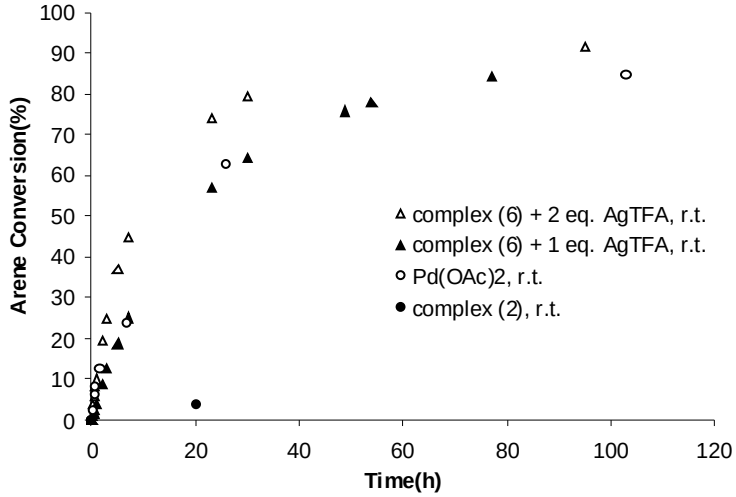

Figure 3.20 Conversion(%) *vs.* time diagram for the reaction between pentamethylbenzene and ethyl propiolate catalysed by complex **(6)**. Effect of the silver salt at room temperature. Reaction conditions: see **Figure 3.19**.

Other experiments, shown in **Figure 3.20**, have been conducted by adding only one equivalent of the silver salt to the reaction mixture containing complex **(6)**. In this case, the initial reaction rate is almost half with respect to the initial rate observed when two equivalents of the salt are used.

This experiments have been useful not only because now it is possible to run the reaction at room temperature, but also because they confirm the need of substituting both halide ligands to make the reaction proceed. Indeed, if one considers that species **(i)** shown in **Figure 3.21** is responsible of the catalytic activity, the reaction rate observed adding 1 or 2 eq. of the silver salt should be similar. Being the initial rate instead very different, and in particular one half of the other, it can be assumed that the active catalytic species needs to possess at least two labile ligands at the metal centre (species **(ii)** in **Figure 3.21**).

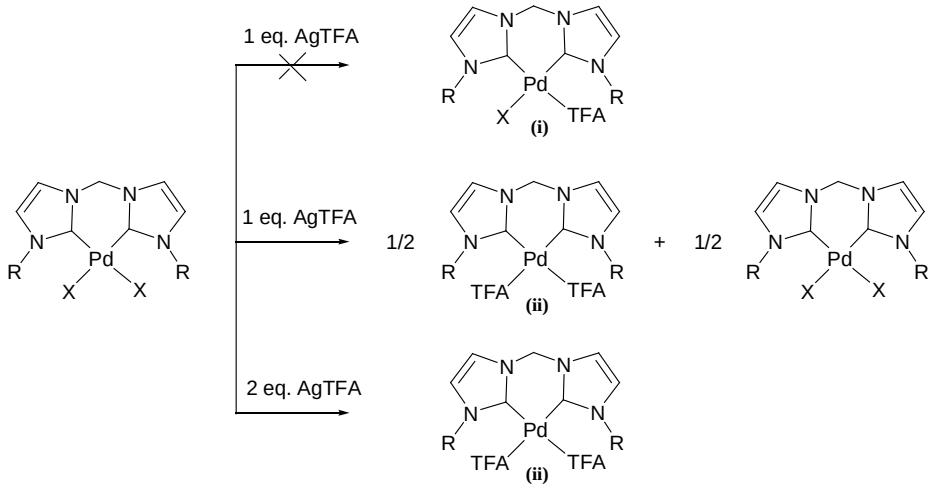

Figure 3.21 Species formed after addition of 1 or 2 eq. AgTFA to dicarbene complexes.

The complex reported in **Figure 3.22**, which possesses two TFA ligands already coordinated to the metal, has been therefore synthesised. Its behaviour should be similar to that obtained with the catalytic system formed by complex **(6)** + 2 eq. AgTFA, and this has been confirmed by the determination of conversion curves, which have resulted identical for both catalytic systems (**Figure 3.23**).

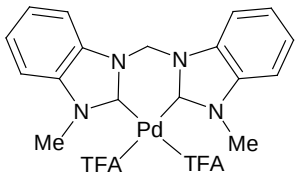

Figure 3.22 Complex **(8)**.

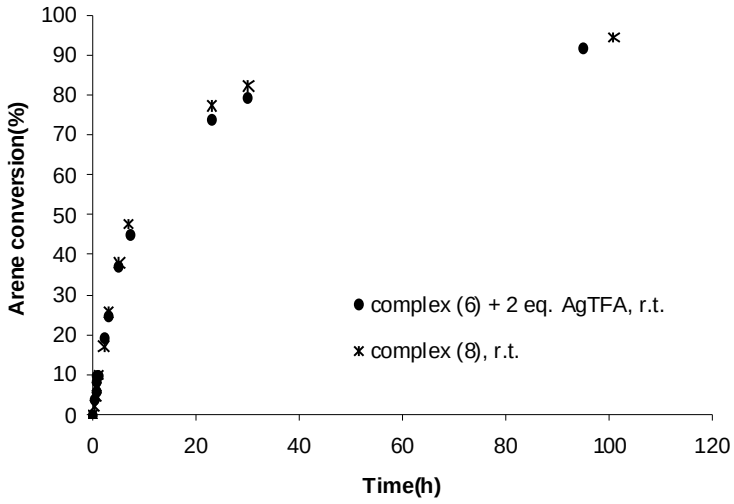

Figure 3.23 Conversion(%) *vs.* time diagram for the reaction between pentamethylbenzene and ethyl propiolate. Reaction conditions: 0.01325 mmol catalyst, 13.25 mmol alkyne, 13.25 mmol arene, solvent: CF_3COOH/DCE = 4mL/1mL, room temperature.

Moreover, the possibility to run the reaction at room temperature increases the selectivity towards the *cis*-product, since isomerisation and hydrolysis reactions have not been observed at this temperature (**Figure 3.24**).

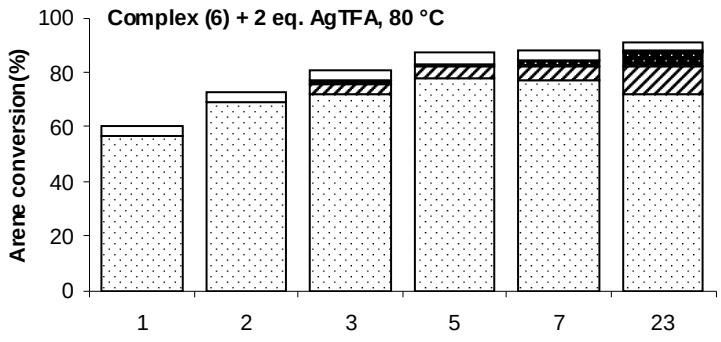

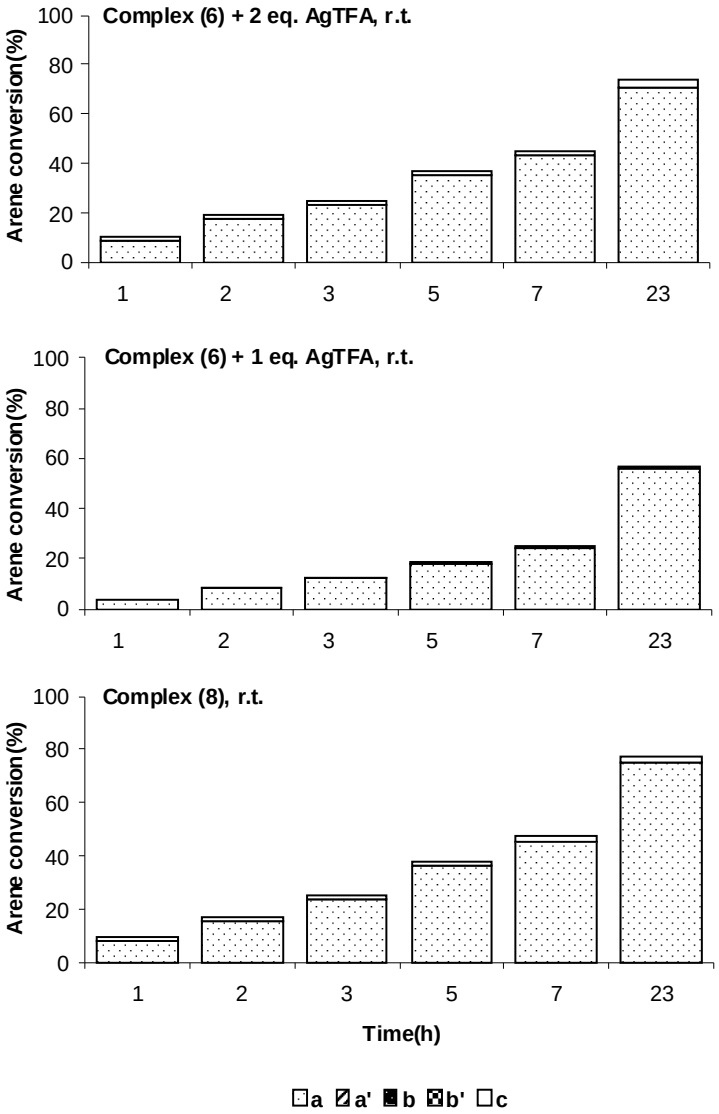

Figure 3.24 Products distribution for the reaction between pentamethylbenzene and ethyl propiolate catalysed by complexes **(6)** in the presence of AgTFA, at 80 °C and at r.t., and by complex **(8)**. Reaction conditions: see **Figure 3.23**.

In conclusion, these last experiments have allowed to develop a useful catalytic system, able to catalyse the reaction also at room temperature and with an enhanced selectivity. Moreover, the nature of the catalytically active species has been elucidated, thereby giving the possibility to design an appropriate catalyst for the reaction.

3.9 Electrochemical studies

Control of both steric and electronic properties at the metal centre is of critical importance for the optimisation of the catalytic activity of the complex, so that the quantification of these characteristics is essential. In the catalytic cycles proposed for the Fujiwara reaction, highly electrophilic species of palladium(II) are involved; therefore the electron density at the metal centre may have an important influence on the efficiency of the catalyst.

Several studies have been made to determine the electron-donating properties of NHC ligands, especially evaluating the CO stretching of CO-containing NHC-complexes [50]. Determination of redox potentials of carbene complexes can be an alternative method and, in particular, the electrochemical analysis of the Pd(II)/Pd(0) reduction potential by cyclic voltammetry can be an useful means of probing the charge density at the metal. Low reduction potentials are indeed expected when the ligands coordinated to the metal are strongly electron-donating. Demonceau, Noels *et al.* have determined the redox potentials, $E^{\ominus}$, of NHC-Ru complexes, showing the existence of a correlation between $E^{\ominus}$ and their catalytic activity in atom transfer radical polymerisation (ATRP) [51]. However, electrochemical investigations on carbene complexes are still limited [52].

On the basis of the results obtained through the kinetic studies (see **paragraph 3.7**), which have shown an influence of the nature of dicarbene ligand on the activity of the catalyst, the electrochemical behaviour of palladium dicarbene complexes bearing different NHC ligands (**Figure 3.25**) has been investigated under different experimental conditions in the laboratories of Prof. Armando Gennaro, Università degli Studi di Padova.

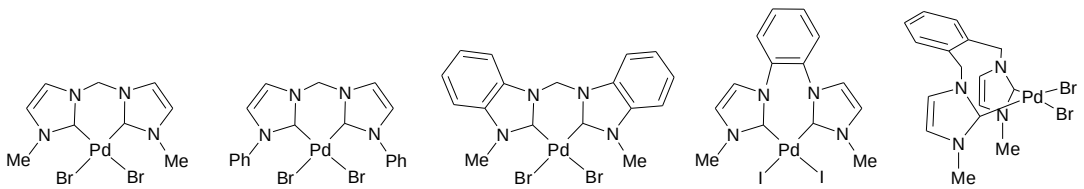

Figure 3.25 Dicarbene complexes utilised in this study.

The CVs of the complexes have been registered at 25 °C in DMSO containing tetra-*n*-butylammonium perchlorate (Bu_4NClO_4) 0.1 M as supporting electrolyte. For detailed experimental conditions see **Chapter 7** and the **Experimental Section**. DMSO has been chosen as solvent, since the analysed complexes are readily soluble in it and trifluoroacetic acid can not be used because of H_2 discharge (due to the reduction of HTFA at the electrode), which partially overlaps the peaks under observation. However, in a first approximation approach, the redox potentials obtained in DMSO can be correlated to the catalytic activity of the complexes, despite the different solvent used.

The complexes exhibit quite similar voltammetric features displaying an irreversible behaviour, and the observed reduction peaks between -1.5 and -2.0 V can be attributed to the reduction of Pd(II) to Pd(0):

$$Pd(II) + 2e^- \rightarrow Pd(0)$$

The main voltammetric peak observed in the CVs of all the complexes at low scan rates (for example at 0.2 V s^{-1}) is related to the mono-solvento species $[Pd(dicarbene)(X)(DMSO)]^+$ **(na)** (**n** is meant a general complex reported in **Figure 3.25**). Target experiments have indeed demonstrated that the complexes, introduced into solution as $[Pd(dicarbene)X_2]$, upon dissolution in DMSO containing Bu_4NClO_4 0.1 M substitute one bromide ion with a solvent molecule giving the mixed complexes **(na)**. At more negative potentials it is however present, in some cases, also the peak associated to the reduction of $[Pd(dicarbene)X_2]$ **(n)**. When silver salts, as for example AgTFA, are added into the solution the main species becomes the bis-solvento complex $[Pd(dicarbene)(DMSO)_2]^{2+}$ **(nb)** (**Figure 3.26**).

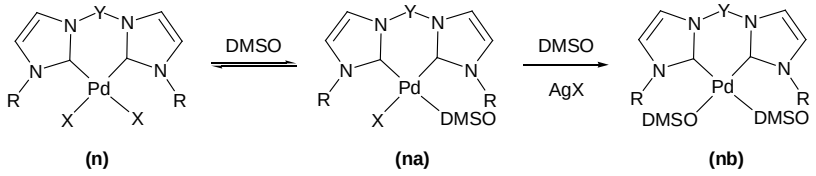

Figure 3.26 Species formed upon dissolution of a generic dicarbene complex **n** in DMSO + Bu_4NClO_4 0.1 M before and after addition of a silver salt.

The order of the reduction potentials of these species is in general **(nb)** > **(na)** > **(n)**: for example, reduction of the di-halide complex **(2)** occurs at the most negative potentials (–2.0 V *vs* Fc^+/Fc), that of the mixed complex **(2a)** at slightly less negative potentials (about –1.9 V *vs* Fc^+/Fc), whereas the di-solvento complex **(2b)**, with a peak potential around –1.7 V, is the most easily reducible complex.

The identification of the species disclosed in solution has allowed the subsequent determination of their reduction potential, which are summarised in **Table 3.6**. Unfortunately, the standard reduction potentials $E^{\ominus}$ of these Pd(II) complexes can not be measured because of the irreversibility of the ET, but the reduction potentials, E_p may be anyway utilised for the comparative analysis of the redox properties of the complexes.

Table 3.6 Voltammetric data for the reduction of mono-solvento **(na)** and bis-solvento **(nb)** Pd(II) complexes in DMSO + Bu_4NClO_4 0.1 M.

Complex	E_{pc}[a] **[V *vs* Fc^+/Fc]**	
(n)	**(na)**	**(nb)**
(2)	-1.87	-1.72
(4)	-1.88	-1.69
(6)	-1.82	-1.59
(9)	-1.94	-1.80
(10)	-2.00	-

[a] Cathodic peak potential, E_{pc}, determined for species **(na)** and species **(nb)** at v = 0.1 V s^{-1}.

Analysis of the peak potentials in the **(na)** and **(nb)** series reveals that in some cases the E_{pc} values depends on the nature of the ligand set.

If we assume that the reduction potential is related to the charge density on Pd, in the sense that the greater the positive charge on the metal the higher the reduction potential, ligands with higher electron-donating abilities will form Pd(II) complexes with smaller positive charge density on the metal and, consequently, the reduction potential will shift to more negative values.

As shown in **Tables 3.6**, the reduction peak potentials measured for complexes **(na)** and **(nb)** become more negative in the following order:

(6a) > (2a) ~ (4a) > (10a)

(6b) > (4b) > (2b) > (9b)

These trends correspond to the decreasing in the charge density present on Pd(II).

Species **(9a)** has not been considered in the comparison because it has one iodide instead of one bromide ligand, and this difference could influence the charge density on Pd providing an additional contribution to E_p.

In the series of species **(nb)**, instead, **(10b)** has not been considered because its reduction potential could not be measured with a reasonable accuracy.

The positive charge on Pd(II) is the highest for species **(6a)**, which shows the least negative reduction potential in the series. In contrast, species **(10a)** and **(9b)** have the most negative potential and, hence, the lowest charge density on the metal.

Correlating the data obtained through the voltammetric studies both for species **(na)** and **(nb)** with the catalytic activity displayed by the same complexes in the Fujiwara reaction (**(10)<<(6)~(2)~(9)<(4)** at 3h of reaction), it is evident that the electron density present on the metal centre does not significantly influence the catalytic performance of the complex, since the observed trend is not the same. This is easily observed in the following graphs (**Figure 3.27**).

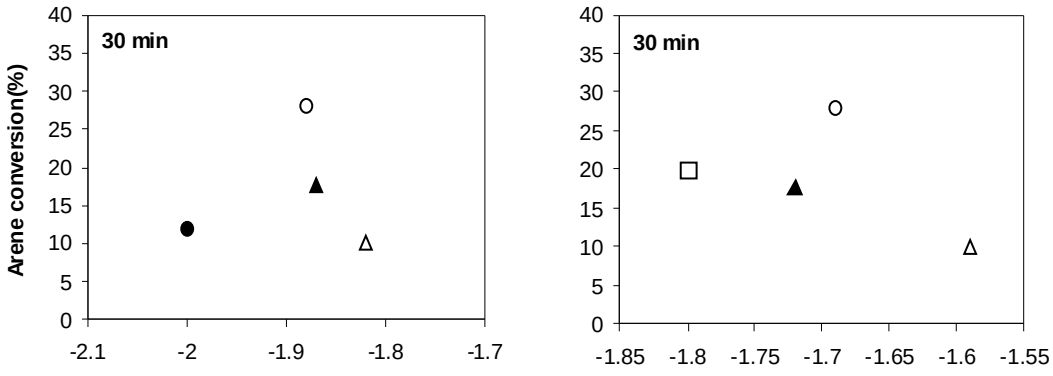

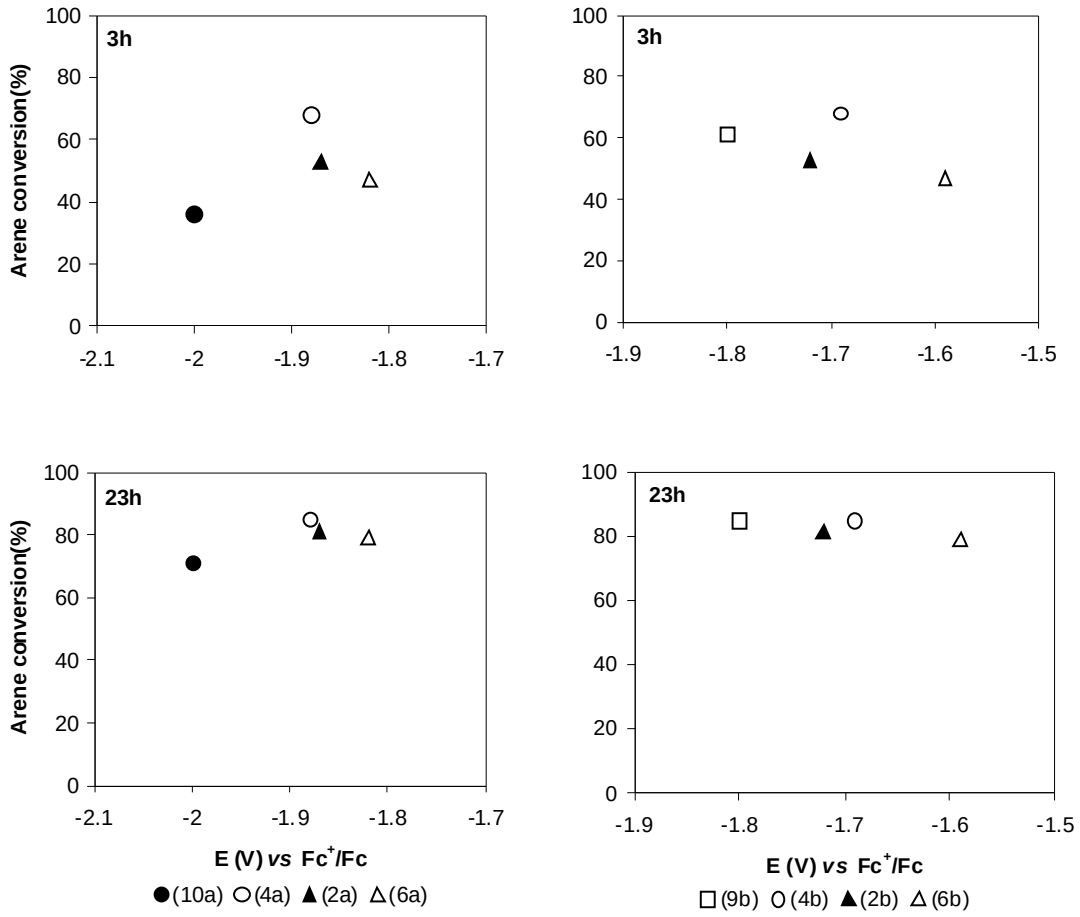

Figure 3.27 Correlation of the catalytic activity of Pd(II) dicarbene complexes at 30 min, 3h and 23h with the reduction potential values determined at 0.1 V s^{-1} for species **(na)** and **(nb)**.

The catalytic efficiency of the complexes, therefore, seems to be prevalently connected to the steric hindrance at the metal centre. This is easily evidenced by a comparison among the X-ray structures reported in the literature for the same or for closely related complexes (**Figure 3.28**).

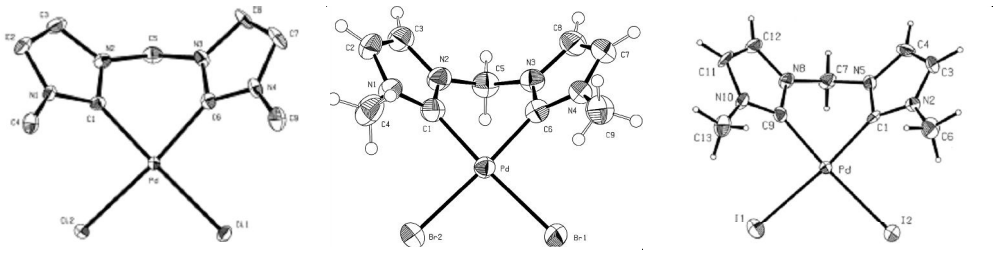

(1)[19b] **(2)**[44h] **(3)**[44b]

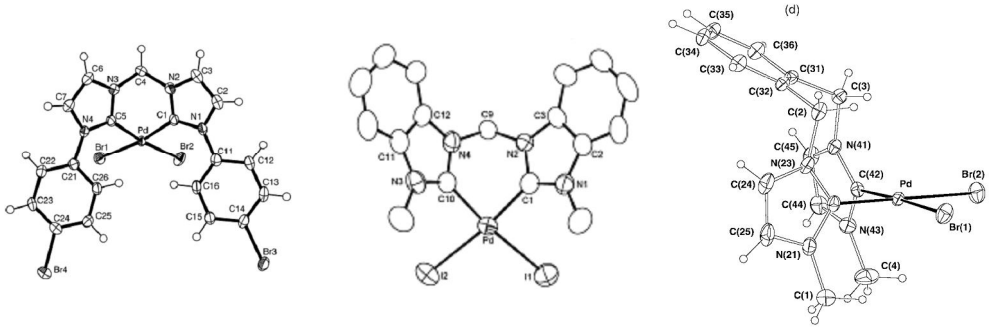

(4)[53a] **(6)**[44c] **(10)**[53b]

Figure 3.28 X-ray structure reported in the literature for complexes **(1)-(3)**, **(6)**, **(10)** and for a complex closely related to **(4)**.

The steric hindrance at the catalytic site is obviously very similar for complexes **(1)**, **(2)**, **(3)**, which possess the same dicarbene ligand. Among the complexes bearing different dicarbene ligands, complex **(4)** is the most hindered one, possessing two bulky phenyl wingtips at the nitrogen atoms; complex **(10)** displays, instead, the least hindered palladium centre, since the angle among the two carbene units and the metal is narrower than in the other complexes. These observations support the scale of reactivity displayed by the complexes: the more hindered complex **(4)** shows the best catalytic activity, whereas complex **(10)** resulted the least active catalyst.

CHAPTER 4
SCOPE OF THE FUJIWARA REACTION

The optimisation of the reaction conditions, made in **Chapter 3**, has allowed to develop a more convenient protocol for the Fujiwara reaction, which can be run with only 0.1% of palladium(II) dicarbene complexes, in few hours and with the substrates in a stoichiometric ratio.

After these encouraging results, the work has been continued evaluating the generality of this catalytic system with respect to both the alkyne and the arene, by testing complex **(6)** as standard catalyst.

4.1 Screening of alkynes [49]

Differently substituted alkynes have been reacted with pentamethylbenzene and the results are reported in **Table 4.1**; the reaction time has not been optimised for any of the alkynes employed.

The dicarbene-based catalytic system displays higher activities and selectivities than Fujiwara's one, which requires larger amounts of catalysts and/or longer reaction times [26b]. Moreover, the observed regio- and stereoselectivity are very much dependent on the nature of the employed alkyne. In fact electron-poor terminal alkynes are very reactive and afford β-aryl substituted alkenes exclusively, whereas internal alkynes substituted with two electron-withdrawing groups are converted more sluggishly. In particular, internal alkynes conjugated with phenyl groups react to give uniquely α-arylalkenes (Markovnikov-type adducts), as it is invariably the case with metal-catalysed hydroarylations [23, 26, 30-33, 35, 37, 42].

Terminal alkynes with electron-withdrawing group such as CO_2H, CO_2Me and CO_2Et as well as 1-phenylpropine afford predominantly aryalkenes with *cis* stereochemistry; these products, however, isomerise to a small extent generating the more thermodinamically stable *trans*-arylalkenes. 3-butyn-2-one is the only alkyne which gives the *E*-product exclusively; probably the *cis*/*trans* isomerisation is faster than in the other cases.

Table 4.1 Conversion(%) for the reaction of pentamethylbenzene with different alkynes catalysed by complex **(6)**.

Alkyne	Time(h)	Products	Yield(%)[a] (*Z*:*E*)
H—≡—CO_2Et	5	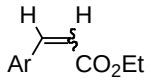	58(57:1)
	7		66(32:1)
	23		83(9:1)
H—≡—CO_2Me	5	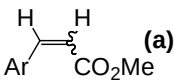 **(a)**	**(a)** 56(18:1) **(b)** 11(10:1)
	24	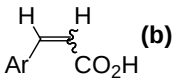 **(b)**	**(a)** 30(2:1) **(b)** 58(4:1)
H—≡—CO_2H	5	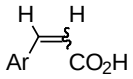	79(25:1)
	24		81(7:1)
MeO_2C—≡—CO_2Me	5	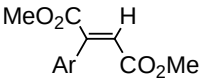	-
	24		9
	48		28
Ph—≡—CO_2Et	5	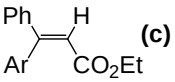 **(c)**	**(c)** 20 **(d)** 5
	24	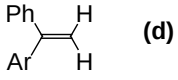 **(d)**	**(c)** 23 **(d)** 25
Ph—≡—H	5	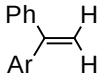	20
	24		20
Ph—≡—Ph	5	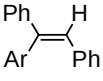	35
	24		35
Ph—≡—Me	5	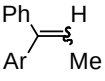	39(7:1)
	24		43(4:1)
H—≡—COMe	2	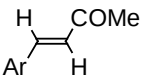	86
	5		87

Reaction conditions: 0.00265 mmol complex **(6)**, 2.65 mmol alkyne, 2.65 mmol arene, solvent: CF_3COOH/DCE = 4mL/1mL, 80 °C. [a] Yields(%) determined by ^{1}H-NMR. For more details see the Experimental Section.

With phenylacetylene as substrate the yield in the α-arylated product is surprisingly low, but it has to be remarked that in this case alkyne polymerisation and hydration by traces of water are found to be serious competitive reactions. ^{1}H NMR of the reaction mixture has indeed revealed the formation of a large amount of acetophenone; addition of TFA to the triple bond and subsequent hydrolysis to give ketones has been demonstrated to be Pd-catalysed and is also observed by Fujiwara in absence of arene or with inactive arenes [26b]. Ethyl phenylpropiolate is also hydrated to a small extent under the employed reaction conditions, thus explaining the moderate conversions observed. Traces of water may also hydrolyse ester functions: limited hydrolysis of the reaction product has been indeed observed with ethyl propiolate and most notably with methyl propiolate, whereas in the case of ethyl phenylpropiolate the reaction product was a mixture of the expected ester and of the corresponding decarboxylated compound, presumably deriving from ester hydrolysis with subsequent rapid decarboxylation. Phenyl 1-propine has found to provide higher yields in the product than the other alkynes conjugated with phenyl groups, giving a mixture of isomers *Z* and *E*. The ratio *Z*/*E* decreases by prolonging the reaction times because of a thermal isomerisation process. This is in contrast with the product distribution observed in the hydroarylation of phenyl 1-propine catalysed by metal triflates, where the isomer ratio *Z*/*E* increases in the course of the reaction [29-30].

4.2 Screening of arenes [49]

The screening of arene substrates has been performed upon reacting ethyl propiolate with arenes differently activated towards the SE_{Ar}, both in terms of the number of substituents and of their nature. The products that can be obtained in these reactions are reported in **Figure 4.1**.

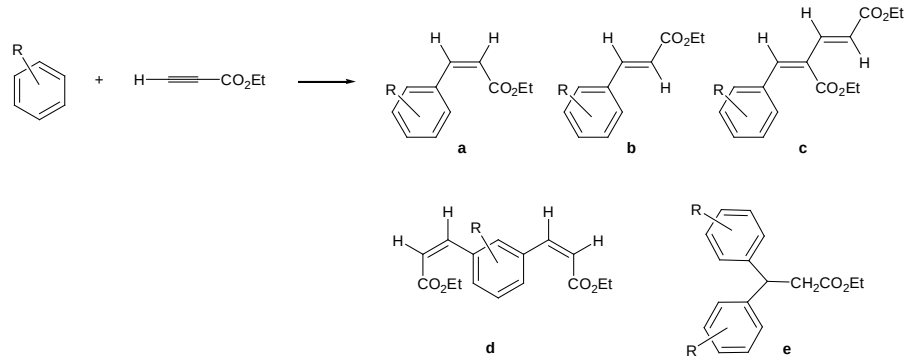

Figure 4.1 Possible reaction products in the reaction between differently substituted arenes and ethyl propiolate.

Table 4.2 Conversion(%) for the reaction of ethyl propiolate with different arenes catalysed by complex **(6)**.

Arene	Time(h)	Arene/Alkyne Conversion(%)[a]	Yield(%)[a] a[b]	b[b]	c	d	e
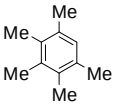	5	73/75	64(5)	1(1)	2	-	-
	23	87/89	50(25)	7(3)	2	-	-
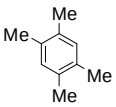	5	58/65	47(4)	-	3	4	-
	24	81/88	62(11)	1	3	4	-
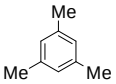	5	74/85	58(4)	1	3	8	-
	24	81/95	34(25)	5(3)	4	10	-
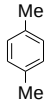	5	10/12	5(1)	2	2	-	-
	24	30/33	7(14)	6	3	-	-
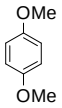	5	20/12	4	-	-	-	8

Reaction conditions: 0.0043 mmol complex **(6)**, 4.3 mmol alkyne, 4.3 mmol arene, solvent: CF_3COOH/DCE = 4mL/1mL, 80 °C. [a] Conversions(%) and yields(%) determined by ^{1}H-NMR. [b] In parenthesis yields in the hydrolysed product. For more details see the Experimental Section.

The results reported in **Table 4.2** show that most of methyl-substituted benzenes are good substrates irrespective of the number of substituents, although the yield recorded with *p*-xylene is unexpectedly low. In this last case the yields could be improved by prolonging the reaction time, but this also results in the extensive hydrolysis of the ester function of the product.

The distribution of side products (see **Figure 4.1**) also changes significantly upon considering different methyl-substitutes benzenes: while in the case of 1,2,4,5-tetramethylbenzene and 1,3,5-trimethylbenzene the double hydroarylation product (**d**) is the main side product, for *p*-xylene it is the *trans*-arylalkene product (**b**). This is evidently the consequence of the decreased reactivity of the aromatic ring towards hydroarylation, as well as of the possible greater incidence of thermal isomerisation through a dipolar mechanism already proposed by Fujiwara and by Alper (**Figure 4.2**) [26b, 44a].

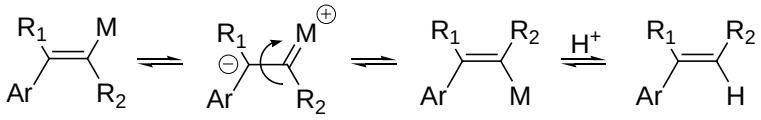

Figure 4.2 Isomerisation process from *cis*-arylalkene to *trans*-arylalkene.

A slow reaction has been observed also with *p*-dimethoxybenzene, as also reported by Fujiwara and Nolan [26b, 42]; however, in our case the arene/alkyne 2/1 adduct (**e**) is the main reaction product (**Figure 4.1**), while Nolan's group obtained exclusively the *cis*-arylalkene (**a**) and Fujiwara's group predominantly **a** and a small percentage of **e**. The formation of **e** occurs through a mechanism already proposed in the literature [26b], which involves the formation of a cationic intermediate. If this intermediate is sufficiently stabilised, it can be attacked by a second arene molecule to give the final product (**Figure 4.3**).

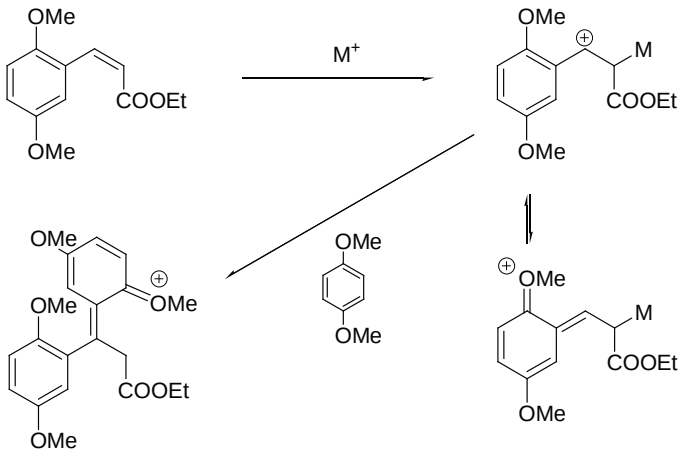

Figure 4.3 Proposed mechanism for the formation of product **e** with *p*-dimethoxybenzene.

Prolongation of the reaction time affords an increase in conversion but also the formation of oligomeric products presumably deriving from further electrophilic substitution reactions (attack of another product molecule to the arene rings of the 2:1 adduct **e**) (**Figure 4.4**).

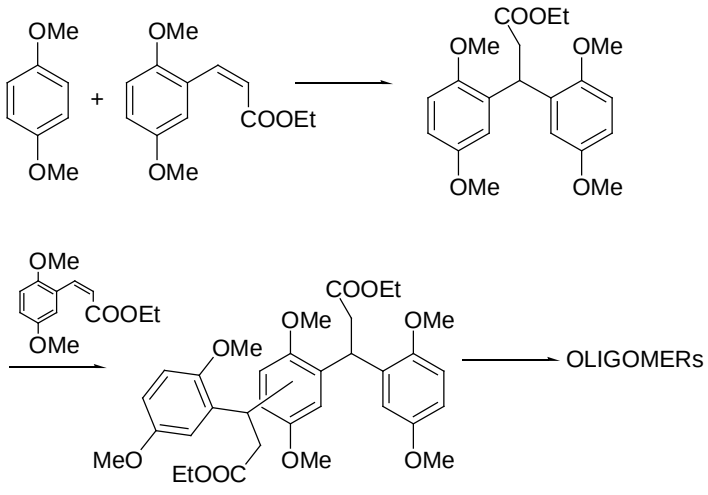

Figure 4.4 Oligomerisation reactions occurring with *p*-dimethoxybenzene at long reaction times.

Finally, the presence of halide substituents has a deleterious effect on the reaction, *p*-bromotoluene being almost inactive and *p*-bromoanisole being only slowly converted with poor selectivity [49]. However, it has to be remarked that arenes substituted with electron withdrawing substituents are usually inactive for this reaction; indeed, the only aryl bromide that is known to be converted to an appreciable extent is mesityl bromide [23, 26, 30-33, 35, 37, 42].

Electron-poor arenes, such as *p*-xylene, have shown a very low reactivity in the reaction with ethyl propiolate catalysed by complex **(6)** at 80 °C (**Table 4.2**). Also the selectivity of the reaction towards the *cis*-product is very low, hydrolysis and isomerisation being very competitive reactions especially for long reaction times.

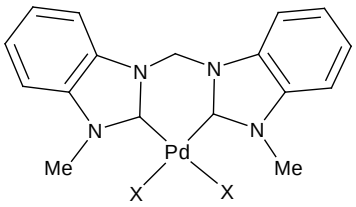

Figure 4.5 Complex **(6)** with $X^- = Br^-$, complex **(8)** with $X^- = CF_3COO^-$.

Other tests have been therefore carried out using complex **(8)** (**Figure 4.5**). The lability of TFA anion and the possibility to run the reaction at room temperature could, indeed, facilitate the coordination of the substrates, thus avoiding collateral reactions.

By employing complex **(8)** the reaction proceeds at room temperature with low conversions, although with complete selectivity towards the *cis*-product (**a**). Increasing of the reaction temperature allows to improve the yield which is however comparable to that obtained using catalyst **(6)** since other collateral reactions, such as polimerisation of the alkyne, take place in these conditions (**Table 4.3**).

Table 4.3 Conversion(%) for the reaction between *p*-xylene and ethyl propiolate catalysed by complex **(8)**.

Temperature	Time(h)	Arene/Alkyne Conversion(%)[a]	Yield(%)[a] a[b]	b[b]	c	d	e
r.t.	5	1/1	1	-	-	-	-
	24	3/3	3	-	-	-	-
	48	6/6	6	-	-	-	-
80 °C	5	13/29	10	2	1	-	-
	24	30/74	15(6)	4(2)	1	-	-

Reaction conditions: 0.013 mmol complex **(8)**, 13.2 mmol alkyne, 13.2 mmol arene, solvent: CF_3COOH/DCE = 4mL/1mL. [a] Conversions(%) and yields(%) determined by ^{1}H-NMR. [b] In parenthesis the yield in the hydrolysed product. For more details see the Experimental Section.

4.3 Fujiwara reaction with Pt(II) dicarbene complexes [49]

A preliminary evaluation of a dicarbene platinum(II) complex **(14)** as catalyst for this reaction (**Figure 4.6**) has been also performed and the results obtained in the arene and alkyne screening are reported in **Table 4.4**, **4.5** and **Table 4.6** respectively. The reagents have been utilised in an equimolar ratio, while the amount of catalyst has been varied from 0.1 to 1 mol% loading.

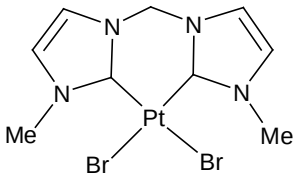

Figure 4.6 Complex **(14)**.

As with palladium complexes, the screening of arenes has been performed upon reacting ethyl propiolate with differently substituted arenes. Complex **(14)** has displayed slightly lower activities and selectivities than Fujiwara's platinum catalytic systems ($PtCl_2$/2AgOAc or $PtCl_2$/2AgOTf), which however require higher catalyst loading (5 mol%) and longer reaction times (24 hours) [35].

Table 4.4 Conversion(%) for the reaction of ethyl propiolate with different arenes catalysed by complex **(14)**.

Arene	Time(h)	Arene/Alkyne Conversion(%)[a]	Yield(%)[a] a[b]	b[b]	c	d	e
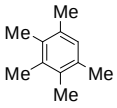	5	72/72	63(6)	1(1)	-	-	-
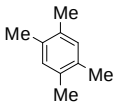	5	56/61	47(4)	-	1	4	-
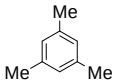	5	63/75	45(4)	1(1)	-	12	-
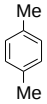	5	4/4	3(1)	-	-	-	-

Reaction conditions: 0.0079 mmol complex **(14)**, 7.9 mmol alkyne, 7.9 mmol arene, solvent: CF_3COOH/DCE = 4mL/1mL, 80 °C. [a] Conversions(%) and yields(%) determined by ^{1}H-NMR. [b] In parenthesis yields in the hydrolysed product. For more details see the Experimental Section.

Comparing the results reported in **Table 4.4** with the ones obtained with the analogous palladium complex **(6)** (see **Table 4.2**), it is evident that the platinum complex is less active but displays in some cases better selectivities.

It is important to notice that the arene steric hindrance does not influence the reaction rate, since pentamethylbenzene is the most active substrate among the arenes analysed, as already observed in the previous studies.

Another arene screening has been made using 1 mol% catalyst (**Table 4.5**).

Table 4.5 Conversion(%) for the reaction of ethyl propiolate with different arenes catalysed by complex **(14)**.

Arene	Time(h)	Arene/Alkyne Conversion(%)[a]	Yield(%)[a] a[b]	b[b]	c	d	e
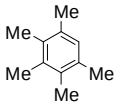	5	94/94[c]	78(12)	3(1)	-	-	-
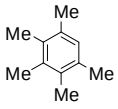	5	77/77	64(11)	2	-	-	-
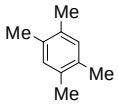	5	52/54	43(5)	2	-	2	-
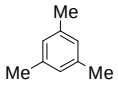	5	73/88	46(8)	3(1)	-	15	-

Reaction conditions: 0.0079 mmol complex **(14)**, 0.79 mmol alkyne, 0.79 mmol arene, solvent: CF_3COOH/DCE = 4mL/1mL, 80 °C. [a] Conversions(%) and yields(%) determined by ^{1}H-NMR. [b] In parenthesis yields in the hydrolysed product. [c] 0.0079 mmol complex **(14)**, 0.79 mmol alkyne, 1.61 mmol arene. For more details see the Experimental Section.

Different alkynes have been subsequently reacted with pentamethylbenzene using 0.1% catalyst, giving the results reported in **Table 4.6**.

Compared to the Pd(II) dicarbene complex **(6)** (see **Table 4.1**), complex **(14)** has given in general higher yields in products, even if it needs to be remarked that in this screening the molar concentration of catalyst and substrates is about three times higher than the one used with Pd(II)-based catalyst. It is important to notice that diphenylacetylene reaches the highest yield in product after 5 h, whereas for phenyl 1-propine it is reached just after 30 minutes. As in the palladium case, the *Z/E* ratio decreases for longer reaction times because of a thermal isomerisation process.

Table 4.6 Conversion(%) for the reaction of pentamethylbenzene with different alkynes catalysed by complex **(14)**.

Alkyne	Time(h)	Products	Yield(%)[a] (*Z*:*E*)
H—≡—CO_2Et	5	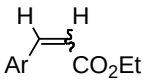	72(35:1)
Ph—≡—Ph	5	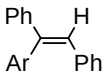	51
	24		51
Ph—≡—Me	0.5	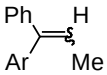	43(11:2)
	2		44(11:2)
	5		45(7:2)

Reaction conditions: 0.0079 mmol complex **(14)**, 7.9 mmol alkyne, 7.9 mmol arene solvent: CF_3COOH/DCE = 4mL/1mL, 80 °C. [a] Conversions(%) and yields(%) determined by ^{1}H-NMR. For more details see the Experimental Section.

4.4 Screening of aromatic heterocycles

The optimised catalytic system has been also evaluated in the C-H functionalisation of aromatic heterocycles [21d, 54].

The functionalisation of heteroaromatic moieties is a highly effective synthetic tool for chemical industry, being heterocycles readily accessible building blocks for the synthesis of a wide range of biologically active compounds, natural products and pharmaceuticals. The classical synthetic methodologies employed for heterocycle functionalisation usually involve cross-coupling reactions [55], thus requiring the use of pre-functionalised substrates. Very recently, several efforts have been aimed at avoiding substrate pre-functionalisation, like halogenation, in order to render the process more convenient both economically and environmentally. For example, it has been reported that several aromatic heterocycles (**1**, **Figure 4.7**) react very fast with terminal and internal alkynes (**2**), at room temperature in acetic acid employing $Pd(OAc)_2$ as catalyst [39]. Products of formal hydroarylation of the triple bond (**3**) are obtained.

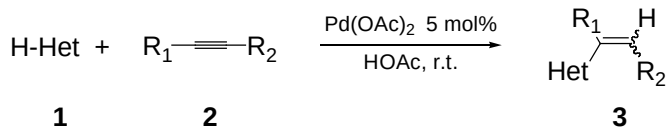

Figure 4.7 Reaction between aromatic heterocycles and alkynes catalysed by $Pd(OAc)_2$.

The initial proposed mechanism [39a] invokes formation of a σ-heterocycle palladium(II) complex through an electrophilic aromatic substitution with cationic Pd(II) species, followed by insertion of the alkyne into the Pd-heterocycle bond. Acetic acid provides the proton necessary to protonolyse the formed Pd-vinyl bond, affording the final product, and has also the role to facilitate the formation of the electrophilic palladium(II) species. Moreover, isotopic experiments have evidenced that the cleavage of the C-H bond of the heterocycle is the possible rate determining step in dichloromethane as solvent [39a].

However, the generally accepted mechanism, proposed later on by the same authors in the addition of propiolic acids to thiophenes catalysed by a Pt(II)-based system in TFA as solvent [56], implies the initial coordination of the metal to the alkyne followed by attack of the heterocycle to the resulting activated triple bond.

Other catalytic systems have been reported in the recent literature in regard to this reaction. Chelate-assisted addition of heterocycles to silyl-alkynes is promoted by metal centres in low oxidation state (e.g. Ru(0)) [57]. Rh_4CO_{12} catalyses the present reaction under CO pressure a 220 °C, functionalisating aromatic heterocycles with diphenylacetylene in the following rate order: furan > thiophene > N-methypyrrole [58]. Metal triflates catalysts, instead, afford bis(heteroaryl)propionates (**4, Figure 4.8**) in neutral conditions at room temperature [59]; this type of products is obtained, together with the common hydroarylation products, also by a $AuCl_3$/AgOTf-based system using N-methylindole and benzofurane [32a, 60] and by a cationic dinuclear catalyst $[(Mes_3PAu)_2Cl]BF_4$ using 2-substituted furans [61].

The platinum system K_2PtCl_4/4AgOTf applied to the hydroarylation of thiophenes in TFA as solvent is also able to catalysed the formation of 3,3-bis(thienyl)propionates and -propionic acids in good yields at 40 °C [56].

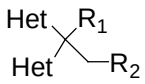

4

Figure 4.8 bis(heteroaryl)propionates.

A dinuclear palladium(II) complex, in the presence of trialkylboranes at 100 °C, promotes the addition reaction between alkynes and N-substituted pyrrole and thiophenes, whereas the reaction does not occur with N-unsubstituted pyrroles and furans [62]. In this case, however the stereoselectivity of the reaction is different from the one observed with the other catalytic systems, since the addition here occurs in a *cis*-fashion.

Despite the existence of a large series of effective catalysts, the potential of this reaction may be deeply investigated by utilising palladium complexes whose electronic and steric properties can be easily tuned in order to modulate both the activity and the selectivity of the catalytic system.

Firstly, catalytic efficiency of complex **(8)** pre-formed or generated *in situ* by adding 2 eq. of silver trifluoroacetate (AgTFA) to complex **(6)** has been investigated under the reaction conditions adopted by Fujiwara (1 mmol alkyne, 2 mmol heterocycle, 1 mL HOAc, 2h, r.t.), but decreasing the catalyst load from 5 mol% to 1 mol%.

It has been previously demonstrated that, in the presence of TFA counter-anions, the complex displays an enhanced efficiency, being trifluoroacetate ligands more easily displaced than bromides. Complex **(8)** has been properly designed to have two labile ligands already coordinated to the metal and it has been found to display the same catalytic activity of the complex formed *in situ* in the previous studies on alkynes hydroarylation (see **Chapter 3**).

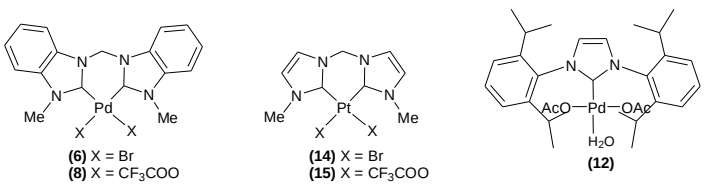

Figure 4.9 NHC carbene complexes employed in this work.

Table 4.7 Conversions(%) and yields(%) for the reaction between pyrrole **1a** and ethyl phenylpropiolate **2a** catalysed by complex **(6)**.

Entry	Catalyst/ Co-catalyst	Time (h)	Temperature	Alkyne Conversion(%)[a]	Yield(%)[a] *Z*-3a	4a
1	(6)/-	2	r.t.	-	-	-
2	(6)/-	3	50 °C	2	2	-
3	(6)/2AgTFA	2	r.t.	4	4	-
4	(6)/2AgTFA	3	50 °C	55	30	8
5	(6)/2AgTFA	22	50 °C	95	21	37
6	(6)/2AgTFA	24	50 °C	99	18	40

Reaction conditions: 0.01 mmol catalyst, 0.02 mmol AgTFA, 1 mmol alkyne, 2 mmol heterocycle, solvent: 1mL HOAc. [a] Conversions(%) and yields(%) determined by GC-MS and/or ^{1}H-NMR. For more details see the Experimental Section.

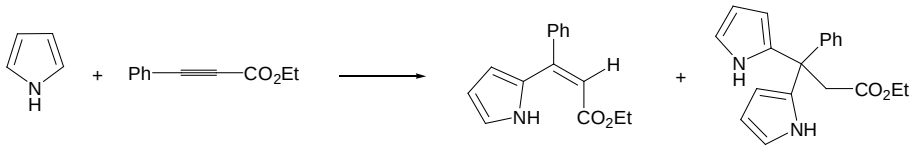

1a **2a** ***Z*-3a** **4a**

Figure 4.10 observed products in the reaction between pyrrole **1a** and ethyl phenylpropiolate **2a**.

In the reaction between pyrrole **1a** and ethyl phenylpropiolate **2a**, complex **(6)** alone has been found to be almost inactive both at room temperature and at 50 °C, reaching in this last run only 2% yield in ***Z*-3a** after 3 hours. Rather unexpectedly, even in the presence of 2 eq. AgTFA the yield reached after 2h at room temperature is low (4%), but the reaction goes to completion within 24 hours at 50 °C, despite the afforded yield in the desired product ***Z*-3a** is just 18%. The selectivity of the reaction towards this product is indeed decreased by hydration and polymerisation reactions of the alkyne and, most notably, by the formation of 3-diarylpropanoate **4a** in 40% yield (**Figure 4.10**), which becomes the main reaction product at long reaction times. With this two substrates, the diaddition product **4a** is observed in the literature with a K_2PtCl_4/AgOTf system [63] but not with $Pd(OAc)_2$ [39a]. This fact has been attributed to the higher activity of the Pt(II)-based system with respect to the Pd(II)

one. In the case of palladium-catalysed reactions, pyrrole and indole afford double hydroarylation only when ethyl but-2-ynoate and oct-2-ynoate are used [39a].

Upon considering the reaction between pyrrole **1a** and a terminal alkyne, namely ethyl propiolate, complex (**6**) has afforded the *trans*-hydroarylation product in 10% yields after 24h at room temperature. In the presence of 2 eq. of AgTFA the same complex has given a comparable yield (11%) after 5h of reaction at room temperature and the yield could not be further increased because of the complete alkyne conversion to hydrated and polymerised products. Because of this last process, the use of terminal alkynes has been avoided and ethyl phenylpropiolate has been used as standard alkyne in the following tests.

Therefore, with these preliminary observations at hand, investigation of other aromatic heterocycles has been pursued choosing ethyl phenylpropiolate **2a** as substrate and complex **(8)** pre-formed as catalyst, in order to avoid the use of silver salt. Aromatic heterocycles of different nature (**Figure 4.11**) have been reacted with **2a** at room temperature and the data are reported in **Table 4.8**; the reaction outcome has been checked after 24h, but the reaction time has not been optimised for any of the heterocycle employed.

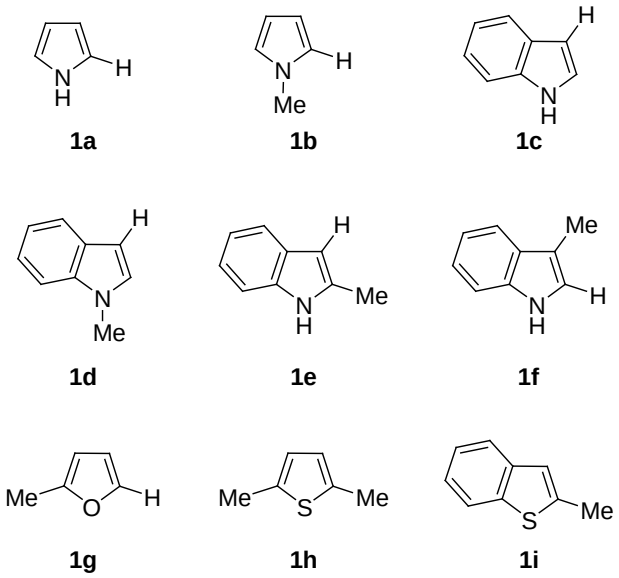

Figure 4.11 Heterocycles employed as substrates.

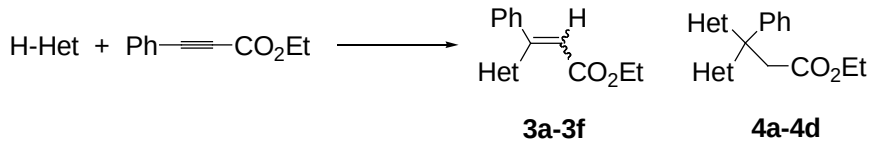

3a-3f **4a-4d**

Figure 4.12 observed products in the reaction between heterocycles **1a-1f** and ethyl phenylpropiolate **2a**.

Table 4.8 Conversions(%) and yields(%) for the reaction of ethyl phenylpropiolate **2a** with different aromatic heterocycles catalysed by complex **(8)**.

Heterocycle	Time (h)	2a Conversion(%)[a]	Yield(%)[a] (*Z*:*E*)			
1a	24	90	**3a**	46	**4a**	18
1b	24	43	**3b**	36(17:1)	**4b**	1
1c	24	22	**3c**	20(1:3)	**4c**	2
1d	24	26	**3d**	17(5:12)	**4d**	9
1e	24	54	**3e**	54(10:17)	-	-
	48	77		77(10:38)	-	-
1f	24	20	**3f**	20(17:3)	-	-

Reaction conditions: 0.01 mmol catalyst, 1 mmol alkyne, 2 mmol heterocycle, solvent: 1mL HOAc, 25 °C. [a] Conversions(%) and yields(%) determined by GC-MS and/or ^{1}H-NMR. For more details see the Experimental Section.

The obtained results have confirmed the general trend in this type of reactions: pyrrole and furane substrates undergo reaction at 2-position of the aromatic ring, as it is invariably the case in aromatic substitution reactions; however, if the 2-position is occupied by substituents, the reaction can occur at the 3-position. For indole substrates, instead, functionalisation normally takes place at 3-position, but it can occur at 2-position if the 3-position of the aromatic ring is substituted.

Moreover, the rate and the selectivity of the reaction have found to be strongly dependent on the nature of the heterocycle employed.

In particular, pyrrole **1a** has displayed the highest conversion among the analysed substrates (90%) with 51% selectivity towards the desired product ***Z*-3a**, being 18% the yield in the adduct **4a** and 23% the yield in another product not yet identified. Compared to simple pyrrole, 1-methylpyrrole **1b** has exhibited a lower reactivity

(43%), which is probably a consequence of the increased steric hindrance at the attack site.

Upon considering different kinds of indoles, it has been observed that the most reactive is 2-methylindole **1e** with 54% alkyne conversion, whereas the other indoles **1c**, **1d** and **1f** present a lower reactivity (26-20% conversion).

The nature of the heterocycle considerably influences the selectivity of the reaction as well: the main side-product observed is also in this case the 3-diarylpropanoate **4**, whose formation is influenced mainly by steric factors. For example it is not formed with 2-methylindole **1e** and 3-methyindole **1f**, which possess an enhanced steric hindrance at the functionalisable C-H bond.

However, all the analysed heterocycles have given a mixture of isomers *Z*/*E*, because of the occurrence of an isomerisation process from the *Z* product to the more thermodynamically stable *E*-arylalkene. In the case of 1-methylpyrrole **1b** also a small percentage (5%) of an hydroarylated product deriving from the functionalisation of the heterocycle in 3-position has been observed together with the correspondent diadduct **4b'**.

In general, the dicarbene-based catalytic system has exhibited good activities compared with the Fujiwara's one, which requires higher amounts of catalyst (5 mol%) [39a]. Yields can be increased prolonging the reaction times, as done with 2-methylindole **1e** which has reached 77% alkyne conversion after 48 h, although this entails a change in selectivity evidenced by the decreased *Z*/*E* ratio. Moreover, in the case of heterocycles **1a-1d** affording diaddition products, prolonging the reaction time the amount of **4** increases at the expense of hydroarylation product **3**. This may be interesting for the production of 3-diarylpropanoates.

Subsequently, a screening of different catalytic systems in the reaction between 1-methylpyrrole **1b** and ethyl phenylpropiolate **2a** has been performed. The nature of the counter-anion, of the metal and the kind of complex has been varied and the results are listed in **Table 4.9**.

Table 4.9 Conversion(%) and products distribution for the reaction between 1-methylpyrrole **1b** and ethyl phenylpropiolate **2a** catalysed by different catalytic systems.

Entry	Catalyst	2a	Yield(%)[a]					Selectivity(%)[a]
		Conversion(%)[a]	*Z*-3b	*E*-3b	3b'	4b	4b'	in *Z*-3b
1	$Pd(OAc)_2$[b]	>99	69	11	19	-	-	70
2	$Pd(OAc)_2$	98	72	7	19	-	-	73
3	$Pd(OAc)_2$[c]	92	65	10	17	-	-	71
4	$Pt_4(OAc)_8$	94	69	10	15	-	-	73
5	$Pd(P^tBu_3)_2$	47	38	3	6	-	-	81
6	$AgBF_4$	-	-	-	-	-	-	-
7	**(6)**/$AgBF_4$	>99	50	20	2	21	7	50
8	**(6)**/AgOTf	>99	50	20	2	21	7	50
9	**(6)**/AgOAc	22	14	4	4	-	-	64
10	**(8)**	43	34	2	5	1	1	79
11	**(14)**/$AgBF_4$	58	24	13	1	15	5	41
12	**(15)**	40	27	5	6	1	1	68
13	**(12)**	>99	78	7	15	-	-	78

Reaction conditions: 0.01 mmol catalyst, excess silver salt, 1 mmol alkyne, 2 mmol heterocycle, solvent: 1mL HOAc, 24h, 25 °C). [a] Conversions(%) and yields(%) determined by GC-MS and/or ^{1}H-NMR. [b] 0.05 mmol catalyst, 1 mmol alkyne, 2 mmol heterocycle. [c] 0.01 mmol catalyst, 1 mmol alkyne, 1 mmol heterocycle. For more details see the Experimental Section.

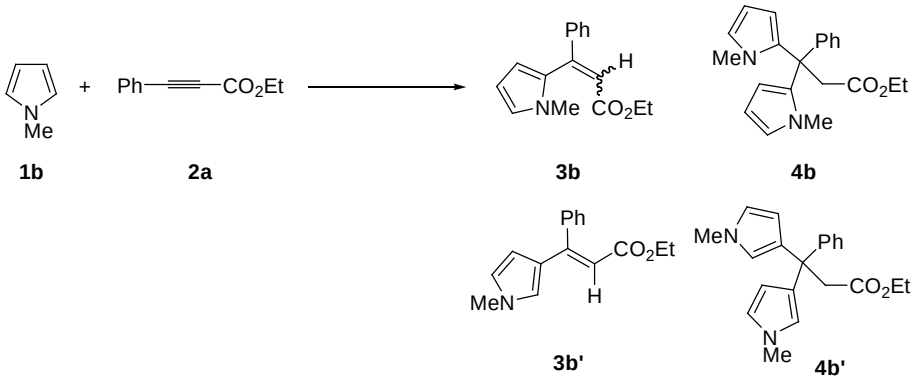

Figure 4.13 Possible products in the reaction between 1-methylpyrrole **1b** and ethyl phenylpropiolate **2a**.

Firstly, a comparative test using 5 mol% palladium acetate has been done with heterocycle/alkyne ratio 2/1 (**entry 1**), obtaining quantitative conversion with 70% selectivity towards the desired product ***Z*-3b**. Other products have been also detected in the reaction mixture, identified as ethyl (2*E*)-3-(2-pyrryl)-phenylpropenoate ***E*-3b** and ethyl (2*E*)-3-(3-pyrryl)-phenylpropenoate **3b'**, in 11% and 19% yield respectively.

At long reaction times (24h), the reaction proceeds very smoothly with excellent yields in the presence of smaller load of palladium acetate (1 mol%, **entry 2**) also using substrates in a stoichiometric ratio (**entry 3**). Moreover, palladium acetate has displayed a slightly better efficiency than platinum acetate tested under the same reaction conditions (compare **entry 1** and **4**), but similar selectivity. A Pd(0) compound has been also tested (**entry 5**) founding an unexpected activity, since the catalytic cycle proposed in the literature involves exclusively Pd(II) species [39, 56]. The observed reactivity is probably due to a partial oxidation of the compound in the reaction conditions.

Considering carbene-based catalytic systems, it is evident that in general they perform quite well in the reaction. Complex **(8)** alone or complex **(6)** in the presence of an excess AgOAc have reacted more sluggishly with respect to the systems formed by complex **(6)**/**$AgBF_4$-AgOTf** (compare **entry 7**, **8** with **entry 9**, **10**); silver additives possessing poor or non-coordinating anions efficiently extract halide ligands from the metal, providing highly cationic complexes able to catalyse the reaction with quantitative conversions. Also monocarbene complex **(12)** [44g] has shown an excellent reactivity (>99%) with 78% selectivity towards ***Z*-3b** (**entry 13**).

A controlled experiment has allowed to verify that, under the employed conditions, $AgBF_4$ itself has the only role of removing the halides from the metal and does not take part to the catalytic hydroarylation of ethyl phenylpropiolate (**entry 6**). Differently from the reaction with pyrrole, polymerisation products of the alkyne has not been observed with this heterocycle.

Dicarbene Pt(II) complex **(14)** [44l] shown in **Figure 4.9** in combination with 2 eq. $AgBF_4$ (**entry 11**) and complex **(15)** (**entry 12**) have been also tested as catalysts in the reaction, but they have shown lower activities with respect to the analogues of Pd(II) (**entry 7** and **10**).

The formation of at least two side-products has been observed with all the catalyst employed in this study: the *trans*-arylalkene ***E*-3b** and product **(3b')**, deriving from the functionalisation of the 3-position at the heterocycle.

With dicarbene complexes bearing poor-coordinating anionic ligand (CF_3COO^-, $CF_3SO_3^-$, BF_4^-) two regioisomeric 3-diarylpropanoates **(4b)** and **(4b')** have been additionally obtained. In particular it needs to be noticed that, the more the anionic ligand is weakly- or poor-coordinating ($CF_3SO_3^-$, BF_4^-), the higher is the yield in these adducts, so that their formation seems to be coherently favoured by less-hindered complexes (**entry 7**, **8**, **11**). Furthermore, poor-coordinating species allow generation of highly dicationic complexes thus increasing the metal electrophilicity.

In conclusion, in the reaction between 1-methylpyrrole **1b** and ethyl phenylpropiolate **2a**, simple palladium acetate together with monocarbene complex **(12)** and complex **(6)**/**$AgBF_4$** or **AgOTf** have afforded the best activities among the catalysts investigated.

The system formed by complex **(6)**/**$AgBF_4$** has been subsequently tested in the reaction of **2a** with other heterocycles, in order to evaluate the distribution of diadducts upon changing the substrates. Results obtained using this catalytic system are shown in **Table 4.10**.

Table 4.10 Conversions(%) and yields(%) for the reaction of ethyl phenylpropiolate **2a** with different aromatic heterocycles catalysed by complex **(6)** in the presence of $AgBF_4$.

Heterocycle	2a Conversion(%)[a]	Yield(%)[a] (*Z*:*E*)			
1b	98	**3b**	70(5:2)	**4b**	21
1c[b]	64	**3c**	25(7:18)	**4c**	2
1d	96	**3d**	66(1:23)	**4d**	30
1e[b]	88	**3e**	72(51:21)	-	-
1f[b]	80	**3f**	53(30:23)	**4f**	8
1g	35	**3g**	17(1:0)	**4g**	18
1h	-	-	-	-	-
1i	-	-	-	-	-

Reaction conditions: 0.01 mmol catalyst, excess silver salt, 1 mmol alkyne, 2 mmol heterocycle, solvent: 1mL HOAc, 25 °C, 24h. [a] Conversions(%) and yields(%) determined by GC-MS and/or ^{1}H-NMR. [b] The rest of the conversion of **2a** are other products not yet identified. For more details see the Experimental Section.

It is evident that the catalytic system formed by complex **(6)** and $AgBF_4$ is more efficient than complex **(8)**, although the selectivity of the reaction towards the hydroarylated product is lower. Diadducts products have not been observed with substrate **1e** whereas, in some case, the yields in these products are quite high, as observed for **1b**, **1d**, **1g**. Unsubstituted pyrrole **1a** has displayed very high reactivity (>99%), but with low selectivity because of parallel reaction, like polimerisation and hydration of the alkyne.

S-containing heterocycles **1h** and **1i**, instead, have not undergone reaction, whereas 2-methylfurane **1g** has reacted very slowly affording the arylalkene ***Z*-3g** with 17% yield and the diaddition product **4g** with 18% yield. Despite the electrophilic substitution occurs very easily on these electron-rich substrates, the presence of donor heteroatoms, such as O an S, can inhibit the reaction because of their tendency to bind electrophilic metal centres thus blocking irreversibly the coordination sites [64].

In conclusion, chelating dicarbene Pd(II) and Pt(II) complexes efficiently catalyse the reaction of alkynoates with aromatic heterocycles at room temperature with only 1% catalyst load. More interestingly, design of dicationic and low-hindered complexes adopting suitable additives has led to a considerable change in the outcome of the reaction. It has been indeed observed the unexpected formation of heterocycle/alkyne adducts 2/1 at long reaction times, besides an increase in the efficiency of the complex. Considering that **4a-4d** and **4f** products are a peculiarity of this catalytic system and are not obtained with the other Pd-based systems employed in the literature, it seems noteworthy to develop a new reaction protocol for the production of these molecules with symmetrical and also asymmetrical heterocycle substitution.

CHAPTER 5
INVESTIGATION OF THE REACTION MECHANISM

5.1 Determination of the kinetic law

There is still some controversy about the type of mechanism involved in the Fujiwara reaction. One proposal suggests the initial electrophilic metalation of the arene [26], whereas the second one proposes a preliminary coordination/electrophilic activation of the alkyne [37] (**Figure 5.1**).

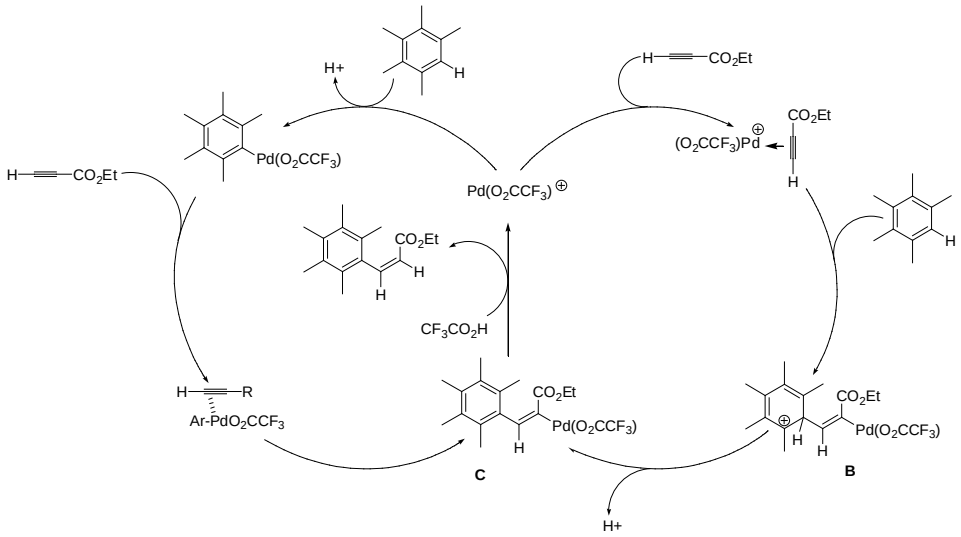

Figure 5.1 Proposed mechanism for the Fujiwara reaction. On the left cycle electrophilic metalation of the arene, on the right cycle electrophilic activation of the alkyne.

During this thesis work, several attempts to clarify the kind of mechanism have been made, firstly through NMR investigations. The limitation of this technique, due the easy exchange between deuterated solvents (CF_3COOD) and both the arene and the alkyne, has not allowed to distinguish the kind of mechanism. Moreover, the low solubility of dicarbene complexes in the common deuterated solvents has further complicated these analyses.

Therefore, studies on the rate of the reaction have been made in order to define the reaction mechanism. The reactions have been performed at 40 °C using complex **(6)** as catalyst in the presence of 2 equivalents AgTFA and the molar concentrations of

reagents and products at different reaction times have been determined by analysing *via* ^{1}H NMR portion of the reaction solution.

The scheme reported in **Figure 5.2** represents the simplest case of a catalytic reaction involving two reactive substrates [65] (substrate **1** and substrate **2**), whose concentration simultaneously changes during the reaction. The intermediate **4**, which can be in this case identified as the catalyst, reacts with substrate **1** affording intermediate **5**. Subsequently, species **5** reacts with substrate **2** giving the product **3** and regenerating the catalyst **4**.

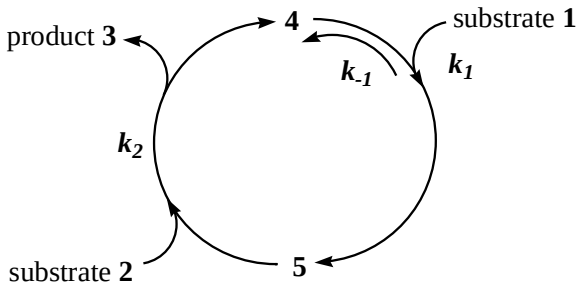

Figure 5.2 Simplest scheme of a mechanism involving a catalytic reaction with two reagents.

The kinetic equation defines the reaction rate *v* as a function of the reagents' concentration and, for this reaction, it can be represented in a first approximation as equation **(5.1)**:

$$v = \frac{k_1 k_2 [1][2][4]_{tot}}{k_{-1} + k_1[1] + k_2[2]} \qquad \textbf{(5.1)}$$

in which $\mathbf{[4]_{tot}}$ is the concentration of the introduced catalyst and consequently the sum of the concentrations of intermediates **4** and **5** in every stage of the reaction.

In order to gain more information about the kinetic law, the reaction rate has been determined by varying the concentration of one substrate, while maintaining fixed the concentration of the other components of the kinetic law.

Firstly, the reaction order in arene has been determined. This has been done by determining the conversions curves in the presence of a large excess alkyne with respect to the arene and by maintaining unchanged the concentrations of catalyst, AgTFA and trifluoroacetic acid. For simplicity, substrate **1** has been associated to the alkyne and substrate **2** to the arene; furthermore, some modifications have been brought to the previously reported kinetic law, since the dependence of the reaction rate on the acid concentration has been now expressed. In the presence of a large excess of substrate **1**, [1]>>[2] and the rate equation **(5.1)** is reduced to **(5.2)**.

$$v = k_2[2][4]_{tot} = k_{oss}[2] \qquad \textbf{(5.2)}$$

where, in this specific case, $k_{oss} = k_2[4]_{tot}[H^+]^n$

i.e. the k_{oss} contains a term describing the dependence of the reaction rate on the acid concentration. For simplicity this dependence is now described by the generic term *n*, but the dependence on the acid could be even more complicated.

Several tests have been carried out and the experimental conditions are reported in **Table 5.1**. The dependence of arene concentration on time is reported in **Figure 5.3**, whereas the logarithm of arene concentration as a function of time has been represented in **Figure 5.4** obtaining a straight line, indicative of a first order reaction.

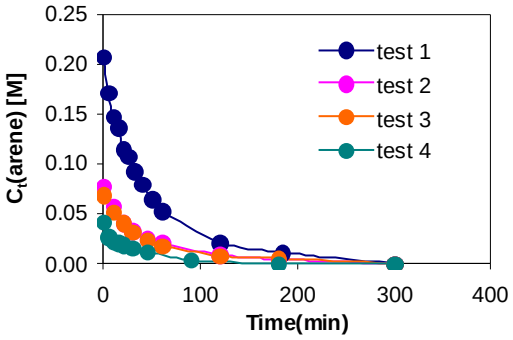

Figure 5.3 Arene concentration *vs* time in the presence of a large excess alkyne.

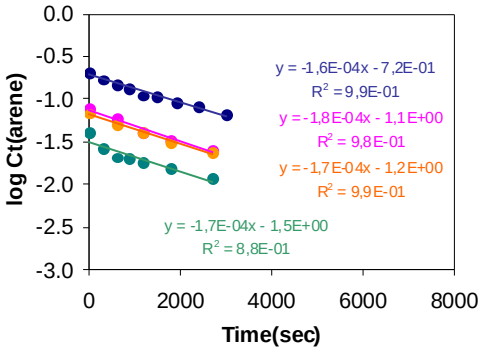

Figure 5.4 Linear interpolation of the logarithm of arene concentration *vs* time.

The integrate equation of the kinetic law is therefore a pseudo-first order law in arene **(5.3)**, confirming the form of the proposed law, and the concentration of the species under exam decreases exponentially with time.

$$\log[arene]_t = \log[arene]_0 - (k_{oss}/2.303)t \qquad \textbf{(5.3)}$$

From this expression is possible to derive the k_{oss} value and thus $k_2[H^+]^n$ using equation **(5.2)** (where $[4]_{tot}$ = [cat]).

In **Table 5.1** the experimental conditions and the obtained values of k_{oss} and $k_2[H^+]^n$, are reported.

Table 5.1 Experimental conditions and values of k_{oss} for the test conducted in the presence of a large excess alkyne.

Test	[arene] [M]	[alkyne] [M]	[arene]/[alkyne]	k_{oss} [a] [s^{-1}]	$k_2[H^+]^n = k_{oss}/[cat]$ [s^{-1} M^{-1}]
1	0.207	2.079	1/10	3.73 E-04	0.18
2	0.077	1.162	1/15	4.20 E-04	0.20
3	0.069	2.079	1/30	3.97 E-04	0.19
4	0.041	2.079	1/50	4.02 E-04	0.19

Reaction conditions: complex **(6)** = $2.079 \cdot 10^{-3}$ M, AgTFA = $4.198 \cdot 10^{-3}$ M, solvent: CF_3COOH/DCE = 4mL/1mL, 40°C. Conversions(%) determined by ^{1}H-NMR. [a] k_{oss} = p·2.303, where p is the slope of the line interpolating the data in **Figure 5.4**.

The diagram of k_{oss} as a function of alkyne concentration shows that k_{oss} (and consequently $k_2[H^+]^n$) has a constant value (**Figure 5.5**). This fact means that the rate limiting step of the reaction is the attack of substrate **2** to intermediate **5**, since the high concentration of alkyne used implies that most catalyst is present as intermediate **5** and the reaction rate becomes independent of k_1.

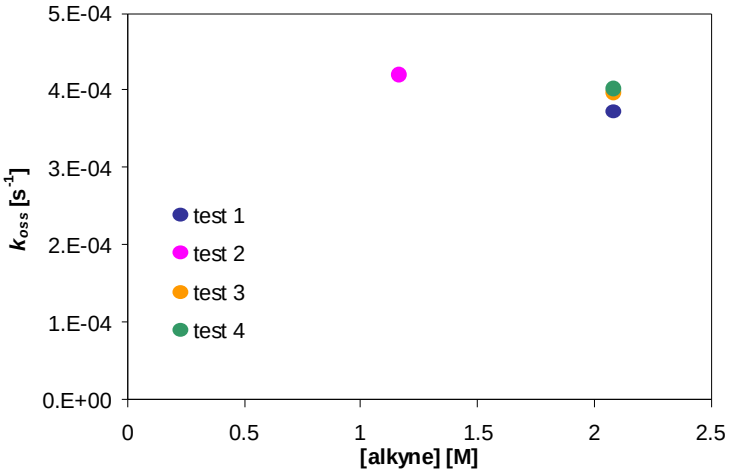

Figure 5.5 k_{oss} values determined for tests 1-4 *vs* alkyne concentration.

Similarly, the order in alkyne has been evaluated, using a large excess of arene (substrate **2**) with respect to the alkyne. The rate equation **(5.1)** is reduced in this case to equation **(5.4)**.

$$v = k_{oss'}[alkyne] = k_1[1][4]_{tot}[H^+]^n \qquad \textbf{(5.4)}$$

$$\log[alkyne]_t = \log[alkyne]_0 - (k_{oss'}/2.303)t$$

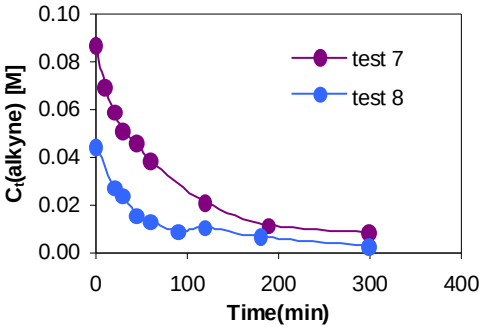

Figure 5.6 Alkyne concentration *vs* time in the presence of a large excess arene.

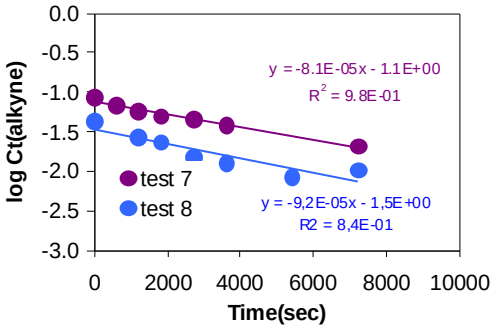

Figure 5.7 Linear interpolation of the logarithm of alkyne concentration *vs* time.

Under the employed conditions the reaction turned out to be first order also in alkyne; consequently, through the linear interpolation of the data shown **Figure 5.7**, values of $k_{oss'}$ and of $k_1[H^+]^n$ have been determined (**Table 5.2**).

Table 5.2 Experimental conditions and values of $k_{oss'}$ for the test conducted in the presence of a large excess arene.

Test	[arene] [M]	[alkyne] [M]	[arene]/[alkyne]	$k_{oss'}$,[a] [s^{-1}]	$k_1[H^+]^n = k_{oss'}$/[cat] [s^{-1} M^{-1}]
7	1.310	0.088	15/1	1.88 E-04	0.09
8	0.658	0.044	15/1	2.12 E-04	0.10

Reaction conditions: complex **(6)** = $2.079 \cdot 10^{-3}$ M, AgTFA = $4.198 \cdot 10^{-3}$ M, solvent: CF_3COOH/DCE = 4mL/1mL, 40 °C. Conversions(%) determined by ^{1}H-NMR. [a] $k_{oss'}$ = p·2.303, where p is the slope of the line interpolating the data in **Figure 5.7**.

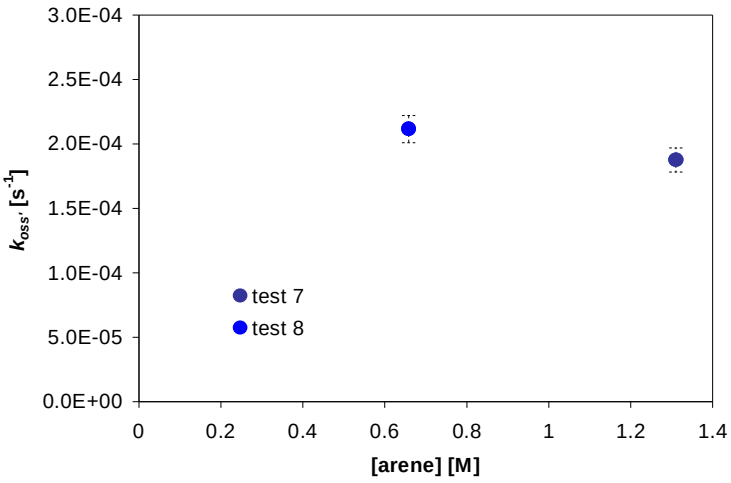

Figure 5.8 $k_{oss'}$ values determined for tests 7-8 *vs* arene concentration.

Under these reaction conditions, the catalyst is prevalently present in form **4** and the rate determining step is represented by the attack of alkyne to the metal (i.e. attack of substrate **1** to intermediate **4**).

This type of kinetic studies does not allow to determine the sequence of substrate to metal interaction, so that it has not been clarified if the arene or the alkyne first coordinates the catalyst.

As expected, the reaction turned out also to be first order in palladium and this is clearly evidenced by **Figure 5.10** and **5.11**.

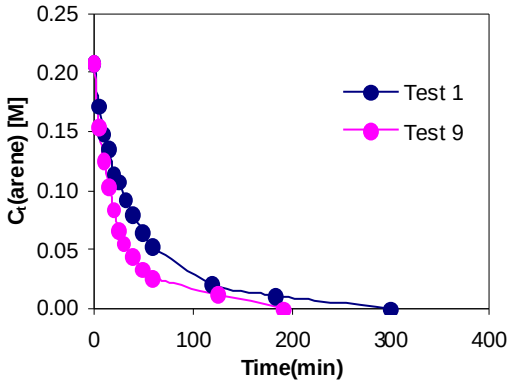

Figure 5.9 Arene concentration *vs* time in conditions of large excess alkyne and different amounts of catalyst.

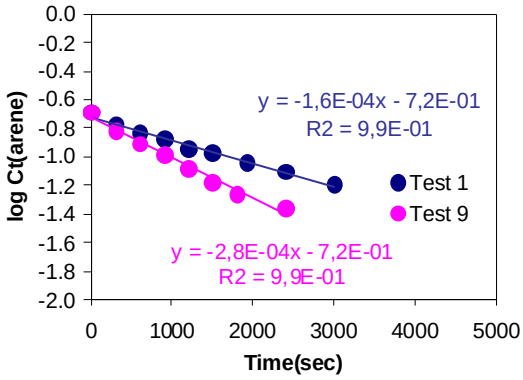

Figure 5.10 Linear interpolation of the logarithm of arene concentration *vs* time, using different amounts of catalyst.

In **Table 5.3** the experimental conditions and the obtained values of k_{oss}'' are reported.

Table 5.3 Experimental conditions and values of k_{oss}'' for the test conducted in the presence of a large excess arene and using different amounts of catalyst **(6)**.

Test	[Pd] [M]	[AgTFA] [M]	[arene] [M]	[alkyne] [M]	[arene]/ [alkyne]	k_{oss}''^{a} [s^{-1}]
1	2.084 E-03	4.14 E-03	0.207	2.079	1/10	3.73 E-04
9	4.167 E-03	8.28 E-03	0.207	2.079	1/10	6.55 E-04

Reaction conditions: solvent: CF_3COOH/DCE = 4mL/1mL, 40 °C. Conversions(%) determined by ^{1}H-NMR. ^{a} k_{oss}'' = p·2.303, where p is the slope of the line interpolating the data in **Figure 5.10**.

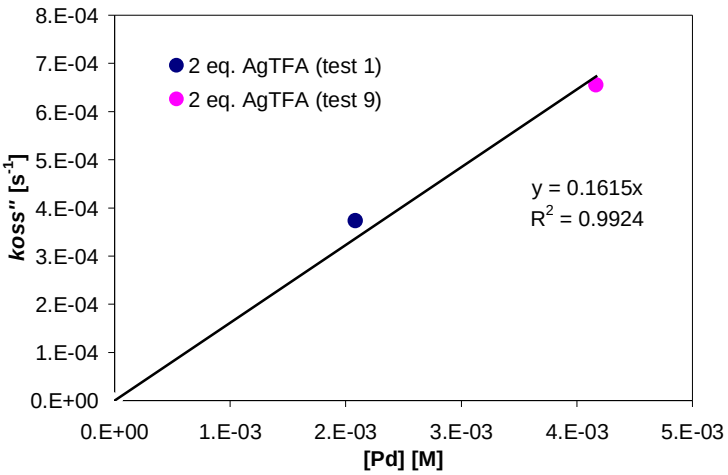

Figure 5.11 k_{oss}'' values determined for tests 1 and 9 *vs* palladium concentration.

It remains to determine the dependence of the reaction rate on the acid concentration. Indeed, in the previous experiments, the amount of acid is high enough to not influence the rate of the reaction. At lower acid amounts the reaction rate is instead significantly lower, as also demonstrated in the studies performed in **Chapter 3** (see page 46).

These kinetic results should be considered preliminary and a much more complex rate equation may be necessary to take into account the acidity contribution.

CHAPTER 6
CATALYTIC APPLICATION OF CHELATING DICARBENE COMPLEXES TO OTHER AROMATIC C-H BOND FUNCTIONALISATION REACTIONS

6.1 Oxidative coupling of anilides with olefins

The arylation of olefins is another useful method to form new C-C bonds and it usually involves aryl halides as substrates. A mild synthetic process for *ortho*-functionalising anilide derivatives with olefins, catalysed by palladium acetate in the presence of cheap oxidants, has been reported in the recent literature (**Figure 6.1**) [66a]. This method does not require prefunctionalisation of substrates, offering an important breakthrough in the synthesis of anilide derivatives. The reaction between acetanilide and *n*-butyl acrylate proceeds at room temperature and implies the use of 2 mol% catalyst and benzoquinone (BQ) as stoichiometric oxidant, giving the Heck-like product (*E*)-3-(2-(acetylamino)phenyl)propenoic acid butyl ester as the only product. A mixture of HOAc and toluene is commonly employed as solvent since the use of stronger acids, as trifluoroacetic acid, does not bring significant improvements to the yields.

Figure 6.1 Functionalisation of the aromatic C-H bond of acetanilide with *n*-butyl acrylate.

The importance of the *ortho*-directing effect of the amide group is evidenced by the high selectivity of the reaction towards the 2-substituted product, being 3- or 4-substituted anilides never obtained. Moreover, neither products resulting from N-H bond activation nor C-H functionalisation of the toluene, employed as solvent, have been observed.

In agreement with the mechanism proposed by Fujiwara for the coupling of arenes with olefins [23b] the reaction involves the initial formation of a σ-arylpalladium complex, through electrophilic metalation of the aromatic C-H bond, and the subsequent olefin coordination to the palladium centre. The *sin*-insertion of the olefin is followed by a β-elimination reaction to give the final product and Pd(0) species. Benzoquinone is added to reoxidate Pd(0) to Pd(II) through *in situ*-formation of BQ-Pd(0) species; BQ can also act as a ligand, stabilising the different Pd species formed during the catalytic cycle.

A substoichiometric amount (0.5 - 1.0 eq.) of an acid co-catalyst (such as *p*-toluenesulfonic acid) is also necessary to make the reaction proceed, because it probably forms *in situ* highly electrophilic Pd(II) species. Additionally, the acid seems to help the decomposition of the Pd(0)-BQ intermediate, thus facilitating Pd(0) reoxidation. A high amount of this co-catalyst promotes, on the contrary, an acid-catalysed polimerisation of the olefin.

Dicarbene complexes **(2)**, **(6)** and monocarbene complex **(12)** shown in **Figure 6.2** have been tested in the reaction between acetanilide and *n*-butyl acrylate and the results are listed in **Table 6.1**.

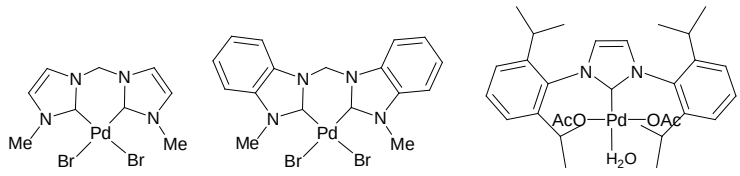

Figure 6.2 Carbene complexes of Pd(II) employed in this work.

Dicarbene complex **(2)** has resulted completely inactive both at room temperature and at 80 °C (**entry 1** and **2**), whereas complex **(6)** in the presence of an excess of $AgBF_4$ has shown reactivity only at 80 °C, affording 21% yield in the product (**entry 4**). The addition of a silver salt possessing a non-coordinating anion helps the creation of free coordination sites, thus enhancing the activity of the complex, although yields are still low. Coordination of acetanilide at the metal centre [67], which is probably the first

step of the reaction, seems to be easier when the steric hindrance is limited and probably this step requires two free coordination sites. This fact could explain the different reactivity between complex **(2)** and the system formed by complex **(6)** + **$AgBF_4$**. For this latter system coordination of the amide group to the metal probably occurs easily because of the minor steric hindrance, thus favouring the C-H activation process.

Table 6.1 Yields(%) in the reaction between acetanilide and n-butyl acrylate catalysed by 2 mol% carbene complexes.

Entry	Catalyst/ Co-catalyst	Oxidant	Temperature	Yield(%)[a]
1	**(2)**	1 eq. BQ	r.t.	-
2	**(2)**	1 eq. BQ	80 °C	-
3[b]	**(6)/$AgBF_4$**	1 eq. BQ	r.t.	-
4[b]	**(6)/$AgBF_4$**	1 eq. BQ	80 °C	21
5	**(12)**	1 eq. BQ	r.t.	10
6	**(12)**	1 eq. BQ	80 °C	73
7	**(12)**	O_2 atm.	80 °C	7
8	**(12)**	1 eq. BQ, O_2 atm.	80 °C	72
9[c]	**(12)**	1 eq. BQ	80 °C	29

Reaction conditions: acetanilide (1 eq., 0.5 mmol), *n*-butyl acrylate (1.1 eq., 0.55 mmol), catalyst (0.02 eq., 0.01 mmol), ***p*-toluenesulfonic acid** (0.5 eq., 0.25 mmol), solvent: HOAc/toluene = 0.75mL/0.37mL, 16h. [a] Yields(%) determined by ^{1}H-NMR. [b] Excess of silver salt. [c] **0.5 eq. trifluoroacetic acid** instead of *p*-toluenesulfonic acid. For more details see the Experimental Section.

On the contrary, monocarbene complex **(12)** has been found to be active also at room temperature (**entry 5**), although with low yields (10%), and it has presented a good reactivity at 80 °C (73%, **entry 6**), but slightly lower than the reactivity of palladium acetate at room temperature (85%) [66a]. Attempts to increase the yields adding other type of oxidants, such as oxygen, have not given better results (**entry 7** and **8**). Furthermore, the substitution of *p*-toluenesulfonic acid with trifuoroacetic acid (**entry 9**) has given worse yields in the desired product, confirming that *p*-toluenesulfonic acid is the best additive for the reaction.

The same dicarbene complexes gave unsatisfactory results in previous studies performed by this research group on the oxidation of alcohols and in Wacker-type oxidative couplings [68], which require a reoxidation step as well. Chelating dicarbene palladium(II) complexes can be therefore regarded as quite inefficient catalysts for reactions which involve a catalyst reoxidation step.

CHAPTER 7
ELECTROCHEMISTRY OF DICARBENE Pd(II) COMPLEXES

7.1 Introduction to electrode processes [69]

An electrochemical system is essentially constituted by an electrolyte solution and a pair of electrodes, connected through an electrical circuit. The main process involved is the transport of charge taking place across different types of interfaces, in particular between an electronic (*electrode*) and an ionic (*electrolyte*) conductor. The charge is transported through the electrode by the movement of electrons and holes and some typical electrode materials are for example solid metals (Pt, Au), liquid metals (Hg, amalgams), carbon (graphite or glassy carbon) and semiconductors (In-Sn oxide, Si). In the electrolyte phase, instead, the charge is carried by the movement of ions which most commonly are H^+, Na^+, Cl^- in water.

A common electrochemical cell is constituted by at least two electrodes immersed in an electrolytic solution where a redox couple is dissolved. In equation **(7.1)** is represented a typical redox reaction where the species of interest passes from its oxidated state (O) to its reduced form (R), through the exchange of *n* electrons with an electrode.

$$O + ne \rightleftharpoons R \qquad \textbf{(7.1)}$$

This reaction takes place only if an appropriate potential difference is present between the two electrodes.

An electrochemical experiment is generally built up to study both the kinetics and termodynamics of this electrochemical reaction. The cell used for electroanalytical measurements (**Figure 7.1**) is normally made in pyrex glass, due to the transparency and general chemical inertness of this material. The electrode where the above reduction reaction occurs is called the *working electrode* (WE), while an oxidation reaction occurs at the *counter electrode* (CE), allowing the current to pass from the external circuits through the cell. However, there are often three electrodes in the system: the WE, the CE and a *reference electrode* (RE), made up with phases having

essentially constant composition, so that its potential is fixed (**Figure 7.2**). The potentials applied to the other electrodes are then referred to the RE used and any changes in the cell are ascribable just to the WE. *The combination of the solvent, electrolyte and specific working electrode material determines the useful range of potential in which measurement can accomplished.*

Figure 7.1 Typical oxygen-free pirex glass cell used in the electroanalytical measurements. http://www.xenosystem.com/ckseo/als/010914-2.jpg

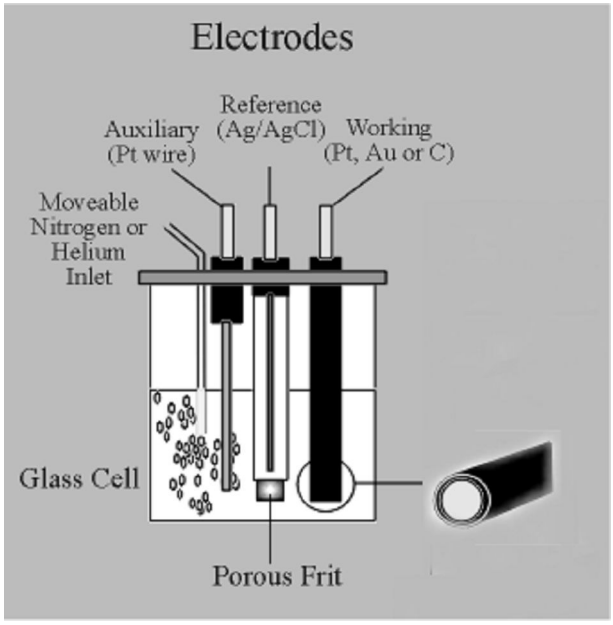

Figure 7.2 Example of an electrochemical cell with a *working electrode* (WE), a *counter electrode* (CE), a *reference electrode* (RE) and a flux of inert gas. http://www.chem.ucla.edu/~bacher/CHEM174/equipment/CV1.html

Usually, noble metal electrodes are used as WE, such as Pt, Au and Ag and occasionally Pd, Ni and Cu. Also carbon indicator electrodes are widely employed as WE, and are very useful for both oxidation and reduction processes in aqueous and nonaqueous solutions thanks to their high inertness. As RE, the *saturated calomel electrode (SCE)* or the *Ag/AgCl/KCl electrode* are commonly utilised.

By connecting the WE to the negative side of a generator or a potentiostat, *i.e.* by driving the electrode to more negative potentials, the energy of the electrons is raised and a flow of electrons occurs from the electrode to the solution (*reductive current*).

At the contrary, if a more positive potential is imposed, the electrons transfer from the electrolyte solution to the electrode generates an *oxidation current*. The critical potentials at which these processes take place are related to the *standard potentials* $E^{\ominus}$ for the specific chemical substances in the system, that take or release electrons on the electrode/solution interface, and to the kinetics of the electron transfer (ET).

The number of electrons that crosses the interface is measured as total charge, Q, passed in the circuit (1 Coulomb = 6.24 x 10^{18} electrons) and it is related to the amount of product formed by *Faraday's Law*: *"the passage of 96485.4 C causes the consumption of 1 mole of reactant or production of 1 mole of product in a one-electron reaction*". The current *i* represents the rate of electrons' flow, and 1 A = 1 C/s.

At the electrode surface, it is possible to distinguish two different fundamental processes, named as *Faradaic* and *non-Faradaic*. The first one generates a current that follows *Faraday's law* (the amount of chemical reaction caused by the flow of current is proportional to the amount of electricity passed). From the peak position (peak potential, E_p) and current (i_p) values it is easy to gain information about the thermodynamics (formal potential of the redox process, $E^{0'}$) and kinetics (electron transfer rate constant, k_{ET}) of the reaction. Instead non-Faradaic processes do not involve a charge transfer across the solution-electrode interface. These processes occur under certain conditions, not only at the potentials at which charge transfer reactions occur, but also in the range of potential where the latter do not take place because such reactions are thermodynamically or kinetically unfavourable. Non-Faradaic processes, such as adsorption and desorption, are sensible to variations of the potential and of the composition of the solution and can change the structure of the electrode-solution interface. The process does not involve any chemical reactions (charge transfer); it only gives rise to a current due to accumulation or removal of electrical charges on the electrode and in the electrolyte solution near the electrode. Electrochemical cells where Faradaic currents are flowing are classified either as *galvanic* or *electrolytic cells*. In a galvanic cell the reactions take place spontaneously at the electrodes when they are connected externally by a conductor. In an electrolytic cell the reactions occur after the imposition of an external voltage greater than the *open-circuit potential* of the cell. The *open-circuit potential* is the

potential that would be measured when a high impedance voltmeter is placed across the cell. For some electrochemical cells it is possible to calculate the open-circuit potential from thermodynamic data via the Nernst equation, keeping in mind that there is a true equilibrium, since a redox-couple is present at each electrode.

In both electrolytic and galvanic cells, the electron current from the electrode to the solution is called *cathodic current*, while the inverse electron flow is the *anodic current*. The difference between the two types of cell is that in an electrolytic cell the cathode is negative with respect to the anode, whereas in the galvanic one the cathode is positive with respect to the anode.

In an overall electrode reaction **(7.1)**, the current is generally ruled by the rates of the following processes:

- Mass transfer (of O from the solution to the electrode).
- Electron transfer at the electrode surface.
- Chemical reactions before or after the electron transfer.
- Other surface reactions (adsorption, desorption, crystallisation).

7.2 Introduction to Cyclic Voltammetries (CVs)

The characterisation of redox processes can be achieved through a large variety of electrochemical methods, but the most common and straightforward technique used belongs to the Sweep Voltammetry family. It is based on a single potentiometric experiment in which the external voltage imposed to the electrochemical cell is swept versus time at a constant rate, allowing the direct recording of the curve I-E. The potential is varied linearly with time, so that the applied signal is a voltage ramp (see **Figure 7.3**). The scan rates, v, generally range from 10 mV s^{-1} (1 V traversed in 100 s) to about 1000 V s^{-1} with conventional electrodes (about 0.12 cm^2). When the initial potential is coincident to the final one, the experiment is called Cyclic Voltammetry (CV). A CV is therefore carried out by switching the direction of the scan at a certain time, $t = \lambda$ (or at the *switching potential*, E_λ).

In the case of the example shown in **Figures 7.3** and **7.4**, it is assumed that only the reduced form of the redox couple (R) is initially present. As the voltage is scanned in the positive direction, R is oxidised at the electrode surface to give O. At a particular potential value, the scan direction is reversed and the species O can be reduced to initial R. Once the voltage returns to the initial value, the experiment is terminated. The resulting cyclic voltammogram (CV) is shown in **Figure 7.4**.

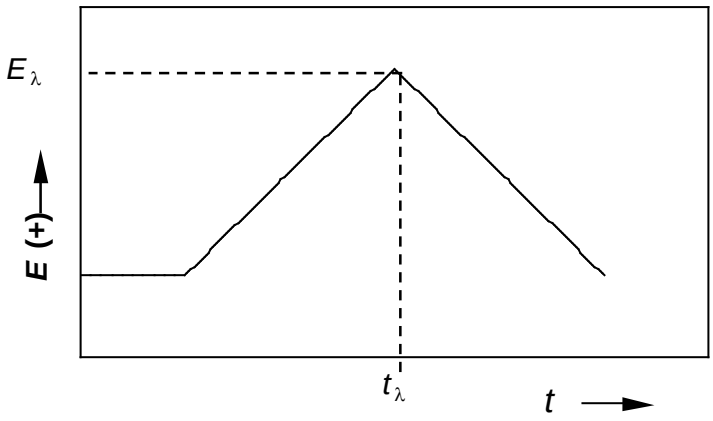

Figure 7.3 Voltage ramp *vs* time in a cyclic voltammetry experiment. t_λ is the time at which the scan potential is reversed.

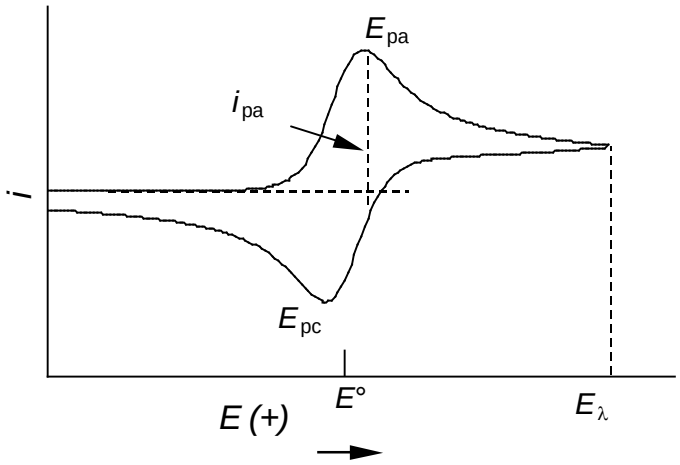

Figure 7.4 A typical cyclic voltammogram (CV) where the current *i* is plotted *vs* potential E. E_{pc} and E_{pa} represent the cathodic and the anodic peak potentials respectively, whereas E_λ is the switching potential.

At the beginning of the experiment, when the potential is lower than the redox potential of the species R in exam, there is no conversion from R to O and the current remains small with a slow growth, due to non-faradaic processes as capacitive charge of the electrode. When the redox potential is approached, there is a net anodic current which increases exponentially with potential. When conversion of R into O starts, concentration gradients are set up for both R and O in the proximity of the electrode surface and diffusion of both species occurs.

At the anodic peak (E_{pa}), the redox potential is sufficiently positive that any R that reaches the electrode is instantaneously oxidised to O so that its concentration on the electrode surface is zero. The current depends, from now, upon the rate of mass transfer from the bulk solution to the electrode surface, which decreases with time because of decreasing concentration gradient (Cotrell-type curve), this is why the CV has an asymmetric shape. Upon scan reversal, the current continues to decay until the potential comes near to the redox potential. At this point, the net reduction of O to R causes a cathodic current and the production of a reverse peak (E_{pc}**)**.

If the redox system remains in equilibrium throughout the potential scan, i.e. concentration of O and R are maintained at the values required by the Nernst equation, the electrochemical reaction is *reversible*. Otherwise, when electron transfer is slow or chemical reactions involving reactants and/or products take place, the electrochemical reaction is called *irreversible*.

Cyclic voltammetry of a reversible redox system is characterised by the following parameters: the peak potential separation ($\Delta E_p = E_{pa}-E_{pc}$) is equal to 57/n mV at 25 °C (n = number of electrons transferred in the redox process); the half peak width (difference between E_p and the potential at half peak height) is 28.5/n mV at 25 °C; the peak current ratio (i_{pa}/i_{pc}) is 1 and the peak current increases linearly as a function of the square root of *v*; the peak potentials are independent on scan rate and can be used to determine the formal potential $E^{0'} = (E_{pc}+E_{pa})/2$.

In the case of totally irreversible systems the peak current of a peak under diffusion control is given by the following equation [69]:

$$i_p = (2.99 \cdot 10^5)(\alpha D v)^{1/2} nAC^* \qquad \textbf{(7.2)}$$

where α is the electron transfer coefficient, *A* is the area of the electrode, *n* is the number of electrons exchanged in the overall process, and *D* and *C** are the diffusion coefficient and bulk concentration of the electroactive species. According to this equation, i_p is expected to increase linearly with $v^{1/2}$, if all other experimental parameters are kept constant and a plot of $i_p/v^{1/2}$ versus $v^{1/2}$ should give a zero-slope straight line.

In particular, if the electrode process is kinetically controlled by the electron transfer, E_p can be expressed by equation **(7.3)** [69]:

$$E_p = E^{0'} - \frac{RT}{\alpha F}\left[0.780 + \ln\left(\frac{D^{1/2}}{k^o}\right) + \ln\left(\frac{\alpha F v}{RT}\right)^{1/2}\right] \qquad \textbf{(7.3)}$$

where *k*° is the standard electron transfer rate constant and *F* is the Faraday constant. The peak potential E_p for an irreversible process is a function of scan rate and shifts in the negative direction (for a reduction process) and in the positive direction (for an oxidation process) of 29.6/α mV at 25 °C for each tenfold increase of *v*. The peak potential value (E_p) is therefore found beyond $E°'$ and it is not possible in this case to obtain the formal potential $E°'$.

As already mentioned before, in several cases the electron transfer reaction **(7.4)** is coupled with chemical reactions involving reactants and/or products. Often R is not stable and reacts with the solvent or the supporting electrolyte to give P **(7.5)**.

$$O + ne \rightleftharpoons R \qquad \textbf{(7.4)}$$

$$R \rightleftharpoons P \qquad \textbf{(7.5)}$$

where P can be an electroctive or a non-electroactive species in the potential range of interest. This kind of reaction occurs very frequently, since reactive species are often produced after electrochemical oxidation or reduction of a substance. In the specific case of an electron transfer reaction involving an organometallic species or a coordination compound, oxidation or reduction can be followed by loss of a ligand or rearrangement of the molecule.

In general, when the product of the redox reaction (R) reacts to give non-electroactive species, the parameters describing the redox reaction are perturbed. In the presence of a chemical reaction of R, indeed, $i_{pa}/i_{pc} < 1$ since R is removed from the proximity of the electrode both by diffusion and by the chemical reaction. Of course, the measured parameters of an electrode process are affected depending on the extent to which the chemical reaction occurs during the electrochemical measurement.

The transfer coefficient α, which appears in equation **(7.3)**, may assume values between 0 and 1, quite often it ranges between 0.3 and 0.7. Therefore, at 25 °C, a value of $dE_p/d\log v$ significantly smaller than -30 mV clearly indicates an electrochemical process with a rate-determining electron transfer. If $dE_p/d\log v \geq -30$ mV, the process is instead kinetically controlled by a slow chemical reaction following a reversible (or fast) ET. However, in both cases, the overall process will give rise to an irreversible voltammetric peak.

7.3 Cyclic voltammetries of dicarbene complexes

The electrochemical behaviour of palladium dicarbene complexes bearing different NHC ligands has been investigated in collaboration with Prof. Armando Gennaro and Dr. Abdirisak Ahmed Isse, Università degli Studi di Padova.

Cyclic voltammograms of the complexes have been obtained in a three-electrode electrochemical cell at 25 °C in DMSO containing tetra-*n*-butylammonium perchlorate (Bu_4NClO_4) 0.1 M as supporting electrolyte. In these experiments a glassy carbon disk has been used as working electrode, together with a Pt counter-electrode and a $Ag/AgI/I^-$ (0.1 M in DMF) reference electrode. At the end of every experiment, the reference electrode has been calibrated against the ferricinium/ferrocene (Fc^+/Fc) couple, used as an internal standard, to which all potentials reported here are referred.

The analysed complexes are readily soluble only in the solvent mixture HTFA/DCE, used in the Fujiwara reaction, and in DMSO or hot CH_3CN. Unfortunately, trifluoroacetic acid can not be used as a solvent in these electrochemical studies because H_2 discharge, due to the reduction of HTFA at the electrode, partially

overlaps with the peaks under observation. Therefore, DMSO has been chosen as solvent. Indeed, in a first approximation approach, the redox potentials obtained in DMSO can be correlated to the catalytic activity of the complexes, despite the different solvent used.

Voltammetric behaviour of Pd(II) dicarbene complexes

The electrochemical behaviour of Pd(II) dicarbene complexes **(2)**, **(4)**, **(6)**, **(9)** and **(10)** has been analysed by cyclic voltammetry under different experimental conditions. The complexes have exhibited quite similar voltammetric features, which will be illustrated in details in the case of complex **(2)** (**Figure 7.5**), chosen as an example. A cyclic voltammogram of **(2)** recorded at a scan rate (v) of 0.2 V s^{-1} is shown in **Figure 7.6**.

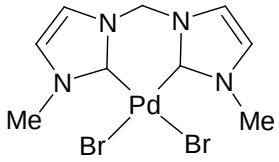

Figure 7.5 Complex **(2)**.

The complex displays a well defined reduction peak, followed by a second reduction peak of much less current intensity. No anodic peaks, associated with these reduction peaks have been observed in the reverse positive-going scan.

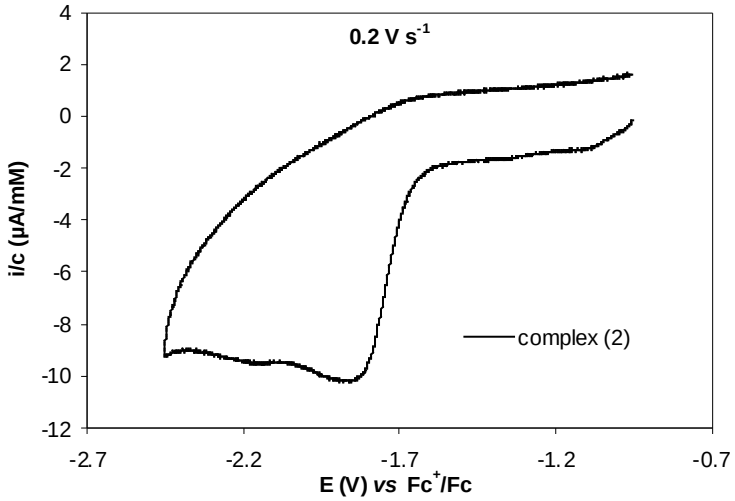

Figure 7.6 Cyclic voltammetry of **(2)** 1.51 mM in DMSO + Bu_4NClO_4 0.1 M at v = 0.2 V s^{-1}.

Considering the well known redox properties of palladium, the observed reduction peaks can be attributed to the reduction of Pd(II) to Pd(0):

$$Pd(II) + 2e^- \rightarrow Pd(0) \qquad \textbf{(7.6)}$$

The absence of anodic partners of the reduction peaks is indicative of irreversibile processes. Irreversibility may be due to slow electron transfer to Pd(II) (electrochemical irreversibility) or to instability of the reduced species of Pd(0) (chemical irreversibility) or both of them.

Although the existence of Pd(0)-bis(carbene) complexes has been reported [70], voltammetric investigations of Pd(II)-bis(carbene) complexes of similar structure as those under examination here have shown very small re-oxidation peaks for the electrogenerated Pd(0) complexes [52a], indicating that such species are not very stable.

A quite interesting feature of the voltammetric behaviour of the complex is the presence of two peaks, although of highly dissimilar height. This indicates the presence of different species in solution, which can be formed through the substitution of the halide anions bound to the metal with coordinating solvent molecules. Therefore, a precise assignment of the reduction peaks has been firstly attempted, considering all the possible complexation equilibria involving Pd(II) species.

The complex is introduced into solution as Pd(dicarbene)Br_2, but, upon dissolution in DMSO, it may lose one or both bromide ions, which are substituted by solvent molecules. The equilibria reported in **Figure 7.7** show the species that can be formed dissolving the complex in DMSO in the presence of a strong electrolyte as Bu_4NClO_4. It is known, indeed, that dicarbene complexes can easily substitute one of the halide ligands with a solvent molecule in the presence of salts like $NaPF_6$, giving the mixed complex **(2a)**. The second halide is generally substituted only using silver salts as additives and, in this case, complex **(2b)** is obtained [71].

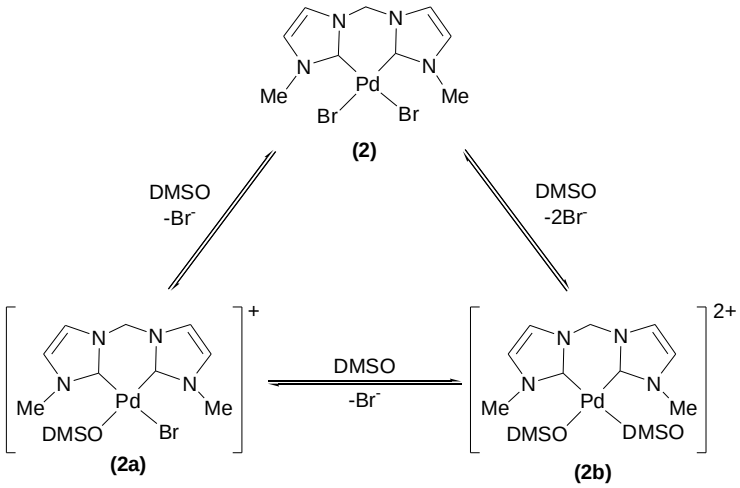

Figure 7.7 Species formed dissolving complex **(2)** in DMSO containing Bu_4NClO_4 0.1 M.

The presence of the equilibria reported in **Figure 7.7** has been confirmed by examination of the effect of *v* on the voltammetric response of complex **(2)**. This is illustrated in **Figure 7.8**. As the scan rate is increased, the second peak increases at the expense of the first and this is a clear evidence of the existence of at least two Pd(II) species in solution.

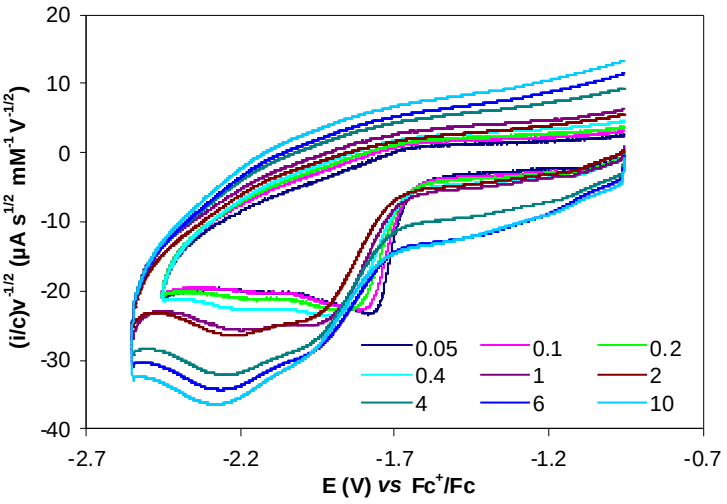

Figure 7.8 Cyclic voltammetry of **(2)** 1.51 mM in DMSO + Bu_4NClO_4 0.1 M recorded at different scan rates.

Analysis of the peak current of the first reduction process also leads to the same conclusion. As it shall be seen later, both the first and second peak represent electrochemically irreversible reduction processes.

The peak current of an irreversible voltammetric peak under diffusion control is given by equation **7.7** [69].

$$i_p = (2.99 \cdot 10^5)(\alpha D v)^{1/2} nAC^* \qquad \textbf{(7.7)}$$

where α is the electron transfer coefficient, A is the area of the electrode, n is the number of electrons exchanged in the overall process, and D and C^* are the diffusion coefficient and bulk concentration of the electroactive species. According to this equation, i_p is expected to increase linearly with $v^{1/2}$, if all other experimental parameters are kept constant. Alternatively a plot of $i_p/v^{1/2}$ versus $v^{1/2}$ should give a zero-slope straight line. Instead, a plot of $i_p/v^{1/2}$ of the first peak as a function of $v^{1/2}$ (**Figure 7.9**) shows a dramatic decrease of the normalised peak current as the scan rate is increased.

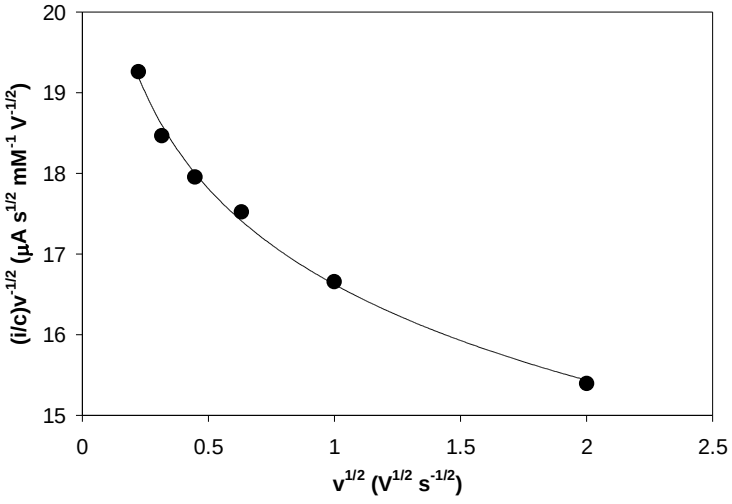

Figure 7.9 Cyclic voltammetry of **(2)** 1.51 mM in DMSO + Bu_4NClO_4 0.1 M. Dependence of the normalised peak current of the first peak on the scan rate.

This is a clear indication that the process underlying the first peak is due to the reduction of a species whose concentration varies during the experiment. In other words, this species is involved in a slow chemical reaction which replenishes it as it is consumed at the electrode. At low scan rates the experiment lasts long enough to allow the chemical reaction to regenerate continuously the electroactive species which continues to participate in the reduction reaction. At higher scan rates the time-scale of the experiment becomes shorter, so that the effect of the chemical reaction is increasingly lowered. Therefore, the current at small *v* values corresponds to an apparent substrate concentration near the electrode, which is higher than the initial equilibrium concentration in the bulk solution. The results so far described are compatible with the occurrence of the equilibria shown in **Figure 7.7**.

To assign correctly each Pd(II) species to the proper reduction peak, further experiments have been carried out with the aim of shifting the equilibrium in favour of one species or another, depending on the reaction conditions. In particular, an experiment has been performed in the presence of excess bromide ions in order to create conditions favouring the predominance of Pd(dicarbene)Br_2. The effect of the addition of increasing amounts (up to 50 equivalents) of tetraethylammonium bromide (TEABr) to a solution of **(2)** is shown in **Figures 7.10** and **7.11** at two different scan rates, namely 0.2 and 2 V s^{-1}.

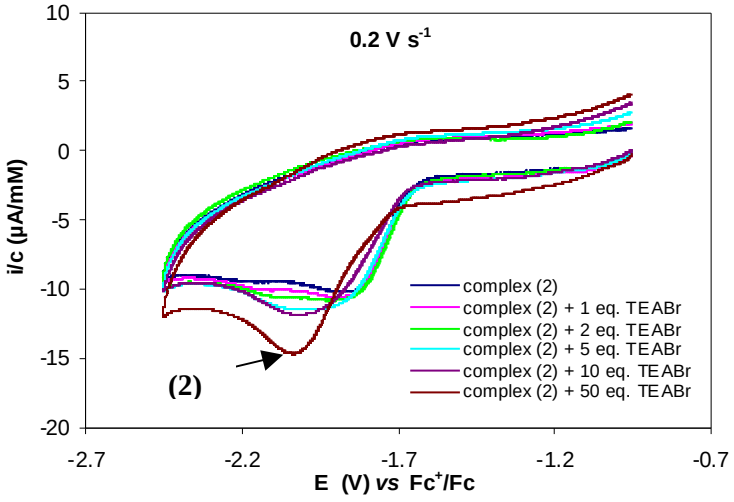

Figure 7.10 Cyclic voltammetry of **(2)** 1.51 mM in DMSO + Bu_4NClO_4 0.1 M recorded at v = 0.2 V s^{-1} in the presence of different amounts of TEABr.

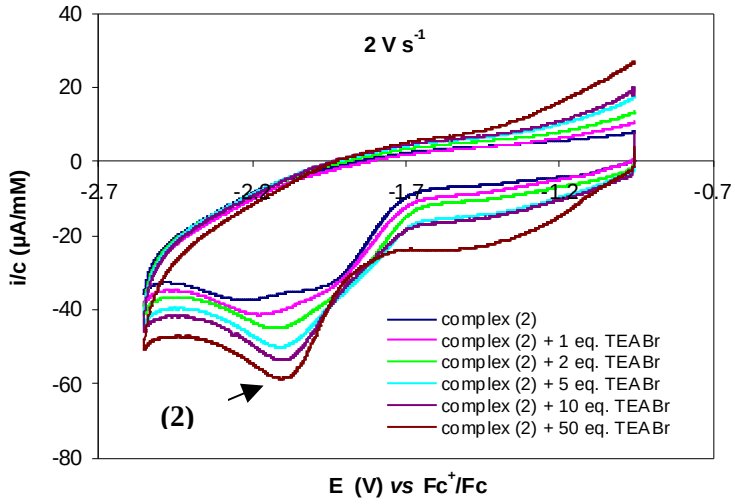

Figure 7.11 Cyclic voltammetry of **(2)** 1.51 mM in DMSO + Bu_4NClO_4 0.1 M recorded at v = 2 V s^{-1} in the presence of different amounts of TEABr.

At both scan rates, as the concentration of Br^- is increased, the second reduction peak increases at the expense of the first. When 50 equivalents of TEABr are added, the first peak almost disappears (only a shoulder can be observed), while the second develops to a well-defined peak. Considering the complexation equilibria depicted in **Figure 7.7**, it is quite reasonable to assume that, in the presence of a large excess of Br^-, the complex with the two bromide ligands is the predominant species in solution. It is therefore possible to assign the second peak at –2.0 V *vs* Fc^+/Fc to the reduction of complex **(2)**.

At low $[Br^-]/[Pd(II)]$ ratios or in the absence of added $[Br^-]$, **(2)** dissociates partially or completely to give **(2a)** and/or **(2b)**. Thus, the first reduction peak is to be attributed to one of these Pd(II) complexes.

To distinguish between these two possibilities, cyclic voltammetry of complex **(2)** has been examined in the presence of 2 equivalents of AgTFA (**Figure 7.12**). As already demonstrated in **Paragraph 3.8**, under these conditions the complex should substitute both halide ligands to give the bis-trifluoroacetate complex. In **Figure 7.12** it is shown that the voltammetric pattern of the complex is strongly modified in these conditions: both the first and the second peak considerably decrease, the latter

completely disappearing, while a new peak appears at -1.7 V *vs* Fc^+/Fc. As it is described later, this new peak is attributable to the reduction of the di-solvento species **(2b)** (see further page 136).

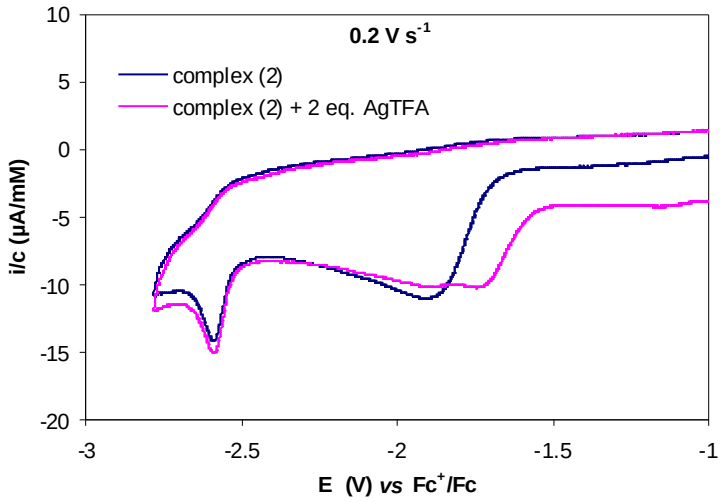

Figure 7.12 Cyclic voltammetry of **(2)** 0.86 mM in DMSO + Bu_4NClO_4 0.1 M recorded at v = 2 V s^{-1} in the absence and presence of 2 eq. AgTFA.

This has allowed identification of the first peak, observed recording the CV of complex **(2)** in the absence of silver salt (blue plot in **Figure 7.12**), which is attributed to the reduction of the complex with one halide ion **(2a)**.

Based on the voltammogram shown in **Figure 7.12**, in the presence of 2 equivalents of silver ions, Pd(II) is mainly present as complex **(2b)** together with a small fraction of **(2a)**. However, according to literature data [71] and the kinetic analysis reported in **Paragraph 3.8**, 2 equivalents of a silver salt should be sufficient to remove both halides from the Pd(II) complex and transform quantitatively **(2)** into **(2b)**; probably, the substitution reaction had not gone to completion when the measurements were carried out; this justifies the presence of a small peak relative to the reduction of **(2a)**.

These preliminary studies have thus allowed the assignment of the observed reduction processes to the different Pd(II) species present in solution. In particular, it has been observed that the order of the reduction potentials of these species is **(2b)** >

(2a) > **(2)**. Reduction of the di-halide complex **(2)** occurs at the most negative potentials (-2.0 V *vs* Fc^+/Fc), that of the mixed complex **(2a)** at slightly less negative potentials (about -1.9 V *vs* Fc^+/Fc), whereas the di-solvento complex **(2b)**, with a peak potential around -1.7 V, is the most easily reducible complex.

The above conclusions are supported by two other observations. The first concerns the formation of the mono-solvento complex due to the substitution of Br^- by DMSO. To confirm the existence of an equilibrium between **(2)** and **(2a)**, the voltammetric investigation on complex **(2)** in DMSO has been extended to positive potentials, where oxidation of bromide ions can be detected. It is worth noting that the electrochemical oxidation of bromides causes a shift of the equilibrium between species **(2)** and **(2a)** towards the release of further bromide anions (**Figure 7.13**).

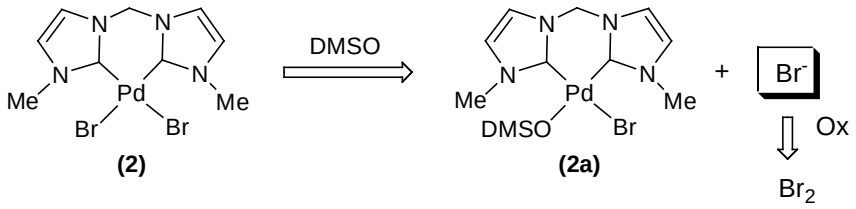

Figure 7.13 Shift of the equilibrium after oxidation of free bromides.

Therefore, if the substitution reaction is fast enough, the voltammetric response for the oxidation of Br^- will depend not only on the equilibrium concentration of the ion at the beginning of the experiment, but also on the rate of conversion of **(2)** into **(2a)**. This situation is quite similar to the one we described for the reduction of **(2a)** (first reduction peak of complex **(2)**).

A series of voltammograms recorded for a solution of complex **(2)** at different scan rates in the potential range -0.25/0.65 is shown in **Figure 7.14**. To make the comparison easier, the voltammograms are plotted as normalised current, $i/v^{1/2}$, versus potential.

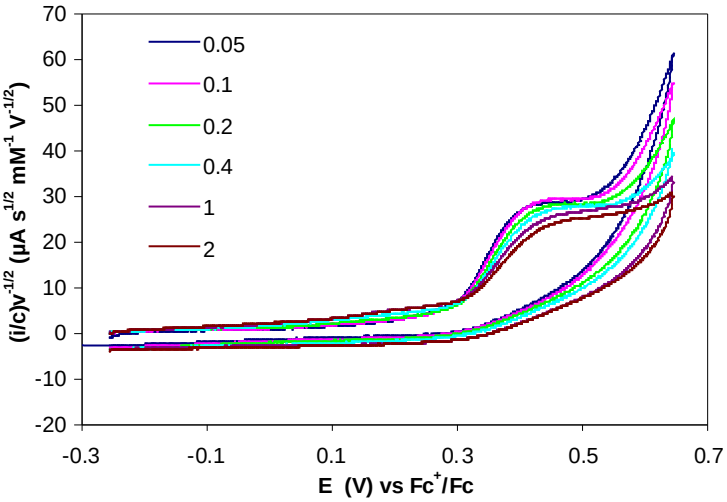

Figure 7.14 Cyclic voltammetry of **(2)** 0.86 mM in DMSO + Bu_4NClO_4 0.1 M recorded at different scan rates.

As can be clearly observed, increasing the scan rate the oxidation peak for bromide ions decreases. This is better illustrated in **Figure 7.15**, which reports a plot of the normalised anodic peak current, $i_{pa}/v^{1/2}$, as a function of $v^{1/2}$.

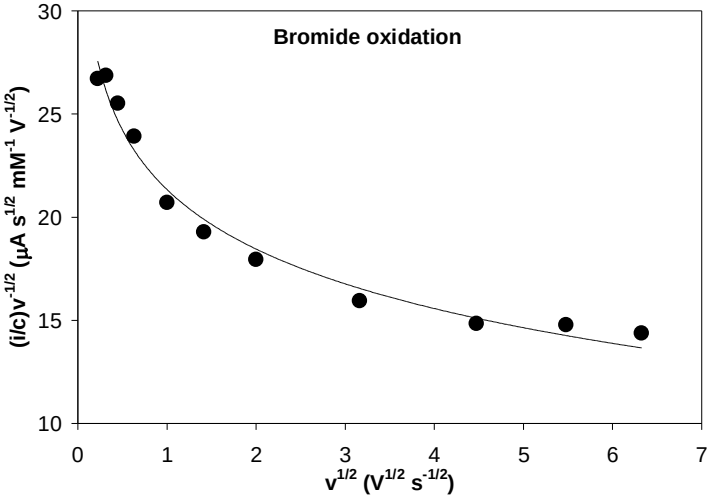

Figure 7.15 Dependence of peak current for the oxidation of Br^-, derived from **(2)**, as a function of scan rate.

The normalised current decreases with increasing *v* and approaches a constant low limiting value at relatively high scan rates. This is a further confirmation of the presence of an equilibrium between complex **(2)** and the mono-solvento complex **(2a)**. At low scan rates the registered current is higher than expected for the initial equilibrium concentration of bromide ions, whereas at high scan rates ($v > 10$ V s^{-1}) the time of the measurement is faster than that needed to shift the equilibrium towards **(2a)** and Br^-. Therefore, currents measured at high *v* values represent the real concentration of bromide ions present in solution under equilibrium conditions.

The second observation deals with the bis-solvento complex assumed to be formed in the presence of 2 equivalents of AgTFA. While there is a clear evidence of the release of Br^-, which precipitates as an insoluble silver salt, defining the structure of the Pd(II) complex is not straightforward. In fact, species containing either 2 TFA ligands, mixed TFA/DMSO ligands or 2 DMSO molecules should be taken into consideration.

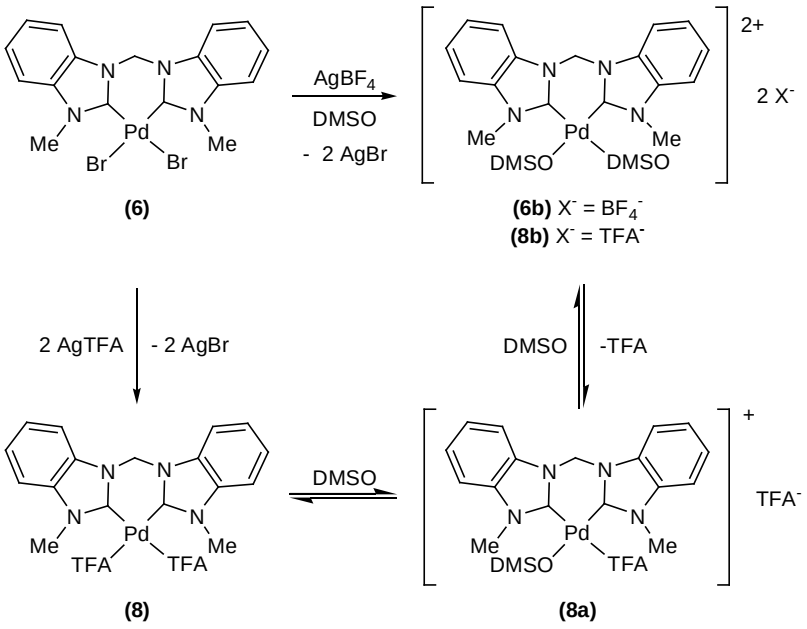

Figure 7.16 Species formed from complex **(6)** in the presence of AgTFA or $AgBF_4$ under the measurement conditions.

To this end, some investigations have been carried out on complex **(6)**. In particular, the effect of two different silver salts, AgTFA and $AgBF_4$, has been examined and the results have been compared with the response of an authentic sample of the complex containing two TFA ligands (complex **(8)**). When 2 equivalents of AgTFA are added to complex **(6)**, all the species reported in **Figure 7.16** (**(8)**, **(8a)** and **(8b)**) can be potentially obtained. Adding $AgBF_4$ to complex **(6)**, instead, species **(6b)** should be directly formed, since BF_4^- is a non coordinating anion.

Comparing the CVs shown in **Figure 7.17**, it is clearly observed that the reduction potential (–1.59 V *vs* Fc^+/Fc) of the newly formed peak is the same in both cases. These results point out that this process is related to the reduction of the bis-solvento species **(6b)** or **(8b)** showed in **Figure 7.16**. Probably, the bis-trifluoroacetate complex **(8)**, formed *in situ* by adding 2 eq. AgTFA to a DMSO solution of **(6)**, easily releases both the TFA^- anions, giving the di-solvento complex **(8b)**.

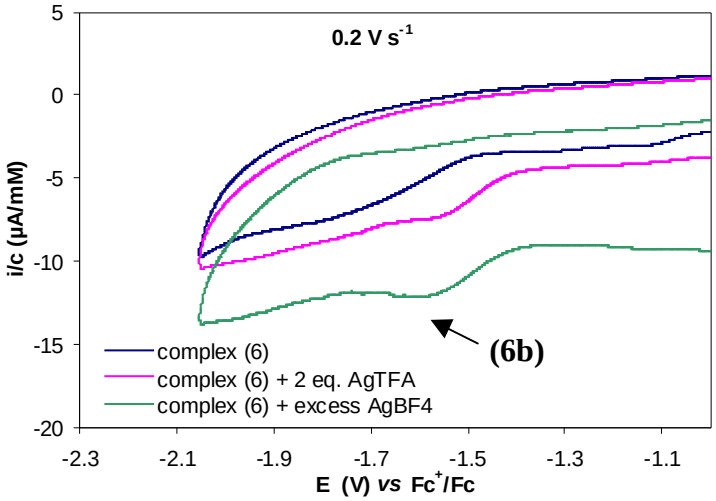

Figure 7.17 Cyclic voltammetry of **(6)** 1.51 mM in DMSO + Bu_4NClO_4 0.1 M recorded at v = 0.2 V s^{-1} in the absence and presence of either AgTFA or $AgBF_4$.

Cyclic voltammetry of the new complex, formed upon addition of either $AgBF_4$ or AgTFA to a solution of **(6)** (green and pink plot in **Figure 7.17**), has been compared to a CV obtained for a DMSO solution of complex **(8)**, which has been prepared and

isolated in a separate experiment. The comparison is shown in **Figure 7.18** and it clearly indicates that the same species, i.e., complex **(8b)**, is formed in all cases.

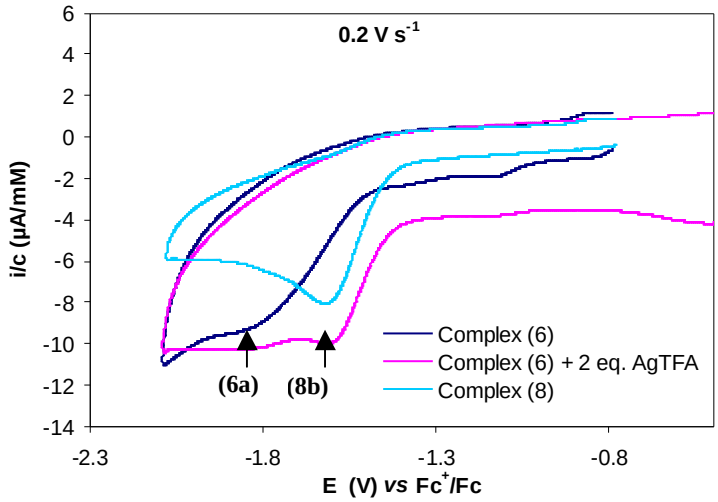

Figure 7.18 Cyclic voltammetry of (i) **(6)** 1.51 mM in DMSO + Bu_4NClO_4 0.1 M in the absence and presence of 2 eq. AgTFA and (ii) **(8)** 1.53 mM; v = 0.2 V s^{-1}.

In conclusion, the main voltammetric peak observed in the CV of complex **(2)** at low scan rates (for example at 0.2 V s^{-1}) is related to the mixed species $[Pd(dicarbene)(Br)(DMSO)]^+$ **(2a)**, since in these conditions just one halide ligand is lost by the Pd(II) complex. When a large excess of Br^- is present, the main Pd(II) species present in solution is $[Pd(dicarbene)(Br)_2]$ **(2)** and the main reduction peak observed in these conditions is related to this complex. When, instead, soluble silver salts are added into the solution, the prevailing species becomes the bis-solvento complex $[Pd(dicarbene)(DMSO)_2]^{2+}$ **(2b)** and its reduction gives a well defined peak at potentials more positive than that of **(2a)**. This systematic analysis enables identification of the species prevailing in solution and determination of their reduction potential.

Keeping in mind the order of reduction of the three possible Pd(II) complexes and the above described protocol of identification, the voltammetric behaviour of the series of complexes shown in **Figure 7.19** has been investigated in DMSO. Some

representative voltammograms are illustrated in **Figure 7.20**. The potential window chosen for complex **(6)** is more narrow than those of the other complexes because of the presence of KBF_4 as a significant impurity, which is reducible at potentials < -2.0 V *vs* Fc^+/Fc.

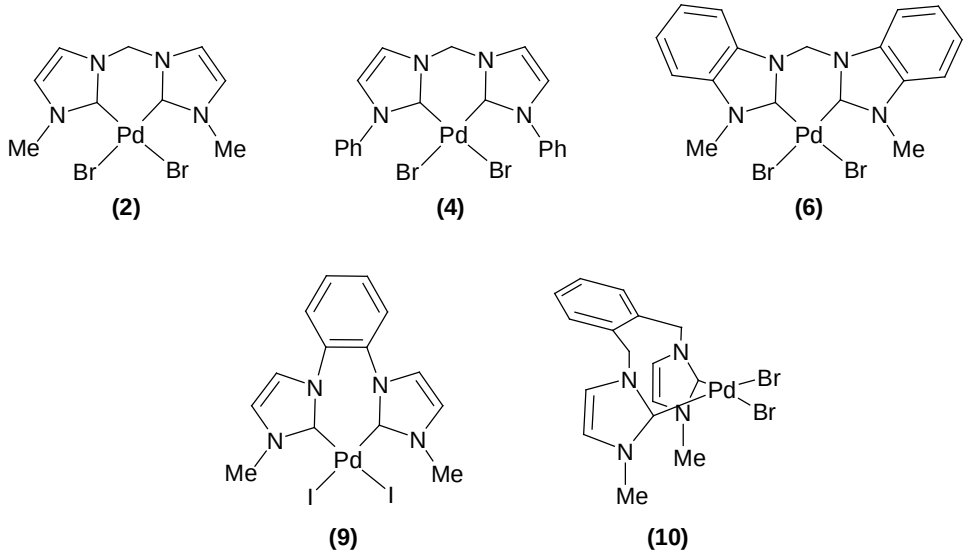

Figure 7.19 Dicarbene complexes utilised in this study.

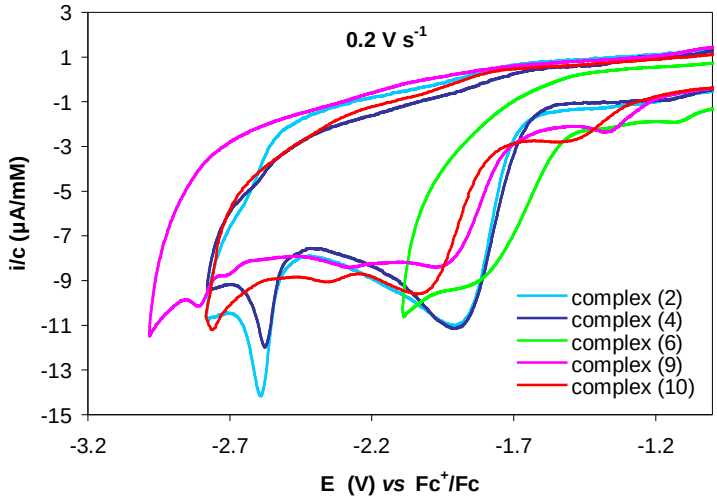

Figure 7.20 Cyclic voltammetry of Pd(II) complexes 0.8-1.5 mM in DMSO + Bu_4NClO_4 0.1 M, recorded at v = 0.2 V s^{-1}.

As shown in **Figure 7.20**, the complexes display very similar voltammetric features; they all exhibit a main reduction peak, which is broad and irreversible, followed, in most cases, by a very small reduction peak located at more negative potentials. This is in line with the finding that in DMSO, without added halides or silver salts, the predominant Pd(II) species is $[Pd(dicarbene)(X)DMSO]^+$. Therefore, in agreement with the previous experiments, the observed main reduction peaks have been assigned to the reduction from Pd(II) to Pd(0) in the mixed species **(na)**.

The voltammetric response of each complex has been examined at different scan rates from 0.05 to 20 V s^{-1}. An example of the effect of the scan rate, *v*, on the voltammetric pattern of the complexes is illustrated in **Figure 7.8**. As *v* is increased, the main peak decreases in height, while a new peak appears at more negative potentials. Both peaks are irreversible even at high scan rates and shift to more negative potentials with increasing *v*. As mentioned earlier, the absence of anodic peaks attributable to the oxidation of the electrogenerated Pd(0) species may be due to instability of Pd(0) complexes or slow electron transfer to Pd(II). In either case, an increase of *v* will cause a cathodic shift of the peak, as is actually observed. A careful analysis of the dependence of the peak potential, E_p, on the scan rate may provide some insight into the reduction mechanism. In particular, if the electrode process is kinetically controlled by the electron transfer, E_p can be expressed by the following equation [69]:

$$E_p = E^{0'} - \frac{RT}{\alpha F}\left[0.780 + \ln\left(\frac{D^{1/2}}{k^o}\right) + \ln\left(\frac{\alpha F v}{RT}\right)^{1/2}\right] \qquad \textbf{(7.8)}$$

where $k°$ is the standard electron transfer rate constant and *F* is the Faraday constant. Thus, at 25 °C, E_p shifts in the negative direction by $29.6/\alpha$ mV for each tenfold increase in *v*. In principle, the transfer coefficient, α, may assume values between 0 and 1, quite often $0.3 < \alpha < 0.7$. It follows that a linear variation of E_p as a function of log*v* with a slope $dE_p/d\log v$ significantly smaller than -30 mV is a clear indication

of an irreversible ET, i.e., overall electrode process with a rate-determining ET. If, by contrast, $dE_p/d\log\nu \geq -30$ mV, the process is kinetically controlled by a chemical reaction following ET to the substrate. In other words, this is the case of a reversible (or fast) ET followed by a relatively slow chemical reaction. Obviously, in both cases, the overall process will give rise to an irreversible voltammetric peak. This being the case for all complexes investigated in this study, the dependence of E_p on logν has been analysed. For each Pd(II) complex, voltammetric experiments have been performed under different experimental conditions and the E_p values obtained at different scan rates have been plotted versus logν. Examples of such plots are reported in **Figure 7.21**, which illustrates the dependence of E_p for **(2)**, **(2a)** and **(2b)** on scan rate. These data have been obtained for the mono-halide complex **(2a)** by examining a DMSO solution of **(2)** as such, whereas data for the di-halide complex **(2)** and the di-solvento complex **(2b)** have been obtained after addition of either 50 eq. TEABr or 2 eq. AgTFA, respectively. The slopes obtained for the complexes **(2)** , **(2a)** and **(2b)** are -81.9, -123.1 and -64.8 mV, respectively. These values are much more negative than -30 mV, indicating reduction processes under kinetic control of the ET.

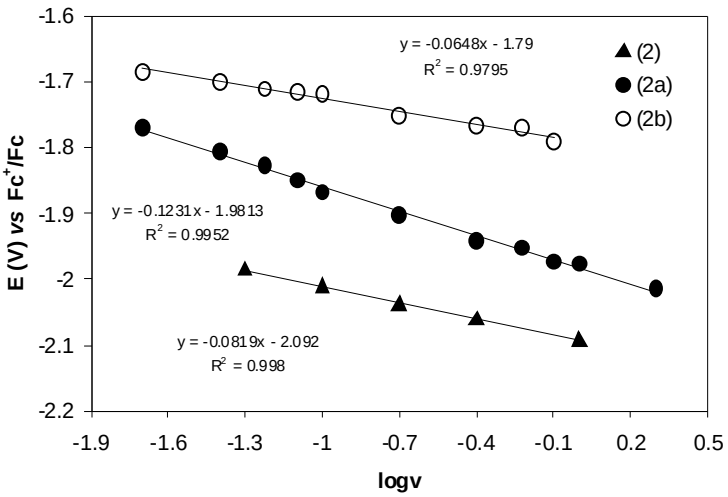

Figure 7.21 Voltammetric reduction of complex **(2)** in DMSO + Bu_4ClO_4 0.1 M in the absence and presence of either TEABr or AgTFA. Dependence of E_p of **(2)**, **(2a)** and **(2b)** on scan rate.
▲ Complex **(2)** 0.86 mM alone; ● Complex **(2)** 0.86 mM + 2 eq. AgTFA; ○ Complex **(2)** 1.51 mM + 50 eq. TEABr.

In **Table 7.1** the main parameters, calculated from the CVs of the mono-halide complexes **(na)**, are summarised. In particular, the peak potentials recorded at 0.1 V s^{-1} together with the slopes of the E_p versus log*v* plots are reported. The values of the transfer coefficients α, calculated from the slopes of the linear plots, are also reported in the table (last column). These values are typical of sluggish electron transfer processes. The activation free energy of an ET process can be expressed as the sum of two contributions coming from the outer and inner reorganisation energies. When ET is not accompanied by appreciable inner reorganisation of the redox couple (change of bond lengths, bond angles, coordination number, etc), the activation free energy is often quite small, being mainly due to solvent reorganisation. Electron transfer, under such circumstances, is always very fast (reversible) with a transfer coefficient of *ca* 0.5. In the case of the Pd(II) complexes considered in this study ET is very slow, possibly because considerable structural changes accompany the passage from Pd(II) to Pd(0) upon ET.

Unfortunately, the standard reduction potentials of these Pd(II) complexes cannot be measured because of the irreversibility of the ET. Since, however, the peak potentials are related to the standard potentials, E_p may be used in place of E^o for a comparative analysis of the redox properties of the complexes. It should be stressed that E_p contains also kinetic effects (see equation **(7.7)**), which for simplicity have been neglected here.

Table 7.1 Voltammetric data for the reduction of mono-solvento Pd(II) complexes in DMSO + Bu_4NClO_4 0.1 M.

Complex	c [mM]	E_{pc}[a] [V *vs* Fc^+/Fc]	dE_{pc}/dlogv [mV]	α[b]
(2a)	0.86	-1.87	-123	0.24
(4a)	0.84	-1.88	-99	0.30
(6a)	1.51	-1.82	-123	0.24
(9a)	0.85	-1.94	-84	0.35
(10a)	0.87	-2.00	-80	0.37

[a] Cathodic peak potential, E_{pc}, measured at v = 0.1 V s^{-1}.
[b] $\alpha = -29.58/[(dE_{pc}/d\log v)]$.

Comparing the peak potentials obtained at 0.1 V s^{-1} for the different species **(na)**, it is evident that some of them differ significantly from others. If it is assumed that the reduction potential is related to the charge density on Pd in the sense that the greater the positive charge on the metal the higher the reduction potential, the charge density present on Pd(II) increases in the following order:

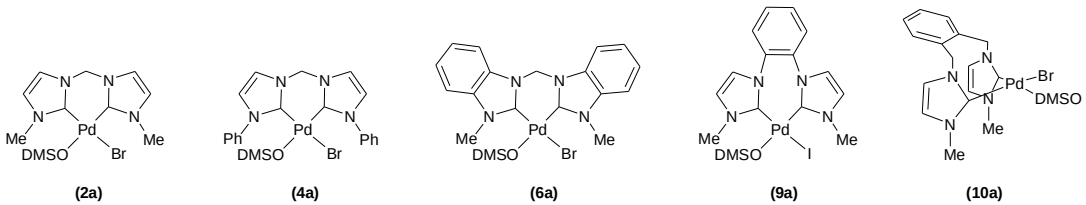

(10a) < (4a) ~ (2a) < (6a)

The positive charge on Pd(II) is the highest for species **(6a)**, which shows the least negative reduction potential in the series. In contrast, species **(10a)** has the most negative potential and, hence, the lowest charge density on the metal.

It is to be noted that species **(9a)** has not been considered in the comparison because it has one iodide instead of one bromide ligand, and this difference can influence the charge density on Pd, thus providing an additional contribution to E_p.

To compare species bearing, besides the dicarbene ligand, only solvent molecules, further CVs have been registered in the presence of 2 equivalents of AgTFA (**Figure 7.22**). As already demonstrated in the previous experiments, complexes **(nb)** should be obtained in all cases. The reduction potentials are, in this case, directly correlated to electronic properties of the specific dicarbene ligand, the other ligands being always the same. The reduction potentials of the series of di-solvento species **(nb)** lie in the range of -1.6/-1.8 V *vs* Fc^+/Fc. These values are less negative than the reduction potentials of the corresponding monohalide complexes **(na)**, since dicationic species $[Pd(dicarbene)(DMSO)_2]^{2+}$ are more easily reduced than the monocationic species $[Pd(dicarbene)(X)(DMSO)]^+$.

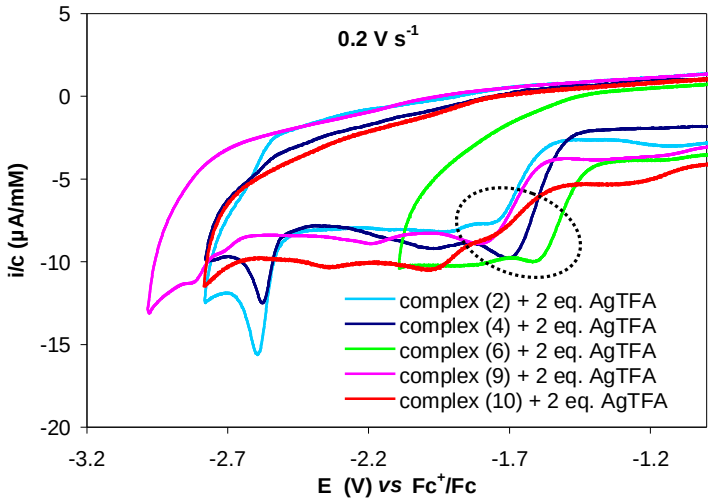

Figure 7.22 Cyclic voltammetry of Pd(II) complexes 0.8-1.5 mM in DMSO + Bu_4NClO_4 0.1 M, recorded at v = 0.2 V s^{-1} in the presence of 2 eq. AgTFA.

In **Table 7.2** the main parameters, calculated analysing cyclic voltammograms at different scan rates, are reported. The slopes of the E_p versus log$v$ plots for these species are less negative than those of the monohalide complexes. Consequently, α values of the di-solvento complexes move closer to 0.5 than the ones obtained for species **(na)**, and therefore the ET to species **(nb)** is faster than that of complexes **(na)**.

Table 7.2 Voltammetric data for the reduction of di-solvento Pd(II) complexes in DMSO + Bu_4NClO_4 0.1 M.

Complex[a]	c [mM]	E_{pc}[b] [V *vs* Fc^+/Fc]	dE_{pc}/dlog$v$ [mV]	α[c]
(2b)	0.86	-1.72	-65	0.46
(4b)	0.84	-1.69	-60	0.50
(6b)	1.51	-1.59	-70	0.42
(9b)	0.85	-1.80	-76	0.39

[a] Prepared *in-situ* by additon of 2 eq. AgTFA to a solution of Pd(dicarbene)(X_2).
[b] Cathodic peak potential, E_{pc}, measured at v = 0.1 Vs^{-1}.
[c] α = -29.58/[(dE_{pc}/dlog$v$)].

Based, as before, on the reduction potentials, the order of increasing charge density on Pd in the di-solvento complexes may be written as follows.

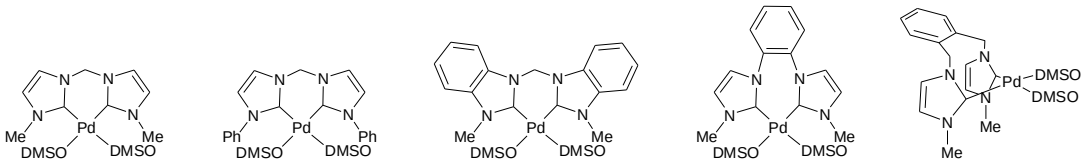

(9b)<(2b)~(4b)<(6b)

Species **(10b)** has not been considered in this comparison because its reduction potential could not be measured with a reasonable accuracy. In fact, as shown in **Figure 7.22**, a well defined peak is not obtained for **(10b)**. For complex **(10)**, the exchange reaction with the silver salt appears to be slower than for the other complexes.

Voltammetric behaviour of ligand precursors

With the aim of verifying if the carbene ligands give rise to reduction waves, CVs of the corresponding imidazolium salts, shown in **Figure 7.23**, which have been used as precursors in the synthesis of dicarbene ligands, have also been registered in DMSO + Bu_4NClO_4 0.1 M.

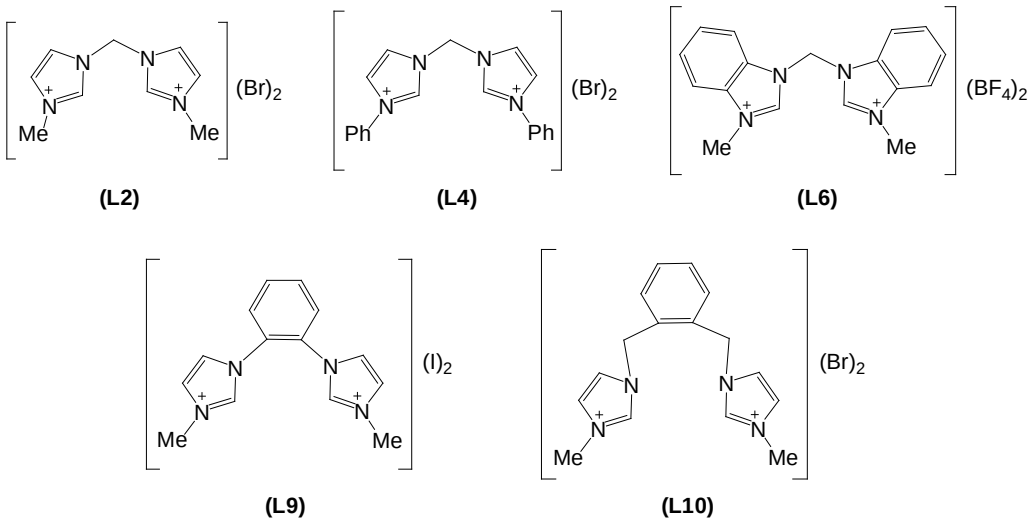

Figure 7.23 Imidazolium salts employed as precursors for the synthesis of dicarbene complexes used in this study.

Cyclic voltammograms of the imidazolium salts display well defined reduction peaks at very negative potentials and anodic peaks associated with the reduction peaks (**Figure 7.24**).

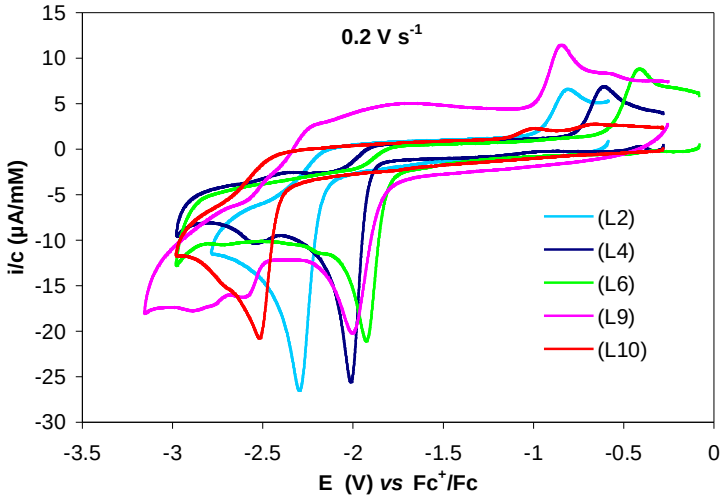

Figure 7.24 Cyclic voltammograms of imidazolium salts **(L2)-(L10)** 0.85 mM in DMSO + Bu_4NClO_4 0.1 M recorded at 0.2 V s^{-1}.

Preliminary studies carried out in our laboratories on imidazolium monocations and also other literature reports [72] have demonstrated that these salts are electrochemically reduced to the corresponding carbenes, which are highly reactive species. The anodic peaks, appearing in **Figure 7.24** at approximately -0.8 V *vs* Fc^+/Fc, are attributable to the oxidation of electrogenerated dicarbenes. The peak currents observed for the oxidation processes are smaller than those of the reduction peaks, indicating that carbenes are reactive species that are not very stable in the reaction medium. In this context ligand **(L10)** displays the lowest anodic current, so that the corresponding carbene species results to be the most unstable in solution. Both reduction of the imidazolium cations and oxidation of dicarbenes are irreversible processes. The electrochemical processes responsible of the cathodic and anodic peaks may be represented by the reactions shown in **Figure 7.25**.

Cathodic process:

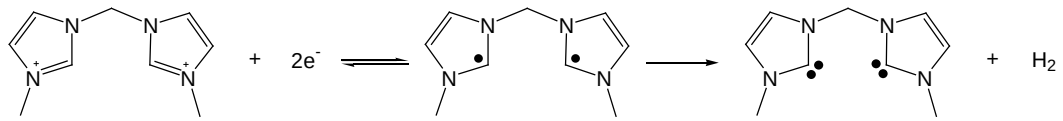

Anodic process:

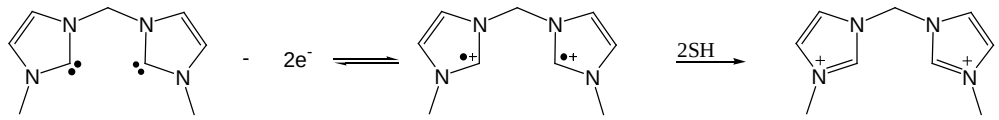

Figure 7.25 Electrochemical processes responsible of cathodic and anodic peaks shown in **Figure 7.24**.

As done before, the main parameters have been calculated analysing both the reduction and the oxidation peaks and are reported in **Table 7.3**. Obviously, the charge density on the metal in the complexes is not necessarily related to the redox properties of the imidazolium salts, since in the complexes also the bond contributions and the orbital overlaps have to be considered. However, even if these data are not directly correlated to the charge density at the catalytic centre, they are useful to gain information about the redox properties of dicarbene ligands and their precursors for which the current electrochemical literature is still poor [72].

Table 7.3 Voltammetric data for the reduction of imidazolium salts **(L2)-(L10)** in DMSO + Bu_4NClO_4 0.1 M.

Compound	**c [mM]**	E_{pc} [a] **[V *vs* Fc^+/Fc]**	**dE_{pc}/dlogv [mV]**	E_{pa} [a] **[V *vs* Fc^+/Fc]**	**dE_{pa}/dlogv [mV]**
(L2)	0.86	-2.29	-38	-0.84	49
(L4)	0.85	-2.01	-31	-0.62	34
(L6)	0.85	-1.92	-30	-0.42	30
(L9)	0.86	-1.99	-50	-0.86	41
(L10)	0.85	-2.51	-48	-1.03	47

[a] Cathodic and anodic peak potentials, E_{pc} and E_{pa}, measured at v = 0.1 V s^{-1}.

Analysis of the CVs, recorded for the ligand precursors at different scan rates, allows determination of the slopes of the dependence of E_p on log$v$ for both the cathodic and the anodic peaks. The values of the slopes dE_p/dlog$v$ are reported in **Table 7.3**. For imidazolium cations **(L4)** and **(L6)**, as well as their respective dicarbenes, $|dE_p/d\log v|$ values of about 30 mV are obtained. This means that electrode processes undergone by these compounds can be described as reversible electron transfers followed by rate-determining chemical reactions. Higher $|dE_p/d\log v|$ values are observed for the other compounds of the series. In these cases the ET steps are less reversible and the overall processes are under mixed kinetic control by both ET and chemical reactions.

For the sake of comparison, CVs at 0.1 V s^{-1} of each complex, in the absence and presence of 2 eq. AgTFA, and of the corresponding imidazolium salt are reported in **Figure 7.26**, in succession from **(2)** to **(10)**. It can be immediately noticed that reduction of the ligands requires potentials that are considerably more negative than those of the complexes, especially those of the type **(a)** or **(b)**. The reported CVs are those of the precursors, which implies that dicarbenes are formed in the negative-going scan and are oxidised in the reverse positive-going scan. Now, the fact that oxidation peaks attributable to dicarbenes can be observed means that they are stable in the time scale of the voltammetric experiment. However, reduction peaks other than those of the precursors are not observed, which clearly indicates that reduction of dicarbenes occurs at potentials more negative than those of the imidazolium cations. Actually these potentials occur beyond the accessible potential window as no other reduction peaks were observed up to the cathodic discharge of the solvent-electrolyte system. A reduction peak at E < -2.5 V *vs* Fc^+/Fc is observed for some complexes. This peak has not been assigned. Certainly, it cannot be attributed to a Pd centre reduction process, not only because Pd(II) has already been reduced to Pd(0) but also this peak does not resemble those of the Pd(II)/Pd(0) couple; it is more similar to the voltammetric peaks of the ligands and ligand precursors. It is more likely to be due to some impurity of the complex.

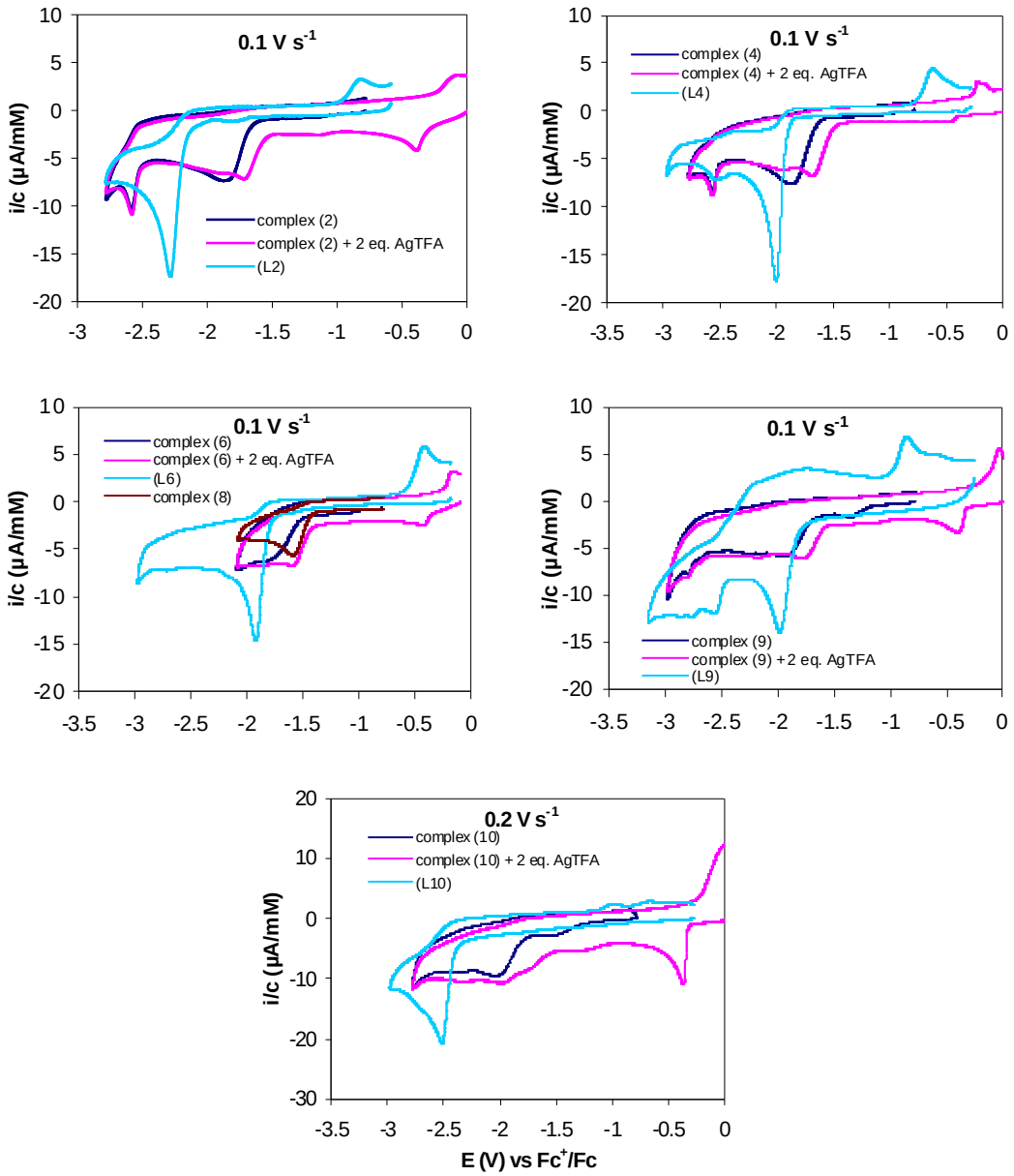

Figure 7.26 Cyclic voltammograms of each complex in the absence and presence of 2 eq. AgTFA and of the corresponding imidazolium salt in DMSO + Bu_4NClO_4 0.1 M, recorded at 0.1 or 0.2 V s^{-1}.

The reduction potentials of the imidazolium cations span in a range of potentials (-1.92/-2.51 V) which is much larger than that of the complexes (for the **(na)** series for example, -1.82/-2.00 V). Also the oxidation potentials of the dicarbene ligands show a great variation (from -0.42 V to -1.03 V), which is of the same order of that of their precursors. If we correlate the reduction potential with the positive charge density on

the electroactive centre (N for the ligand precursors and Pd for the complexes), we expect an anodic shift of the potential with an increase of charge density. A similar reasoning for the oxidation of dicarbenes leads to the conclusion that more electron rich carbenes should have less positive oxidation potentials.

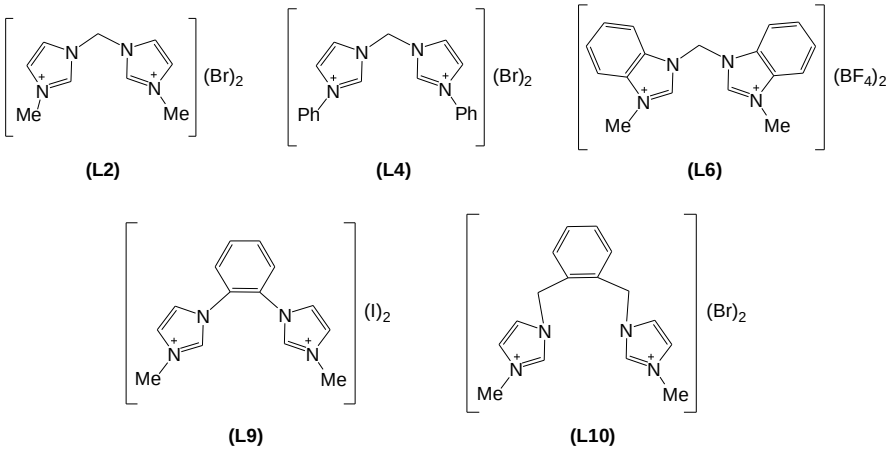

Reduction of the precursors shows the following trend of increasing reduction potential, which corresponds to increasing charge density on the nitrogen atom:

(L10) < (L2) ~ (L4) < (L9) < (L6)

The species reducible at the most negative potentials (**(L10)** and **(L2)**) bear alkyl groups directly bonded to the nitrogen atoms, whereas the species with least negative potentials (**(L6)**, **(L9)** and **(L4)**) are those bearing phenyl groups. Oxidation of the dicarbenes follows a similar trend, i.e., the greater the electron density on :C, the lower the oxidation potential. In this case, it is easier to remove an electron from a species with high electron density than one with lower electron density. The order of increasing oxidation potential of the dicarbene ligands **(L′)**, which coincides with the order of decreasing electron density, is

(L′10) < (L′9) < (L′2) < (L′4) < (L′6)

The order of increasing electron density on :C in the dicarbenes may be compared with the reduction potentials of the Pd(II) complexes. If one assumes that the redox properties of the metal complexes exclusively depend on the polar effects of the dicarbene ligands, one would expect an opposite trend for the reduction potentials of the complexes. In other words, ligands with higher electron-donating abilities will form Pd(II) complexes with smaller positive charge density on the metal and, consequently, the reduction potential will shift to more negative values. As shown in **Tables 3.6** and **3.7**, the reduction peak potentials measured for complexes **(na)** and **(nb)** decrease, i.e., become more negative, in the following order:

(6a) > (2a) ~ (4a) > (10a)

(6b) > (4b) > (2b) > (9b)

whereas the electron donating ability of the dicarbene ligands increases in the order:

(L′6) < (L′4) < (L′2) < (L′9) < (L′10)

In general, the agreement between the trend of electron-donating ability of the ligands and those of the reduction potentials of Pd(II) complexes is fairly good, especially in the case of the di-solvento complexes **(nb)**. Of course, the polar effect of the ligands alone is not responsible for the variations of the redox properties of the complexes; other factors such as steric hindrance and optimal geometric configuration around each component of the redox couple should also be taken into consideration. Last, it should be kept in mind that we are comparing peak potentials of irreversible electrode processes rather than standard potentials. As shown in equation **(7.7)** peak potentials contain both thermodynamic ($E^{\ominus}$) and kinetic parameters. In carrying out the foregoing comparison, we assumed the kinetic contributions to be the same in the whole series, but this might not be correct, resulting in deviations of E_p from the expected trend.

CONCLUSIONS

The research work has shown that the use of chelating N-heterocyclic carbene ligands can improve the stability of the catalyst under the reaction conditions as well as its reactivity. In the Fujiwara reaction these dicarbene complexes have displayed a higher reactivity than the systems reported as catalysts in the literature (simple palladium acetate, monocarbene palladium complexes, Pt salts). Dicarbene Pd(II) and Pt(II) complexes are indeed able to catalyse the hydroarylation of alkynes at 80 °C, with excellent conversions and selectivities at low catalyst loading (0.1 mol%) and with equimolar amounts of reagents.

The optimised reaction protocol has resulted quite general with respect to the alkyne, while its applicability to arene substrates is at present limited to electron-rich molecules, although this is a limitation occurring with all Pd- and Pt-catalytic systems reported in the literature. Moreover it has been demonstrated that, in the presence of silver salts (like AgTFA) as co-catalysts, the reaction can be run at room temperature with a better selectivity than at 80 °C, being collateral reactions such as isomerisation and hydrolysis totally suppressed.

The optimised catalytic system has been used with other substrates, such as aromatic heterocycles; in this case the selectivity of the reaction can be controlled through the appropriate choice of anionic ligands at the metal centre. Poor-coordinating anions, indeed, favour the formation of diadducts products because of the limited steric hindrance and the high positive charge on the metal.

Another part of the work has concerned the identification of the catalytic active species. Mechanistic studies, performed at 80 °C, suggested that the catalytic active species retains the dicarbene ligand in its coordination sphere. Halide anionic ligands are instead removed from the complex by exchange with the trifluoroacetate anion deriving from the acidic solvent media. Thereby, the catalytic efficiency is not sensitive on the kind of halide ligands, but it is influenced by the nature of the dicarbene ligand.

Electrochemical studies have been subsequently used to evaluate the electron density at the metal centre as a function of the ligand. However, the scale of reduction potentials Pd(II)/Pd(0) is not correlated to the scale of catalytic activity shown by the

complexes. Therefore, in the Fujiwara reaction the steric hindrance at the metal centre seems more important in determining the efficiency of the dicarbene complex.

It needs to be remarked that, in principle, strongly electron-donating carbene ligands are not suitable ligands in reactions which require electrophilic metal centres, as the Fujiwara reaction. The important breakthrough in the present procedure is the combination of the high stability given to the catalyst by the dicarbene ligand with the creation of highly cationic species through the use of non-coordinating anions.

Chelating dicarbene complexes have resulted even more active than the monocarbene ones thanks to the enhanced stability arising by their chelated structure. The rigide conformation, moreover, in some cases may also increase the selectivity towards a determined product.

A preliminary investigation of the reaction mechanism through kinetic studies has been also started, since at present there is still some controversy about the reaction mechanism, and further studies are still ongoing.

Dicarbene complexes of palladium(II) have not been particularly efficient, instead, in the *ortho*-functionalisation of acetanilides, in which monocarbene complexes have proven a better reactivity, although very similar to the one displayed by palladium acetate.

EXPERIMENTAL SECTION

8.1 General remarks

All manipulations have been carried out using standard Schlenk techniques under an atmosphere of argon. The reagents have been purchased as high-purity products and generally used as received. The complexes, the imidazolium salts and $Pt_4(OAc)_8$ have been synthesised according to literature procedures. Tetra-*n*-butylammonium perchlorate has been re-crystallised before use from a solvent mixture ethanol/water 2/1. All solvents have been used as received as technical grade solvents. NMR spectra have been recorded on a Bruker Avance 300 MHz (300.1 MHz for ^{1}H and 75.5 for ^{13}C) at room temperature; the chemical shifts (δ) are reported in units of ppm relative to the residual solvent signals and multiplicities of the peaks are expressed as s (singlet), br s (broad singlet), d (doublet), t (triplet), q (quartet), m (multiplet).

GC-MS analyses have been carried out with a Varian Saturn 2100T gas chromatograph/mass spectrometer (injector temperature 220 °C, column Supelco SPB 50); the temperature has been programmed from 100 °C (1 min) to 240 °C with a gradient of 15 °C/min.

Electrochemical measurements have been performed on a computer-controlled Autolab PGSTAT30 (Eco-Chimie, Utrecht, Netherlands) potentiostat. All experiments have been carried out at 25 °C in a three-electrode cell system using glassy carbon (GC) as a working electrode. As counter-electrode and reference electrode a Pt ring and $Ag/AgI/I^-$ have been respectively used. All potentials reported in this thesis are quoted versus the redox couple ferricinium/ferrocene. This has been achieved by calibrating the $Ag/AgI/I^-$ reference system at the end of each experiment.

As working electrode a 3-mm diameter disc embedded in glass has been utilised and it has been polished to a mirror finish with silicon carbide papers of decreasing grain size (Struers, grit: 500, 1000, 2400, 4000) followed by diamond paste (3-, 1-, 0.25-mm particle size). Before every experiment it has been refreshed by polishing with a 0.25-mm diamond paste, followed by ultrasonic rinsing in ethanol for about 5 minutes.

8.2 Reagents and solvents

AgOAc	silver acetate	Aldrich-Chemie
$AgBF_4$	silver tetrafluoborate	Aldrich-Chemie
AgOTf	silver triflate	Aldrich-Chemie
AgTFA	silver trifluoroacetate	Aldrich-Chemie
$MgSO_4$	magnesium sulfate (97%)	Carlo Erba
NaCl	sodium chloride	Carlo Erba
Na_2CO_3	sodium carbonate (97%)	Carlo Erba
Na_2SO_4	sodium sulfate (97%)	Carlo Erba
$Pd(OAc)_2$	palladium acetate	Aldrich-Chemie
$Pd(P^tBu_3)_2$	bis(tri-*tert*-butylphosphane) palladium (0)	Strem
$CDCl_3$	chloroform-d_1 (99.8%, 0.03% TMS)	Aldrich-Chemie
$(CD_3)_2SO$	dimethylsulphoxide-d_6 (99%) (DMSO-d_6)	Aldrich-Chemie
CF_3COOD	trifluoroacetic acid-d_1 (DTFA)	Aldrich-Chemie
HCCCOMe	3-butyn-2-one (98%)	Aldrich-Chemie
$HCCCO_2H$	propiolic acid	Aldrich-Chemie
$HCCCO_2Me$	methyl propiolate	Ega Chemie
$HCCCO_2Et$	ethyl propiolate (98%)	Aldrich-Chemie
PhCCH	phenylacetylene (98%)	Merk
PhCCMe	1-phenyl-1-propyne (98%)	Aldrich-Chemie
PhCCPh	diphenylacetylene (98%)	Merk
$PhCCCO_2Et$	ethyl phenylpropiolate (98%)	Aldrich-Chemie
MeO_2CCCCO_2Me	dimethyl acetylenedicarboxylate	Aldrich-Chemie
$C_6H_4(CH_3)_2$	*p*-xylene (99%)	Carlo Erba
$C_6H_3(CH_3)_3$	1,3,5-trimethylbenzene (98%)	Aldrich-Chemie
$C_6H_2(CH_3)_4$	1,2,4,5-tetramethylbenzene (98%)	Aldrich-Chemie
$C_6H(CH_3)_5$	pentamethylbenzene (99%)	Aldrich-Chemie
C_4H_5N	pyrrole (pyr)	Aldrich-Chemie
$C_4H_4N(CH_3)$	1-methylpyrrole	Fluka
$C_4H_3O(CH_3)$	2-dimethylfurane	Aldrich-Chemie
C_8H_7N	indole	Aldrich-Chemie

$C_8H_6N(CH_3)$	1-methylindole	Aldrich-Chemie
$C_8H_6N(CH_3)$	2-methylindole	Aldrich-Chemie
$C_8H_6N(CH_3)$	3-methylindole	Aldrich-Chemie
$C_4H_2S(CH_3)_2$	2,5-dimethylthiophene	Aldrich-Chemie
$C_8H_5S(CH_3)$	3-methylbenzothiophene	Aldrich-Chemie
$CH_3CONHPh$	acetanilide	Aldrich-Chemie
CH_2CHCOO^nBu	*n*-butyl acrylate	Aldrich-Chemie
$CH_3C_6H_4SO_3H \cdot H_2O$	*p*-toluenesulfonic acid	Carlo Erba
$C_6H_4O_2$	*p*-benzoquinone (BQ)	Aldrich-Chemie
CF_3COOH	trifluoroacetic acid (HTFA)	Riedel-de-Haën
CH_2Cl_2	dichloromethane (DCM)	Carlo Erba
$(CH_3)_2SO$	dimethylsulfoxide (DMSO)	Fluka
$ClCH_2CH_2Cl$	1,2-dichloroethane (DCE)	Aldrich-Chemie
$(CH_3CH_2)_2O$	diethyl ether (Et_2O)	Carlo Erba
CH_3COOH	acetic acid (HOAc)	J.T.Baker
$CH_3(CH_2)_4CH_3$	*n*-hexane	Prolabo
CH_3CO_2Et	ethyl acetate (EtOAc)	Carlo Erba
Bu_4NClO_4	tetra-*n*-butylammonium perchlorate	Aldrich-Chemie
Bu_4NBr	tetra-*n*-butylammonium bromide	Fluka

8.3 General procedure for the catalytic tests

General procedure for the functionalisation of arenes: the solid reagents (arene and/or alkyne) and the catalyst (together with the silver co-catalyst, when used) were placed in a 50 mL round bottom flask, previously evacuated and filled with argon. Trifluoroacetic acid and 1,2-dichloroethane or dichloromethane were then added and the resulting solution was stirred at room temperature for 5 min. Finally the liquid reagents (arene and/or alkyne) were added and the reaction mixture was stirred at the indicated temperature for the time noted, under inert atmosphere. Portions of solution

(0.2 mL) were drawn off from the reaction mixture and analysed by ^{1}H-NMR (yields are determined referring to the limiting reagent) or GC-MS.
Reaction conditions as amount of reagents and solvents, reaction times and temperatures are specified under every table or graph reported.

General procedure for the functionalisation of aromatic heterocycles: the heterocycle (when solid, 2 mmol) and the complex (0.01 mmol, together with an excess of the silver co-catalyst, when used) were placed in a Schlenk tube. After three vacuum/argon cycles, acetic acid (1 mL) was added through the rubber septum and the reaction mixture was stirred at the noted temperature for 5 minutes before addition of the liquid reagents (2 mmol heterocycle and/or 1 mmol alkyne). The reactions conducted at 25 °C were appropriately thermostatated. Portions of solutions were drawn off the reaction mixture and analysed by NMR or GC-MS. Otherwise, at the end of the reaction, the mixture was poured with a saturated aqueous solution of NaCl and extracted with ether. The organic layers were dried over Mg_2SO_4 and concentrated under reduced pressure. The residue obtained was separated by silica-gel column chromatography with EtOAc/*n*-hexane 1:6 or Et_2O/*n*-hexane 1:1 as eluent.

General procedure for the oxidative coupling of anilides with olefins: acetanilide (0.5 mmol), the catalyst (0.01 mmol), *p*-toluenesulfonic acid (0.25 mmol) and *p*-benzoquinone (0.5 mmol) were placed in a 50 mL round bottom flask, previously evacuated and filled with argon. Acetic acid (0.75 mL), toluene (0.37 mL) and *n*-butyl acrylate (0.55 mmol) were then added and the resulting solution was stirred at the temperature indicated in **Table 6.1** for 16 hours.
At the end of the reaction, the mixture was poured with a 2.5 M aqueous solution of NaOH and extracted with diethyl ether. The organic layers were dried over Mg_2SO_4, filtered and concentrated under reduced pressure. The residue obtained was analysed by ^{1}H NMR ($CDCl_3$).

8.4 Characterisation of the products

The following product has been obtained in the test performed with pentamethylbenzene and propiolic acid after the workup described in the literature, namely purification with a saturated aqueous solution of NaCl, neutralisation with an Na_2CO_3 aqueous solution and extraction with diethyl ether. During addition of the Na_2CO_3 aqueous solution, formation of a substance insoluble in diethyl ether, water and chloroform has been noticed. The mixture has been therefore filtered and the solid analysed by ^{1}H NMR (DMSO-d_6).

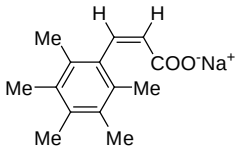

^{1}H NMR (DMSO-d_6, 300 MHz, ppm) δ: 2.07 (s, 12H, 4CH_3), 2.11 (s, 3H, CH_3), 5.95 (d, $^3J_{HH}$ = 12.3 Hz, 1H, *H* vinylic), 6.22 (d, $^3J_{HH}$ = 12.3 Hz, 1H, *H* vinylic).

The following products have been characterised *via* ^{1}H NMR analysis of the reaction mixture.

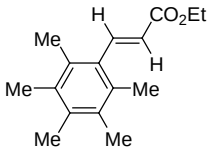

^{1}H NMR ($CDCl_3$, 300 MHz, ppm) δ: 1.35 (t, $^3J_{HH}$ = 7.2 Hz, 3H, OCH_2CH_3), 2.14 (s, 6H, 2CH_3), 2.19 (s, 6H, 2CH_3), 2.22 (s, 3H, CH_3), 4.27 (q, $^3J_{HH}$ = 7.2 Hz, 2H, OCH_2CH_3), 5.87 (d, $^3J_{HH}$ = 16.2 Hz, 1H, *H* vinylic), 7.88 (d, $^3J_{HH}$ = 16.2 Hz, 1H, *H* vinylic).

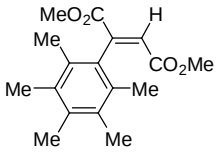

^{1}H NMR ($CDCl_3$, 300 MHz, ppm) δ: 2.05 (s, 6H, 2CH_3), 2.21 (s, 3H, CH_3), 2.27 (s, 6H, 2CH_3), 3.59 (s, 3H, OCH_3), 3.75 (s, 3H, OCH_3), 7.14 (s, 1H, *H* vinylic).

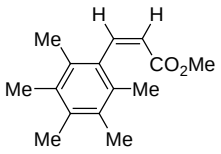

^{1}H NMR ($CDCl_3$, 300 MHz, ppm) δ: 2.14 (s, 6H, 2CH_3), 2.20 (s, 6H, 2CH_3), 2.23 (s, 3H, CH_3), 3.59 (s, 3H, OCH_3), 6.15 (d, $^3J_{HH}$ = 11.7 Hz, 1H, *H* vinylic), 7.15 (d, $^3J_{HH}$ = 11.7 Hz, 1H, *H* vinylic).

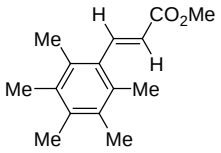

^{1}H NMR ($CDCl_3$, 300 MHz, ppm) δ: 2.14 (s, 6H, 2CH_3), 2.20 (s, 6H, 2CH_3), 2.23 (s, 3H, CH_3), 3.73 (s, 3H, OCH_3), 5.89 (d, $^3J_{HH}$ = 16.5 Hz, 1H, *H* vinylic), 7.90 (d, $^3J_{HH}$ = 16.5 Hz, 1H, *H* vinylic).

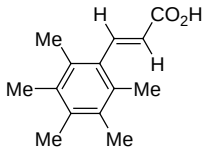

^{1}H NMR (b') ($CDCl_3$, 300 MHz, ppm) δ: 2.14 (s, 6H, 2CH_3), 2.19 (s, 6H, 2CH_3), 2.24 (s, 3H, CH_3), 5.86 (d, $^3J_{HH}$ = 16.5 Hz, 1H, *H* vinylic), 7.96 (d, $^3J_{HH}$ = 16.5 Hz, 1H, *H* vinylic).

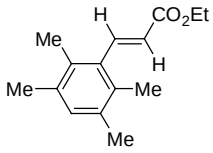

The product has been identified in the ^{1}H NMR spectra by analysis of coupling constants and position of the peaks.
^{1}H NMR ($CDCl_3$, 300 MHz, ppm) δ: 7.96 (d, $^3J_{HH}$ = 16.5 Hz, 1H, *H* vinylic).

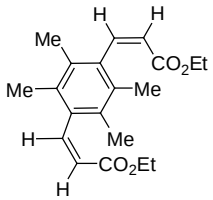

^{1}H NMR ($CDCl_3$, 300 MHz, ppm) δ: 1.11 (t, $^3J_{HH}$ = 7.2 Hz, 6H, 2OCH$_2$CH_3), 2.09 (s, 12H, 4CH_3), 4.02 (q, $^3J_{HH}$ = 7.2 Hz, 4H, 2OCH_2CH$_3$), 6.14 (d, $^3J_{HH}$ = 11.7 Hz, 2H, *H* vinylic), 7.12 (d, $^3J_{HH}$ = 11.7 Hz, 2H, *H* vinylic).

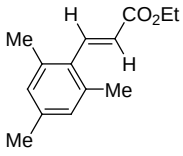

The product has been identified in the ^{1}H NMR spectra by analysis of coupling constants and position of the peaks.
^{1}H NMR ($CDCl_3$, 300 MHz, ppm) δ: 7.95 (d, $^3J_{HH}$ = 16.5 Hz, 1H, *H* vinylic).

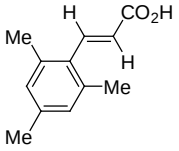

The product has been identified in the ^{1}H NMR spectra by analysis of coupling constants and position of the peaks.

^{1}H NMR ($CDCl_3$, 300 MHz, ppm) δ: 8.15 (d, $^{3}J_{HH}$ = 15.9 Hz, 1H, *H* vinylic).

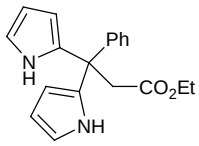

4a

Product **4a** has been isolated filtering the reaction mixture as a white solid insoluble in HOAc.

^{1}H NMR (4a) ($CDCl_3$, 300 MHz, ppm) δ: 1.18 (t, $^{3}J_{HH}$ = 7.2 Hz, 3H, OCH_2CH_3), 3.59 (s, 2H, CH_2), 4.07 (q, $^{3}J_{HH}$ = 7.2 Hz, 2H, OCH_2), 5.71 (m, 2H, pyr), 6.12 (m, 2H, pyr), 6.72 (m, 2H, pyr), 7.01 (dd, 2H, Ph), 7.24 (m, 3H, Ph), 9.06 (br s, 1H, N*H*).

GC-MS: retention time 11.9 min, molecular fragmentation 308 (40%), 221 (100%), 154 (75%).

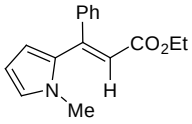

***E*-3b**

Product ***E*-3b** has been isolated through separation in silica-gel chromatographic column EtOAc/*n*-hexane 1:6 (reaction mixture referred to entry 4 in Table 4.9).

^{1}H NMR (*E*-3b) ($CDCl_3$, 300 MHz, ppm) δ: 1.11 (t, $^{3}J_{HH}$ = 7.2 Hz, 3H, OCH_2CH_3), 3.37 (s, 3H, CH_3), 4.03 (q, $^{3}J_{HH}$ = 7.2 Hz, 2H, OCH_2CH_3), 6.08 (s, 1H, *H* vinyl), 6.13-6.10 (m, 2H, pyr), 6.70 (m, 1H, pyr), 7.36-7.25 (m, 5H, Ph).

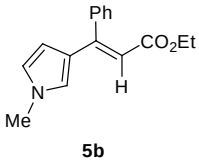

5b

Product ***5*b** has been isolated through separation in silica-gel chromatographic column EtOAc/*n*-hexane 1:6 (reaction mixture referred to entry 4 in Table 4).

^{1}H NMR (5b) ($CDCl_3$, 300 MHz, ppm) δ: 1.09 (t, $^{3}J_{HH}$ = 7.2 Hz, 3H, OCH_2CH_3), 3.55 (s, 3H, CH_3), 3.99 (q, $^{3}J_{HH}$ = 7.2 Hz, 2H, OCH_2CH_3), 6.20 (s, 1H, *H* vinyl), 6.24 (m, 1H, pyr), 6.40 (m, 1H, pyr), 6.58 (m, 1H, pyr), 7.39-7.23 (m, 5H, Ph).

Product **4b** and **6b** have been obtained as a mixture of isomers after separation in silica-gel chromatographic column EtOAc/*n*-hexane 1:6 (reaction mixture referred to entry 7 in Table 4).

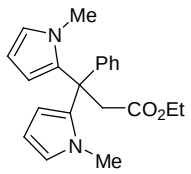

4b

^{1}H NMR (4b) ($CDCl_3$, 300 MHz, ppm) δ: 1.04 (t, $^3J_{HH}$ = 7.2 Hz, 3H, OCH_2CH_3), 3.40 (s, 2H, CH_2), 3.56 (s, 6H, $2CH_3$), 3.93 (q, $^3J_{HH}$ = 7.2 Hz, 2H, OCH_2CH_3), 5.94 (m, 2H, pyr), 6.26 (m, 2H, pyr), 6.50 (m, 2H, pyr), 7.34-7.17 (m, 5H, Ph).

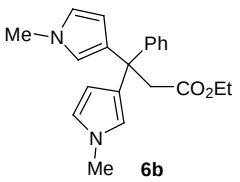

6b

^{1}H NMR (6b) ($CDCl_3$, 300 MHz, ppm) δ: 1.02 (t, $^3J_{HH}$ = 7.2 Hz, 3H, OCH_2CH_3), 3.05 (s, 6H, $2CH_3$), 3.50 (s, 2H, CH_2), 3.92 (q, $^3J_{HH}$ = 7.2 Hz, 2H, OCH_2CH_3), 6.03 (m, 2H, pyr), 6.07 (m, 2H, pyr), 6.57 (m, 2H, pyr), 7.34-7.17 (m, 5H, Ph).

Product ***Z*-3c** has been isolated through separation in silica-gel chromatographic column Et_2O/*n*-hexane 1:1.

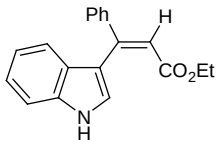

***Z*-3c**

^{1}H NMR (*Z*-3c) ($CDCl_3$, 300 MHz, ppm) δ: 1.16 (t, $^3J_{HH}$ = 7.2 Hz, 3H, OCH_2CH_3), 4.11 (q, $^3J_{HH}$ = 7.2 Hz, 2H, OCH_2), 6.27 (s, 1H, *H* vinyl), 7.00-7.41 (m, 9H, aryl), 7.80 (d, *J* = 7.2 Hz, 1H, aryl), 8.60 (br s, 1H, N*H*).

Product **4c** has been isolated through separation in silica-gel chromatographic column Et_2O/*n*-hexane 1:1.

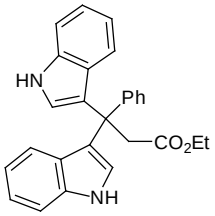

4c

^{1}H NMR (4c) ($CDCl_3$, 300 MHz, ppm) δ: 0.69 (t, $^3J_{HH}$ = 7.2 Hz, 3H, OCH_2CH_3), 3.68 (q, $^3J_{HH}$ = 7.2 Hz, 2H, OCH_2CH_3), 3.83 (s, 2H, CH_2), 6.87 (m, 2H, aryl), 7.03-7.47 (m, 11H, aryl), 7.49 (d, *J* = 7.2 Hz, 2H, aryl), 8.03 (br s, 2H, N*H*).

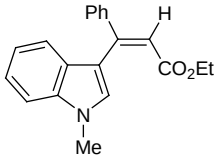

***Z*-3d**

Product ***Z*-3d** has been identified through NMR analysis of the reaction mixture.

^{1}H NMR (*Z*-3d) ($CDCl_3$, 300 MHz, ppm) δ: 1.15 (t, $^3J_{HH}$ = 7.2 Hz, 3H, OCH_2CH_3), 3.82 (s, 3H, CH_3), 4.10 (q, $^3J_{HH}$ = 7.2 Hz, 2H, OCH_2CH_3), 6.15 (s, 1H, *H* vinyl), 6.86 (s, 1H, aryl), 7.12-7.44 (m, 8H, aryl), 7.60 (d, *J* = 7.2 Hz, 1H, aryl).

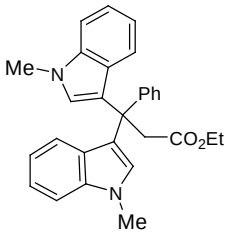

4d

Product **4d** has been identified through NMR analysis of the reaction mixture.

^{1}H NMR (4d) ($CDCl_3$, 300 MHz, ppm) δ: 0.69 (t, $^3J_{HH}$ = 7.2 Hz, 3H, OCH_2CH_3), 3.69 (q, $^3J_{HH}$ = 7.2 Hz, 2H, OCH_2CH_3), 3.70 (s, 6H, $2CH_3$), 3.83 (s, 2H, CH_2), 6.91 (s, 2H, aryl), 7.12-7.44 (m, 11H, aryl), 7.48 (d, *J* = 7.2 Hz, 2H, aryl).

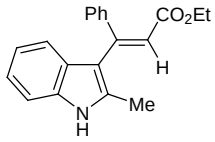

***E*-3e**

Product ***E*-3e** has been isolated through separation in silica-gel chromatographic column Et_2O/*n*-hexane 1:1.

^{1}H NMR (*E*-3e) ($CDCl_3$, 300 MHz, ppm) δ: 1.14 (t, $^3J_{HH}$ = 7.2 Hz, 3H, OCH_2CH_3), 1.97 (s, 3H, CH_3), 4.09 (q, $^3J_{HH}$ = 7.2 Hz, 2H, OCH_2CH_3), 6.18 (s, 1H, *H* vinyl), 6.94-6.38 (m, 9H, aryl), 8.31 (br s, 1H, N*H*).

GC-MS: retention time 21.5 min, molecular fragmentation 305 (100%), 230 (35%).

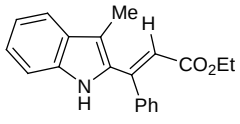

***E*-3f**

Product ***E*-3f** has been isolated through separation in silica-gel chromatographic column Et_2O/*n*-hexane 1:1.

^{1}H NMR (*E*-3f) ($CDCl_3$, 300 MHz, ppm) δ: 1.12 (t, $^3J_{HH}$ = 7.2 Hz, 3H, OCH_2CH_3), 2.27 (s, 3H, CH_3), 4.06 (q, $^3J_{HH}$ = 7.2 Hz, 2H, OCH_2CH_3), 6.31 (s, 1H, *H* vinyl), 7.11-7.44 (m, 8H, aryl), 7.59 (d, *J* = 7.2 Hz, 1H, aryl), 7.66 (br s, 1H, N*H*).

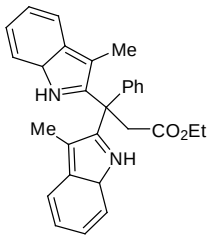

4f

Product **4f** has been isolated through separation in silica-gel chromatographic column Et_2O/*n*-hexane 1:1.

^{1}H NMR ($CDCl_3$, 300 MHz, ppm) δ: 1.03 (t, $^3J_{HH}$ = 7.2 Hz, 3H, OCH_2CH_3), 1.74 (s, 6H, $2CH_3$), 3.88 (s, 2H, CH_2), 3.97 (q, $^3J_{HH}$ = 7.2 Hz, 2H, OCH_2), 7.09-7.60 (m, 13H, aryl), 9.17 (br s, 1H, NH).

The other products have been identified in comparison with literature data [26b, 29, 35c, 39a, 63, 73].

References

[1] a) D. A. Dixon, A. J. Arduengo III, *J. Phys. Chem.* **1991**, *95*, 4180; b) A. J. Arduengo III, H. V. R. Dias, R. L. Harlow, M. Kline, *J. Am. Chem. Soc.* **1992**, *114*, 5530.

[2] W. A. Herrmann, C. Köcher, L. J. Gooßer, G. R. J. Artus, *Chem. Eur. J.* **1996**, *2*, 1627.

[3] a) C. Heinemann, T. Müller, Y. Apeloig, H. Schwarz, *J. Am. Chem. Soc.* **1996**, *118*, 2023; b) C. Boehme, G. Frenking, *J. Am. Chem. Soc.* **1996**, *118*, 2039.

[4] a) N. M. Scott, S. P. Nolan, *Eur. J. Inorg. Chem.* **2005**, 1815; b) S. Díez-González, S. P. Nolan, *Coord. Chem. Rev.* **2007**, *251*, 874.

[5] W. A. Herrmann, C. Köcher, *Angew. Chem. Int. Ed.* **1997**, *36*, 2162.

[6] a) E. Peris, J. A. Loch, J. Mata, R. H. Crabtree, *Chem. Commun.* **2001**, *2*, 201; b) M. Albrecht, J. R. Miecznikowski, A. Samuel, J. W. Faller, R. H. Crabtree, *Organometallics* **2002**, *21*, 3596.

[7] a) T. Weskamp, V. P. W. Böcher, W. A. Herrmann, *J. Organomet. Chem.* **2000**, *600*, 12; b) C. Tubaro, *Tesi di Dottorato in Scienze Chimiche XVII Ciclo*, Università degli Studi di Padova, **2004**; c) C. Tubaro, A. Biffis, M. Basato, F. Benetollo, K. J. Cavell, L. I. Ooi, *Organometallics* **2005**, *24*, 4153; d) C. Tubaro, A. Biffis, C. Gonzato, M. Zecca, M. Basato, *J. Mol. Catal. A: Chemical* **2006**, *248*, 93.

[8] a) M. Regitz, *Angew. Chem. Int. Ed.* **1996**, *35*, 725; b) A. J. Arduengo III, R. Krafczyk, *Chem. Ztg.* **1998**, *32*, 6; c) C. M. Crudden, D. P. Allen, *Coord. Chem. Rev.* **2004**, *248*, 2247.

[9] R. H. Grubbs, *Angew. Chem. Int. Ed.* **2006**, *45*, 3760.

[10] a) I. E. Markò, S. Stérin, O. Buisine, G. Mignani, P. Branlard, B. Tinant, J.-P. Declerq, *Science* **2002**, *298*, 204; b) For applications of chelating carbenes see for example: M. Viciano, E. Mas-Marzà, M. Sanaù, E. Peris, *Organometallics* **2006**, *25*, 3063.

[11] a) H. M. Lee, T. Jiang, E. D. Stevens, S. P. Nolan, *Organometallics* **2001**, *20*, 1255; b) A. C Hillier, H. M. Lee, E. D. Stevens, S. P. Nolan, *Organometallics*

2001, *20*, 4246; c) L. D. Vasquez-Serrano, B. T. Owens, J. M. Buriak, *Chem. Commun.* **2002**, 2518; d) For applications of chelating carbenes see: E. Peris, R. H. Crabtree, *Coord. Chem. Rev.* **2004**, *248*, 2239.

[12] a) A. de Meijere, F. Diederichs, (Eds.), *Metal-catalyzed cross-coupling reactions*, 2nd edn., Wiley-VCH, Weinheim, **2004**; b) H. M. Lee, C. Y. Lu, C. Y. Chen, W. L. Chen, H. C. Lin, P. L. Chiu, P. Y. Cheng, *Tetrahedron* **2004**, *60*, 5807; c) E. A. B. Kantchev, C. J. O'Brien, M. G. Organ, *Angew. Chem. Int. Ed.* **2007**, *46*, 2768.

[13] I. P. Beletskaya, A. V. Cheprakov, *Chem. Rev.* **2000**, *100*, 3009.

[14] a) K. N. Miyaura, A. Suzuki, *Chem. Rev.* **1995**, *95*, 2457; b) T. Weskamp, V. P. W. Böhm, W. A. Herrmann, *J. Organomet. Chem.* **1999**, *585*, 348; c) W. A. Herrmann, V. P. W. Böhm, C. W. K. Gstöttmayr, M. Grosche, C.-P. Reisinger, T. Weskamp, *J. Organomet. Chem.* **2001**, *617-618*, 616; d) N. Hadei, E. A. B. Kantchev, C. J. O'Brien, M. G. Organ, *Org. Lett.* **2005**, *7*, 1991.

[15] a) A. H. Janowicz, R. G. Bergman, *J. Am. Chem. Soc.* **1982**, *104*, 352; b) J. K. Hoyano, W. A. G. Graham, *J. Am. Chem. Soc.* **1982**, *104*, 3723; c) W. D. Jones, F. J. Feher, *Organometallics* **1983**, *2*, 562.

[16] a) B. A. Arndtsen, R. G. Bergman, T. A. Mobley, T. H. Peterson, *Acc. Chem. Res.* **1995**, *28*, 154; b) A. E. Shilov, G. B Shul'pin, *Chem. Rev.* **1997**, *97*, 2879; c) S. S. Stahl, J. A. Labinger, J. E. Bercaw, *Angew. Chem., Int. Ed.* **1998**, *37*, 2181; d) R. H. Crabtree, *Dalton Trans.* **2001**, 2437; e) J. A. Labinger, J. E. Bercaw, *Nature* **2002**, *417*, 507; f) U. Fekl, K. I. Goldberg, *Adv. Inorg. Chem.* **2003**, *54*, 259; g) R. H. Crabtree, *J. Organomet. Chem.* **2004**, *689*, 4083; h) K. I. Goldberg, A. S. Goldman, *Activation and Functionalization of C-H bonds*, ACS symposium Series 885, eds. **2004**; i) M. Lersch, M. Tilset, *Chem. Rev.* **2005**, *105*, 2471; l) A. R. Dick, M. S. Sanford, *Tetrehedron* **2006**, *62*, 2439.

[17] a) A. E. Shilov, G. V. Shul'pin, Activation and Catalytic Reactions of Saturated Hydrocarbons in the Presence of Metal Complexes, *Catalysis by Metal Complexes Vol. 21*, Springer, Heidelberg, **2002**; b) M. Basato, A. Biffis, G. Buscemi, T. Tubaro, *La Chimica e L'Industria*, **2007**, *9*, 148.

[18] a) H. M. L. Davies, T. Hansen, M. R. Churchill, *J. Am. Chem. Soc.* **2000**, *122*, 3063; b) H. M. L. Davies, R. E. J. Beckwith, *Chem. Rev.* **2003**, *103*, 2861.

[19] a) M. Muehlhofer, T. Strassner, W. A. Herrmann, *Angew. Chem. Int. Ed.* **2002**, *41*, 1745; b) T. Strassner, M. Muehlhofer, A. Zeller, E. Herdtweck, W. A. Herrmann, *J. Organomet. Chem.* **2004**, *689*, 1418; c) S. Ahrens, T. Strassner, *Inorg. Chim. Acta* **2006**, *359*, 4789; d) S. Ahrens, A. Zeller, M. Taige, T. Strassner, *Organometallics* **2006**, *25*, 5409.

[20] a) W. J. Keim, *J. Organomet. Chem.* **1969**, *16*, 191; b) J. S. Ricci, J. A. Ibers, *J. Organomet. Chem.* **1971**, *27*, 261; c) M. I. Bruce, R. C. F. Gardner, F. G. A Stone, *Dalton Trans.* **1976**, 81; d) M. Pfeffer, *Pure Appl. Chem.* **1992**, *64*, 335; e) H. C. L. Abbenhuis, M. Pfeffer, J. P. Sutter, A. de Cian, J. Fischer, H. Li Ji, J. H. Nelson, *Organometallics* **1993**, *12*, 4464; f) W. Ferstl, I. K. Sakodinskaya, N. Beydoun-Sutter, G. Le Borgne, M. Pfeffer, A. D. Ryabov, *Organometallics* **1997**, *16*, 411; g) J. Dupont, M. Pfeffer, J. Spencer, *Eur. J. Inorg. Chem.* **2001**, 1917.

[21] a) V. Ritleng, C. Sirlin, M. Pfeffer, *Chem. Rev.* **2002**, *102*, 1731; b) F. Kakiuchi, N. Chatani, *Adv. Synth. Catal.* **2003**, *345*, 1077; c) M. Beller, J. Seayad, A. Tillack, H. Jiao, *Angew. Chem. Int. Ed.* **2004**, *43*, 3368; d) L. A. Goj, T. B. Gunnoe, *Curr. Org. Chem.* **2005**, *9*, 671.

[22] a) S. Murai, K. Kakiuchi, S. Sekine, Y. Tanaka, A. Kamatani, M. Sonoda, N. Chatani, *Nature* **1993**, *366*, 529; b) F. Kakiuchi, Y. Yamamoto, N. Chatani, S. Murai, *Chem. Lett.* **1995**, 682; c) F. Kakiuchi, T. Sato, K. Igi, N. Chatani, S. Murai, *Chem. Lett.* **2001**, 386; d) F. Kakiuchi, K. Igi, M. Matsumoto, T. Hayamizu, N. Chatani, S. Murai, *Chem. Lett.* **2002**, 396; with Rh(I) see: C. P. Lenges, M. Brookhart, *J. Am. Chem. Soc.* **1999**, *121*, 6616.

[23] a) C. Jia, T. Kitamura, Y. Fujiwara, *Acc. Chem. Res.* **2001**, *34*, 633; b) C. Jia, W. Lu, T. Kitamura, Y. Fujiwara, *Org. Lett.* **1999**, *1*, 2097; c) Y. Fujiwara, C. Jia, *Pure Appl. Chem.* **2001**, *73*, 319.

[24] P. W. N. M. van Leeuwen, M. D. K. Boele, G. P. F. van Strijdonck, A. H. M. de Vries, P. C. J. Kamer, J. G. de Vries, *J. Am. Chem. Soc.* **2002**, *124*, 1586.

[25] M. Dams, D. E. De Vos, S. Celen, P. A. Jacobs, *Angew. Chem. Int. Ed.* **2003**, *42*, 3512.

[26] a) C. Jia, D. Piao, J. Oyamada, W. Lu, T. Kitamura, Y. Fujiwara, *Science* **2000**, *387*, 1992; b) Y. Fujiwara, C. Jia, W. Lu, J. Oyamada, T. Kitamura, K. Matsuda, M. Irie, *J. Am. Chem. Soc.* **2000**, *122*, 7252; c) T. Kitamura, *Eur. J. Org. Chem.*, DOI: 10.1002/ejoc.200801054.

For carbopalladation of alkynes by arylpalladium complexes see also: C. Amatore, S. Bensalem, S. Ghalem, A. Jutand, *J. Organomet. Chem.* **2004**, *689*, 4642. For insertion of alkynes into the Pd-C bond of an arylpalladium complex see also: T. Yagyu, M. Hamada, K. Osakada, T. Yamamoto, *Organometallics* **2001**, *20*, 1087. For the synthesis and the structure of the first σ-arylpalladium complex stabilised by IPr N-heterocyclic carbene see also: W. J. Marshall, V. V. Grushin, *Organometallics* **2003**, *22*, 1591.

[27] C. Nevado, A. Echavarren, *Synthesis* **2005**, *2*, 167.

[28] P. Hong, B.-R. Cho, H. Yamazaki, *Chem. Lett.* **1979**, *9*, 339.

[29] M. Y. Yoon, J. H. Kim, D. S. Choi, U. S. Shin, J. Y. Lee, C. E. Song, *Adv. Synth. Catal.* **2007**, *349*, 1725.

[30] a) T. Tsuchimoto, T. Maeda, E. Shirakawa, Y. Kawakami, *Chem. Commun.* **2000**, 1573; b) C. E. Song, D. Jung, S. Y. Choung, E. J. Roh, S. Lee, *Angew. Chem. Int. Ed.* **2004**, *43*, 6183.

[31] a) R. Li, S. R. Wang, W. Lu, *Org. Lett.* **2007**, *9*, 2219; b) C. Dal Zotto, J. Wehbe, D. Virieux, J. Campagne, *Synlett* **2008**, *13*, 2033.

[32] a) M. T. Reetz, K. Sommer, *Eur. J. Org. Chem.* **2003**, 3485; b) A. Hoffmann-Röder, N. Krause, *Org. Biomol. Chem.* **2005**, *3*, 387.

[33] Z. Shi, C. He, *J. Org. Chem.* **2004**, *69*, 3669.

[34] N. Tsukada, T. Mitsuboshi, H. Setoguchi, Y. Inoue, *J. Am. Chem. Soc.* **2003**, *125*, 12102.

[35] a) J. Oyamada, T. Kitamura, *Chem. Lett.* **2005**, *34*, 1430; b) J. Oyamada, T. Kitamura, *Tetrahedron Lett.* **2005**, *46*, 3823; c) J. Oyamada, T. Kitamura, *Tetrahedron* **2007**, *63*, 12754.

[36] a) L. C. Campeau, M. Parisien, A. Jean, K. Fagnou, *J. Am. Chem. Soc.* **2006**, *128*, 581; b) L. C. Campeau, K. Fagnou, *Chem. Commun.* **2006**, 1253; c) D. R. Stuart, *Science* **2007**, *316*, 1172.

[37] a) J. A. Tunge, L. N. Foresee, *Organometallics* **2005**, *24*, 6440; b) E. Soriano, J. Marco-Contelles, *Organometallics* **2006**, *25*, 4542. For vinylidene reactions see also: K. Ohe, *Bull. Korean Chem. Soc.* **2007**, *28*, 2153.

[38] a) T. Kitamura, K. Yamamoto, M. Kotani, J. Oyamada, C. Jia, Y. Fujiwara, *Bull. Chem. Soc. Jpn.* **2003**, *76*, 1889; b) B. M. Trost, F. D. Toste, K. Greenman, *J. Am. Chem. Soc.* **2003**, *125*, 4581; c) M. Kotani, K. Yamamoto, J. Oyamada, Y. Fujiwara, T. Kitamura, *Synthesis* **2004**, *9*, 1466; d) C. Nevado, A. M. Echavarren, *Chem. Eur. J.* **2005**, *11*, 3155; e) K. L. Lindsay, J. A. Tunge, *J. Org. Chem.* **2005**, *70*, 2881; f) J. Oyamada, T. Kitamura, *Tetrahedron* **2006**, *62*, 6918; g) M. Bandini, E. Emer, S. Tommasi, A. Umani-Ronchi, *Eur. J. Org. Chem.* **2006**, 3527.

[39] a) W. Lu, C. Jia, T. Kitamura, Y. Fujiwara, *Org. Lett.* **2000**, *2*, 2927; b) J. Oyamada, W. Lu, C. Jia, T. Kitamura, Y. Fujiwara, *Chem. Lett.* **2002**, *31*, 20.

[40] a) D. Bourissou, O. Guerret, F. P. Gabbai, G. Bertrand, *Chem. Rev.* **2000**, *100*, 39; b) W. A. Herrmann, *Angew. Chem. Int. Ed.* **2002**, *41*, 1290; c) N. M. Scott, S. P. Nolan, *Eur. J. Inorg. Chem.* **2005**, 1815; d) S. P. Nolan, (Ed.), *N-Heterocyclic Carbenes in Synthesis*, Wiley-VCH, Weinheim, **2006**; e) F. Glorius, (Ed.), *N-Heterocyclic Carbenes in Transition Metal Catalysis*, Topics in Organometallic Chemistry, Vol. 21, Springer, Heidelberg, **2007**.

[41] S. Ahrens, E. Herdtweck, S. Goutal, T. Strassner, *Eur. J. Inorg. Chem.* **2006**, 1268.

[42] M. S. Viciu, E. D. Stevens, J. L. Petersen, S. P. Nolan, *Organometallics* **2004**, *23*, 3752.

[43] G. Buscemi, A. Biffis, C. Tubaro, M. Basato**,** *Catal. Today* **2009**, *140*, 84.

[44] For closely related complexes, see: a) Zargarian, H. Alper, *Organometallics* **1993**, *12*, 712; b) W. A. Herrmann, C.-P. Reisinger, M. Spiegler, *J. Organomet. Chem.* **1998**, *557*, 93; c) E. Hahn, M. Foth, *J. Organomet. Chem.* **1999**, *585*, 241; d) G. Gardiner, W. A. Herrmann, C.-P. Reisinger, J. Schwarz, M. Spiegler, *J. Organomet. Chem.* **1999**, *572*, 239; e) W. A. Herrmann, J. Schwarz, M. G. Gardiner, *Organometallics* **1999**, *18*, 4082; f) Magill, D. S. McGuinness, K. J. Cavell, G. J. P. Britovsek, V. C. Gibson, A. J. P. White, D. J. Williams, A. H. White, B. W. Skelton, *J. Organomet. Chem.*

2001, *617–618*, 546; g) D. R. Jensen, M. J. Schultz, J. A. Mueller, M. S. Sigman, *Angew. Chem. Int. Ed.* **2003**, *42*, 3810; h) E. Herdtweck, M. Muehlhofer, T. Strassner, *Acta Crystallogr., Sect. E: Struct. Rep. Online*, **2003**, *m970*; i) S. Ahrens, A. Zeller, M. Taige, T. Strassner, *Organometallics* **2006**, *25*, 5409; l) article in preparation; m) M. Muehlhofer, T. Strassner, E. Herdtweck, W. A. Herrmann, *J. Organomet. Chem.* **2002**, *660*, 121.

[45] Article in preparation.

[46] a) P. Y. Savechenkov, A. P. Rudenko, A. V. Vasil'ev, G. K. Fukin, *Russ. J. Org. Chem.* **2005**, *41*, 1316; b) S. A. Aristov, A. V. Vasil'ev, G. K. Fukin, A. P. Rudenko, *Russ. J. Org. Chem.* **2007**, *43*, 691; c) A. O. Shchukin, A. V. Vasilyev, *Appl. Catal. A* **2008**, *336*, 140.

[47] See for example K. Fagnou, M. Lautens, *Angew. Chem. Int. Ed.* **2002**, *41*, 26.

[48] L. Gazzola, *Tesi di Laurea Specialistica in Chimica*, Università degli Studi di Padova, **2008**.

[49] A. Biffis, C. Tubaro, G. Buscemi, M. Basato, *Adv. Synth. Catal.* **2008**, *350*, 189.

[50] a) W. A. Herrmann, J. Schütz, G. D. Frey, E. Herdtweck, *Organometallics* **2006**, *25*, 2437; b) R. A. Kelly III, H. Clavier, S. Giudice, N. M. Scott, E. D. Stevens, J. Bordner, I. Samardjiev, C. D. Hoff, L. Cavallo, S. P. Nolan, *Organometallics* **2008**, *27*, 202.

[51] L. Delaude, S. Delfosse, A. Richel, A. Demonceau, A. F. Noels, *Chem. Commun.* **2003**, 1526.

[52] a) J. Pytkowicz, S. Roland, P. Mangeney, G. Meyer, A. Jutand, *J. Organomet. Chem.* **2003**, *678*, 166; b) F. Demirhan, Ö. Yıldırım, B. Cetinkaya, *Transition Met. Chem.* **2003**, *28*, 558; c) L. Meres, G. Labat, A. Neels, A. Ehlers, M. Albrecht, *Organometallics* **2006**, *25*, 5648; d) S. Leuthäußer, D. Schwarz, H. Plenio, *Chem. Eur. J.* **2007**, *13*, 7195.

[53] a) M. A. Taige, A. Zeller, S. Ahrens, S. Goutal, E. Herdtweck, T. Strassner, *J. Organomet. Chem.* **2007**, *692*, 1519; b) M. V. Baker, B. W. Skelton, A. H. White, C. C. Williams, *Dalton Trans.* **2001**, 111.

[54] a) N. P. Grimster, C. Gauntlett, C. R. A. Godfrey, M. J. Gaunt, *Angew. Chem. Int. Ed.* **2005**, *44*, 3125; b) E. Capito, J. M. Brown, A. Ricci, *Chem. Commun.*

2005, 1854; c) S. Cacchi, G. Fabrizi, *Chem. Rev.* **2005**, *105*, 2873; d) I. V. Seregin, V. Gevorgyan, *Chem. Soc. Rev* **2007**, *36*, 1173; e) L. Djakovitch, P. Rouge, *Catal. Today* **2009**, *140*, 90.

[55] M. G. Banwell, T. E. Goodwin, S. Ng, J. A. Smith, D. J. Wong, *Eur. J. Org. Chem.* **2006**, 3043.

[56] M. L. Keita, T. Mizuhara, J. Oyamada, T. Kitamura, *Chem. Lett.* **2007**, *36*, 1150.

[57] a) F. Kakiuchi, Y. Yamamoto, N. Chatani, S. Murai, *Chem. Lett.* **1995**, *24*, 681; b) F. Kakiuchi, T. Sato, K. Igi, N. Chatani, S. Murai, *Chem. Lett.* **2001**, *30*, 386.

[58] P. Hong, B-R. Cho, H. Yamazaki, *Chem. Lett.* **1980**, *9*, 507.

[59] T. Tsuchimoto, K. Hatanaka, E. Shirakawa, Y. Kawakami, *Chem. Commun.* **2003**, 2454.

[60] a) Z. Li, Z. Shi, C. He, *J. Organomet. Chem.* **2005**, *690*, 5049; b) C. Ferrer, C. H. M. Amijs, A. M. Echavarren, *Chem. Eur. J.* **2007**, *13*, 1358.

[61] A. S. K. Hashmi, M. C. Blanco, *Eur. J. Org. Chem.* **2006**, 4340.

[62] a) N. Tsukada, K. Murata, Y. Inoue, *Tetrahedron Lett.* **2005**, *46*, 7515; b) N. Tsukada, H. Setoguchi, T. Mitsuboshi, Y. Inoue, *Chem. Lett.* **2006**, *35*, 1164.

[63] J. Oyamada, *PhD Thesis* **2007**.

[64] a) T. J. Williams, J. A. Labinger, J. E. Bercaw, *Organometallics* **2007**, *26*, 281.

[65] D. G. Blackmond, *Angew. Chem. Int. Ed.* **2005**, *44*, 4302.

[66] a) M. D. K. Boele, G. P. F. van Strijdonck, A. H. M. de Vries, P. C. J. Kamer, J. G. de Vries, P. W. N. M. van Leeuwen, *J. Am. Chem. Soc.* **2002**, *124*, 1586; b) J-R. Wang, C-T. Yang, L. Liu, Q-X. Guo, *Tetrahedron Lett.* **2007**, *48*, 5449.

[67] H. Horino, N. Inoue, *J.Org. Chem. Soc.* **1981**, *46*, 4416.

[68] unpublished results.

[69] A. J. Bard, L. R. Faulkner, *Electrochemical Methods*, 2nd ed., Wiley&Sons, New York, **2001**.

[70] a) L. R. Titcomb, S. Caddick, F. G. N. Cloke, D. J. Wilson, D. McKerrecher, *Chem. Commun.* **2001**, 1388; b) N. D. Clement, K. J. Cavell, C. Jones, C. J. Elsevier, *Angew. Chem. Int. Ed.* **2004**, *43*, 1277.

[71] M. G. Gardiner, W. A. Herrmann, C. Reisinger, J. Schwarz, M. Spiegler, *J. Organomet. Chem.* **1999**, *572*, 239.

[72] a) B. Gorodetsky, T. Ramnial, N. R. Branda, J. A. C. Clyburne, *Chem. Comm.* **2004**, 1972; b) J. A. C. Clyburne *Chem. Comm.* **2006**, 1809; R. Hagiwara, Y. Ito, *J. Fluorine Chem.* **2000**, *105*, 221.

[73] J. Oyamada, T. Kitamura, *Chem. Commun.* **2008**, 4992.

PUBLICATIONS

A. Biffis, L. Gazzola, P. Gobbo, **G. Buscemi**, C. Tubaro, M. Basato. "Alkyne hydroarylations with chelating dicarbene palladium(II) complex catalysts: improved and unexpected reactivity patterns disclosed upon additive screening", *submitted.*

G. Buscemi, A. Biffis, C. Tubaro, M. Basato. "Mild hydroarylation of alkynes with chelating dicarbene palladium(II) complexes". *Catal. Today*, **2009**, *140,* 84.

A. Biffis, C. Tubaro, **G. Buscemi**, M. Basato. "Highly efficient alkyne hydroarylation with chelating dicarbene palladium(II) complexes". *Adv. Synth. Catal.*, **2008**, *350*, 189-196.

M. Basato, A. Biffis, **G. Buscemi**, C. Tubaro. "C-H activation: a facile process?". *Chim. Ind. (Milan, Italy),* **2007**, *9*, 148-152.

CONGRESS COMMUNICATIONS

C. Tubaro, A. Biffis, M. Basato, **G. Buscemi**, L. Gazzola, E. Scattolin. *XXIII ICOMC: "C-H functionalization and coupling reactions with poly(N-heterocyclic) carbene catalysts of late transition metals"*. International Conference on Organometallic Chemistry, IC15. Rennes, France (13-18 July 2008).

C. Tubaro, **G. Buscemi***, L. Gazzola, A. Biffis, M. Basato. *XVI ISHC: "Aromatic C-H bond functionalisation with chelating NHC-Pd(II) catalysts: the Fujiwara hydroarylation of alkynes"*. International Symposium on Homogeneous Catalysis, P053. Firenze, Italy (6-11 July 2008).

A. Biffis, C. Tubaro, **G. Buscemi**, M. Basato. *P27: "Highly efficient alkyne hydroarylation with chelating dicarbene metal complex catalysts"*. International Symposium on Catalysis Applied to Fine Chemicals 8th Edition. Verbania, Italy (16-20 September 2007).

G. Buscemi**, A. Biffis, C. Tubaro, M. Basato. *ISOC2007: "Highly efficient alkyne hydroarylation with chelating dicarbene metal complex catalysts"*. International School of Organometallic Chemistry 6th Edition. Camerino, Italy (8-12 September 2007).

Biffis, C. Tubaro, **G. Buscemi**, M. Basato. *INO-P-11: "Catalytic C-H Activation with Chelating NHC Palladium Complexes: the Fujiwara Hydroarylation of Alkynes"*. XXII Congresso Nazionale della Società Chimica Italiana. Firenze, Italy (10-15 September 2006).

Biffis, C. Tubaro, **G. Buscemi**, M. Basato. *P8: "Catalytic C-H activation with chelating NHC palladium complexes: the Fujiwara hydroarylation of alkynes"*. VII Congresso del Gruppo Interdivisionale di Chimica Organometallica. Parma, Italy (9-12 July 2006).

Active attendance to the congress or the school. ** Flash presentation in english language.

Acknowledgements

I wish to express my sincere gratitude to Professor Marino Basato for the constant help and the suggestions during these three years.

Thanks to Dr. Cristina Tubaro e Dr. Andrea Biffis for the useful advices in the experimental development of the work and to all the laboratory's staff: Sig. Antonio Ravazzolo and the master students who contributed to and will continue the research work.

Also the board of examiners composed by Prof. Giulia Licini, Prof. Daniele Marton and Prof. Giuliano Bandoli have contributed to the success of this thesis through helpful tips and proper clarifications, together with the guidance of the director of the school Prof. Maurizio Casarin.

I would like also to acknowledge Professor Armando Gennaro and Dr. Abdirisak Ahmed Isse, for the chance to work in their laboratories discovering and developing a new field of chemistry, which at the beginning was totally unknown to me.

To all my family, and in particular to my parents, who believed with me in the success of the project, supporting and suggesting me in every difficult moment with an incredible patience, thank you!

Gabriella